

SIMULTANEOUS OPTIMIZATION OF QUALITY RETENTION IN
CONDUCTION-HEATED FOODS OF DIFFERENT GEOMETRIES

By

FERRUH ERDOĞDU

A DISSERTATION PRESENTED TO THE GRADUATE SCHOOL
OF THE UNIVERSITY OF FLORIDA IN PARTIAL FULFILLMENT
OF THE REQUIREMENTS FOR THE DEGREE OF
DOCTOR OF PHILOSOPHY

UNIVERSITY OF FLORIDA
2000

To my mother, Aynur, for all her support, love, patience, and the invaluable opportunities she provided me throughout my life for the best life possible; to my sister, Aylin, for all her love, support, and encouragement; to the dear memory of my father, Feran; and to my friends for the precious moments they gave me.

ACKNOWLEDGMENTS

I would like to express my sincere thanks and appreciation to my advisor, Dr. Murat Ö. Balaban, for his invaluable advice, guidance, friendship, help in all aspects of my career, and encouragement to participate in other activities, learn other disciplines, and network with people during my studies at the University of Florida. He is the main reason for most of my achievements and success in my career thus far.

My sincere thanks and appreciation are also extended to Dr. Khe V. Chau for all his time, advice, guidance, friendship, help, and encouragement in all aspects of my studies at the University of Florida.

Appreciation is also extended to Drs. Teixeira, Hsieh, and Sims for their guidance and recommendations for the success of this study.

TABLE OF CONTENTS

ACKNOWLEDGMENTS	iii
LIST OF TABLES	vii
LIST OF FIGURES	xii
NOMENCLATURE	xvii
ABSTRACT	xix
CHAPTERS	
1 INTRODUCTION AND LITERATURE REVIEW	1
Thermal Processing	1
Optimization	2
Optimization of Thermal Processing	3
Complex Method	17
Objectives	19
2 MATERIALS AND METHODS	21
Objective Functions	22
Constraints	24
Explicit Constraints	24
Implicit Constraints	25
Decision Variable	26
Complex Method Algorithm For A Single Geometry System	26
Step 1	26
Step 2	28
Step 3	28
Step 4	29
Step 5	32
Step 6	32
Step 7	34
Algorithm Testing and Application Systems	35

Algorithm of Complex Method For Double Geometry System	41
The Software	43
3 RESULTS AND DISCUSSION	50
The Complex Method	50
Optimization With Single Geometry	50
Objective Function: volume average retention of nutrient	50
Sphere	50
Finite cylinder	69
Objective function: surface retention of nutrient	84
Sphere	84
Finite cylinder	93
Optimization With Double Geometry	98
Uniqueness and Reproducibility Issues	113
Comparison With the Literature Results	116
4 CONCLUSIONS AND RECOMMENDATIONS	119
Conclusions	119
Recommendations	121
APPENDICES	
A THE COMPLEX METHOD	122
B PROCESS AND CENTER TEMPERATURE PROFILES FOR A SPHERE UNDER DIFFERENT PROCESSING CONDITIONS; OBJECTIVE FUNCTION: VACN	131
C PROCESS AND CENTER TEMPERATURE PROFILES FOR A FINITE CYLINDER UNDER DIFFERENT PROCESSING CONDITIONS; OBJECTIVE FUNCTION: VACN	172
D PROCESS AND CENTER TEMPERATURE PROFILES FOR A SPHERE UNDER DIFFERENT PROCESSING CONDITIONS; OBJECTIVE FUNCTION: SCN	194
E PROCESS AND CENTER TEMPERATURE PROFILES FOR A FINITE CYLINDER UNDER DIFFERENT PROCESSING CONDITIONS; OBJECTIVE FUNCTION: SCN	215
F PROCESS AND CENTER TEMPERATURE PROFILES FOR DOUBLE GEOMETRY SYSTEM (A SPHERE and A FINITE CYLINDER) UNDER DIFFERENT PROCESSING CONDITIONS; OBJECTIVE FUNCTION: VACN	222

G	PROCESS AND CENTER TEMPERATURE PROFILES FOR LITERATURE CASES	235
REFERENCES		240
BIOGRAPHICAL SKETCH		245

LIST OF TABLES

<u>Table</u>	<u>page</u>
1-1. Objective functions used to optimize the thermal processing	6
3-1. Optimization results using constant retort temperature profile for model spheres	51
3-2. Simulation conditions for sphere	52
3-3. The calculated variable process temperature profiles (VPTP) of the model sphere-1 ($r=15$ mm) for processing time of 20 min and the discretized time steps of $N=10$ (Objective Function: VACN)	55
3-4. The calculated variable process temperature profiles (VPTP) of the model sphere-1 ($r=15$ mm) for processing time of 20 min and the discretized time steps of $N=20$ (Objective Function: VACN).	56
3-5. The VACN (%), SCN(%), and $F_0(\text{min})$ results of the calculated VPTPs of the model sphere 1 ($r=15$ mm) for the processing time of 20 min and two different discretized time steps of $N=10$ and $N=20$ (Objective Function: VACN)	57
3-6. The calculated variable process temperature profiles (VPTP) of the model sphere-1 ($r=15$ mm) for processing time of 30 min and the discretized time steps of $N=10$ (Objective Function: VACN)	58
3-7. The calculated variable process temperature profiles (VPTP) of the model sphere-1 ($r=15$ mm) for processing time of 30 min and the discretized time steps of $N=20$ (Objective Function: VACN).	59
3-8. The VACN (%), SCN(%), and $F_0(\text{min})$ results of the calculated VPTPs of the model sphere 1 ($r=15$ mm) for the processing time of 30 min and two different discretized time steps of $N=10$ and $N=20$ (Objective Function: VACN)	60

3-9.	The calculated variable process temperature profiles (VPTP) of the model sphere-2 ($r=30$ mm) for processing time of 80 min and the discretized time steps of $N=10$ (Objective Function: VACN)	62
3-10.	The calculated variable process temperature profiles (VPTP) of the model sphere-2 ($r=30$ mm) for processing time of 80 min and the discretized time steps of $N=20$ (Objective Function: VACN)	63
3-11.	The VACN (%), SCN(%), and $F_0(\text{min})$ results of the calculated VPTPs of the model sphere 2 ($r=30$ mm) for the processing time of 80 min and two different discretized time steps of $N=10$ and $N=20$ (Objective Function: VACN)	64
3-12.	The calculated variable process temperature profiles (VPTP) of the model sphere-2 ($r=30$ mm) for processing time of 120 min and the discretized time steps of $N=10$ (Objective Function: VACN)	65
3-13.	The calculated variable process temperature profiles (VPTP) of the model sphere-2 ($r=30$ mm) for processing time of 120 min and the discretized time steps of $N=20$ (Objective Function: VACN)	66
3-14.	The VACN (%), SCN(%), and $F_0(\text{min})$ results of the calculated VPTPs of the model sphere 2 ($r=30$ mm) for the processing time of 120 min and two different discretized time steps of $N=10$ and $N=20$ (Objective Function: VACN)	68
3-15.	Optimization results using constant retort temperature profile for model finite cylinders	70
3-16.	Simulation setup for finite cylinder	70
3-17.	The calculated variable process temperature profiles (VPTP) of the model finite cylinder 1 ($r=15$ mm, $L=15$ mm) for processing time of 20 min and the discretized time steps of $N=10$ (Objective Function: VACN)	72
3-18.	The calculated variable process temperature profiles (VPTP) of the model finite cylinder 1 ($r=15$ mm, $L=15$ mm) for processing time of 20 min and the discretized time steps of $N=20$ (Objective Function: VACN)	73
3-19.	The VACN (%), SCN(%), and $F_0(\text{min})$ results of the calculated VPTPs of the model finite cylinder 1 ($r=15$ mm, $L=15$ mm) for the processing time of 20 min and two different discretized time steps of $N=10$ and $N=20$ (Objective Function: VACN)	74

3-20.	The calculated variable process temperature profiles (VPTP) of the model finite cylinder 1 ($r=15$ mm, $L=15$ mm) for processing time of 30 min and the discretized time steps of $N=10$ (Objective Function: VACN)	75
3-21.	The calculated variable process temperature profiles (VPTP) of the model finite cylinder 1 ($r=15$ mm, $L=15$ mm) for processing time of 30 min and the discretized time steps of $N=20$ (Objective Function: VACN)	76
3-22.	The VACN (%), SCN(%), and $F_0(\text{min})$ results of the calculated VPTPs of the model finite cylinder 1 ($r=15$ mm, $L=15$ mm) for the processing time of 30 min and two different discretized time steps of $N=10$ and $N=20$ (Objective Function: VACN)	77
3-23.	The calculated variable process temperature profiles (VPTP) of the model finite cylinder 2 ($r=30$ mm, $L=60$ mm) for processing time of 90 min and the discretized time steps of $N=10$ (Objective Function: VACN)	78
3-24.	The calculated variable process temperature profiles (VPTP) of the model finite cylinder 2 ($r=30$ mm, $L=60$ mm) for processing time of 90 min and the discretized time steps of $N=20$ (Objective Function: VACN)	80
3-25.	The VACN (%), SCN(%), and $F_0(\text{min})$ results of the calculated VPTPs of the model finite cylinder 1 ($r=30$ mm, $L=60$ mm) for the processing time of 90 min and two different discretized time steps of $N=10$ and $N=20$ (Objective Function: VACN)	81
3-26.	The calculated variable process temperature profiles (VPTP) of the model finite cylinder 2 ($r=30$ mm, $L=60$ mm) for processing time of 135 min and the discretized time steps of $N=10$ (Objective Function: VACN)	83
3-27.	The VACN (%), SCN(%), and $F_0(\text{min})$ results of the calculated VPTPs of the model finite cylinder 1 ($r=30$ mm, $L=60$ mm) for the processing time of 135 min and two different discretized time steps of $N=10$ (Objective Function: VACN)	84
3-28.	The calculated variable process temperature profiles (VPTP) of the model sphere 1 ($r=15$ mm) for processing time of 20 min and the discretized time steps of $N=10$ (Objective Function: SCN)	85
3-29.	The calculated variable process temperature profiles (VPTP) of the model sphere 1 ($r=15$ mm) for processing time of 20 min and the discretized time steps of $N=20$ (Objective Function: SCN)	86

3-30.	The VACN (%), SCN(%), and $F_0(\text{min})$ results of the calculated VPTPs of the model sphere 1 ($r=15 \text{ mm}$) for the processing time of 20 min and two different discretized time steps of $N=10$ and $N=20$ (Objective Function: SCN)	87
3-31.	The calculated variable process temperature profiles (VPTP) of the model sphere 2 ($r=30 \text{ mm}$) for processing time of 80 min and the discretized time steps of $N=10$ (Objective Function: SCN)	88
3-32.	The calculated variable process temperature profiles (VPTP) of the model sphere 2 ($r=30 \text{ mm}$) for processing time of 80 min and the discretized time steps of $N=20$ (Objective Function: SCN)	89
3-33.	The VACN (%), SCN(%), and $F_0(\text{min})$ results of the calculated VPTPs of the model sphere 1 ($r=30 \text{ mm}$) for the processing time of 80 min and two different discretized time steps of $N=10$ and $N=20$ (Objective Function: SCN)	90
3-34.	The calculated variable process temperature profiles (VPTP) of the model finite cylinder 1 ($r=15 \text{ mm}$, $L=15 \text{ mm}$) for processing time of 16 min and the discretized time steps of $N=10$ (Objective Function: SCN)	94
3-35.	The VACN (%), SCN(%), and $F_0(\text{min})$ results of the calculated VPTPs of the model finite cylinder 1 ($r=15 \text{ mm}$, $L=15 \text{ mm}$) for the processing time of 16 min and discretized time steps of $N=10$ (Objective Function: SCN)	95
3-36.	The calculated variable process temperature profiles (VPTP) of the model finite cylinder 1 ($r=30 \text{ mm}$, $L=60 \text{ mm}$) for processing time of 90 min and the discretized time steps of $N=10$ (Objective Function: SCN)	97
3-37.	The VACN (%), SCN(%), and $F_0(\text{min})$ results of the calculated VPTPs of the model finite cylinder 1 ($r=30 \text{ mm}$, $L=60 \text{ mm}$) for the processing time of 90 min and discretized time steps of $N=10$	97
3-38.	The calculated variable process temperature profiles (VPTP) for double geometry system consisting of a sphere ($r=15 \text{ mm}$) and a finite cylinder ($r=15 \text{ mm}$, $L=15 \text{ mm}$) for the processing time of 20 min and discretized time steps of $N=10$ (Objective Function: VACN)	100

3-39.	The VACN (%), SCN(%), and $F_0(\text{min})$ results of the calculated VPTPs of double geometry system consisting of a sphere ($r=15 \text{ mm}$) and a finite cylinder ($r=15 \text{ mm}$, $L=15 \text{ mm}$) for the processing time of 20 min and discretized time steps of $N=10$ (Objective Function: VACN) ...	101
3-40.	The calculated variable process temperature profiles (VPTP) for double geometry system consisting of a sphere ($r=30 \text{ mm}$) and a finite cylinder ($r=15 \text{ mm}$, $L=15 \text{ mm}$) for the processing time of 80 min and discretized time steps of $N=10$ (Objective Function: VACN)	102
3-41.	The VACN (%), SCN(%), and $F_0(\text{min})$ results of the calculated VPTPs of double geometry system consisting of a sphere ($r=30 \text{ mm}$) and a finite cylinder ($r=15 \text{ mm}$, $L=15 \text{ mm}$) for the processing time of 80 min and discretized time steps of $N=10$ (Objective Function: VACN) ...	103
3-42.	The calculated variable process temperature profiles (VPTP) for double geometry system consisting of a sphere ($r=15 \text{ mm}$) and a finite cylinder ($r=30 \text{ mm}$, $L=60 \text{ mm}$) for the processing time of 90 min and discretized time steps of $N=10$ (Objective Function: VACN)	104
3-43.	The VACN (%), SCN(%), and $F_0(\text{min})$ results of the calculated VPTPs of double geometry system consisting of a sphere ($r=15 \text{ mm}$) and a finite cylinder ($r=30 \text{ mm}$, $L=60 \text{ mm}$) for the processing time of 90 min and discretized time steps of $N=10$ (Objective Function: VACN) ...	106
3-44.	The variable process temperature profiles (VPTP) for double geometry system consisting of a sphere ($r=30 \text{ mm}$) and a finite cylinder ($r=30 \text{ mm}$, $L=60 \text{ mm}$) for the processing time of 90 min and discretized time steps of $N=10$ (Objective Function: VACN)	107
3-45.	The VACN (%), SCN(%), and $F_0(\text{min})$ results of the calculated VPTPs of double geometry system consisting of a sphere ($r=30 \text{ mm}$) and a finite cylinder ($r=30 \text{ mm}$, $L=60 \text{ mm}$) for the processing time of 90 min and discretized time steps of $N=10$ (Objective Function: VACN) ...	108

LIST OF FIGURES

<u>Figure</u>	<u>page</u>
2-1. The retort temperature profile after step 1	27
2-2. The retort temperature profile after step 2	29
2-3. The retort temperature profile in step 3 (not achieving the first implicit constraint)	31
2-4. The retort temperature profile in step 3 (achieving both of the implicit constraints)	31
2-5. The algorithm structure of the developed program for a single geometry system	36
2-6. The start-up screen of the Optimization Expert	44
2-7. Screen of options for the Optimization Expert	45
2-8. Screen for the thermophysical properties of the geometries and kinetics of the quality attribute and microorganism	47
2-9. Numerical output for a sphere geometry of radius of 15 mm with the given properties in Figure 2-8	48
2-10. Graphical output for a sphere geometry of radius of 15 mm with the given properties in Figure 2-8	49
3-1. Constant optimum temperature profile for sphere 1 ($r=15$ mm) with the accompanying center temperature	53
3-2. Constant optimum temperature profile for sphere 2 ($r=30$ mm) with the accompanying center temperature profile	53

3-3.	Comparison of the CPTP and the best VPTP with resulting center temperature profiles (Sphere-1: $r=15$ mm, $t=20$ min, $N=10$, Objective Function: VACN)	57
3-4.	Comparison of the CPTP and the best VPTP with resulting center temperature profiles (Sphere-1: $r=15$ mm $t=20$ min, $N=20$, Objective Function: VACN)	58
3-5.	Comparison of the best calculated VPTPs of $N=10$ and $N=20$ for sphere 1 ($r=15$ mm, $t=20$ min, Objective Function: VACN)	60
3-6.	Comparison of the best calculated VPTPs of $N=10$ and $N=20$ for sphere 1 ($r=15$ mm, $t=30$ min, Objective Function: VACN)	61
3-7.	Representation of the CPTP and the best VPTP with resulting center temperature profiles (Sphere-2, $r=30$ mm, $t=80$ min, $N=10$, Objective Function: VACN)	64
3-8.	Representation of the CPTP and the best VPTP with resulting center temperature profiles (Sphere-2: $r=30$ mm, $t=80$ min, $N=20$, Objective Function: VACN)	65
3-9.	Comparison of the best calculated VPTPs of $N=10$ and $N=20$ for sphere 2 ($r=30$ mm, $t=80$ min, Objective Function: VACN)	67
3-10.	Comparison of the best calculated VPTPs of $N=10$ and $N=20$ for sphere 2 ($r=30$ mm, $t=120$ min, Objective Function: VACN)	67
3-11.	Constant optimum temperature profile for finite cylinder 1 ($r=15$ mm, $2l=15$ mm) with the accompanying center temperature profile	71
3-12.	Constant optimum temperature profile for finite cylinder 2 ($r=30$ mm, $2l=60$ mm) with the accompanying center temperature profile	71
3-13.	Comparison of the CPTP and the best VPTP with resulting center temperature profiles (Finite Cylinder-1, $r=15$ mm, $2l=15$ mm, $t=16$ min, $N=10$, Objective Function: VACN)	74
3-14.	Comparison of the CPTP and the best VPTP with resulting center temperature profiles (Finite Cylinder-1, $r=15$ mm, $2l=15$ mm, $t=16$ min, $N=20$, Objective Function: VACN)	75

3-15. Comparison of the best calculated VPTPs of N=10 and N=20 for finite cylinder 1($r=15$ mm, $2l=15$ mm, $t=16$ min, Objective Function: VACN)	77
3-16. Comparison of the best calculated VPTPs of N=10 and N=20 for finite cylinder 1($r=15$ mm, $2l=15$ mm, $t=24$ min, Objective Function: VACN)	78
3-17. Comparison of the CPTP and the best VPTP with resulting center temperature profiles (Finite Cylinder-2, $r=30$ mm, $2l=60$ mm, $t=90$ min, N=10, Objective Function: VACN)	81
3-18. Comparison of the CPTP and the best VPTP with resulting center temperature profiles (Finite Cylinder-2, $r=30$ mm, $2l=60$ mm, $t=90$ min, N=20, Objective Function: VACN)	82
3-19. Comparison of the best calculated VPTPs of N=10 and N=20 for finite cylinder 2($r=30$ mm, $2l=60$ mm, $t=90$ min, Objective Function: VACN)	82
3-20. Comparison of the CPTP and the best VPTP with resulting center temperature profiles (Sphere-1, $r=15$ mm, $t=20$ min, N=10, Objective Function: SCN)	87
3-21. Comparison of the CPTP and the best VPTP with resulting center temperature profiles (Sphere-1, $r=15$ mm, $t=20$ min, N=20, Objective Function: SCN)	88
3-22. Comparison of the CPTP and the best VPTP with resulting center temperature profiles (Sphere-1, $r=30$ mm, $t=80$ min, N=10, Objective Function: SCN)	91
3-23. Comparison of the CPTP and the best VPTP with resulting center temperature profiles (Sphere-1, $r=30$ mm, $t=80$ min, N=20, Objective Function: SCN)	91
3-24. Comparison of the best calculated VPTPs of N=10 and N=20 for sphere 1 ($r=15$ mm, $t=20$ min, Objective Function: SCN)	92
3-25. Comparison of the best calculated VPTPs of N=10 and N=20 for sphere 2 ($r=30$ mm, $t=80$ min, Objective Function: SCN)	92

3-26.	Comparison of the CPTP and the best VPTP with resulting center temperature profiles (Finite Cylinder-1, $r=15$ mm, $2l=15$ mm, $t=16$ min, $N=10$, Objective Function: SCN)	95
3-27.	Comparison of the CPTP and the best VPTP with resulting center temperature profiles (Finite Cylinder-2, $r=30$ mm, $2l=60$ mm, $t=90$ min, $N=10$, Objective Function: SCN)	98
3-28.	Comparison of the sphere 1 ($r=15$ mm) and finite cylinder 1 ($r=15$ mm, $2l=15$ mm) center temperature profiles, subjected to the CPTP for sphere 1 ($r=15$ mm, $t=20$ min, Objective Function: VACN)	101
3-29.	Comparison of the sphere 1 ($r=15$ mm) and finite cylinder 1 ($r=15$ mm, $2l=15$ mm) center temperature profiles, subjected to the optimum VPTP for double geometry system (Objective Function: VACN)	102
3-30.	Comparison of the sphere 2 ($r=30$ mm) and finite cylinder 1 ($r=15$ mm, $2l=15$ mm) center temperature profiles, subjected to the CPTP for sphere 2 ($r=30$ mm, Objective Function: VACN)	103
3-31.	Comparison of the sphere 2 ($r=30$ mm) and finite cylinder 1 ($r=15$ mm, $2l=15$ mm) center temperature profiles, subjected to the optimum VPTP for double geometry system (Objective Function: VACN)	104
3-32.	Comparison of the sphere 1 ($r=15$ mm) and finite cylinder 2 ($r=30$ mm, $2l=60$ mm) center temperature profiles, subjected to the CPTP for finite cylinder 2 ($r=30$ mm, $2l=60$ mm, Objective Function: VACN)	106
3-33.	Comparison of the sphere 1 ($r=15$ mm) and finite cylinder 2 ($r=30$ mm, $2l=60$ mm) center temperature profiles, subjected to the optimum VPTP for double geometry system (Objective Function: VACN)	107
3-34.	Comparison of the sphere 2 ($r=30$ mm) and finite cylinder 2 ($r=30$ mm, $2l=60$ mm) center temperature profiles, subjected to the CPTP for finite cylinder 2 ($r=30$ mm, $2l=60$ mm, Objective Function: VACN)	108
3-35.	Comparison of the sphere 2 ($r=30$ mm) and finite cylinder 2 ($r=30$ mm, $2l=60$ mm) center temperature profiles, subjected to the optimum VPTP for double geometry system (Objective Function: VACN)	109
3-36.	Comparison of the best VPTPs for sphere 1 ($r=15$ mm) and system A (sphere 1: $r=15$ mm; finite cylinder 1: $r=15$ mm, $2l=15$ mm) for $N=10$ (Objective Function: VACN)	110

3-37.	Comparison of the best VPTPs for sphere 2 ($r=15$ mm) and system B (sphere 2: $r=30$ mm; finite cylinder 1: $r=15$ mm, $2l=15$ mm) for $N=10$ (Objective Function: VACN)	110
3-38.	Comparison of the best VPTPs for finite cylinder 2 ($r=30$ mm, $2l=60$ mm) and system C (sphere 1: $r=15$ mm; finite cylinder 2: $r=30$ mm, $2l=60$ mm) for $N=10$ (Objective Function: VACN)	111
3-39.	Comparison of the best VPTPs for finite cylinder 2 ($r=30$ mm, $2l=60$ mm) and system D (sphere 2: $r=30$ mm; finite cylinder 2: $r=30$ mm, $2l=60$ mm) for $N=10$ (Objective Function: VACN)	111
3-40.	The computed graph of y versus x for equation 3-1	116

NOMENCLATURE

<u>Symbol</u>	<u>Definition</u>
ASM	Volume average survival of microorganisms or volume average quality retention (%)
α	Reflection coefficient in complex method
β	Retraction coefficient in complex method
C	Cook value (min)
C_v	Volume average cook value (min)
CPTP	Constant temperature profile
D	Decimal reduction time (min)
D_{ref}	Decimal reduction time at the reference temperature (min)
F_0	Integrated lethality at the slowest heating point (min)
γ	Expansion coefficient in complex method
k	Reaction kinetics constant
L	Full length of a finite cylinder (mm)
n	Degree of reaction
N	Number of discretized time steps
PT	Process temperature profile
PT_L	Lower limit of process temperature profile (°C)

PT_H	Higher limit of process temperature profile (°C)
r	Radius (mm)
r_i	Pseudo-random number
SCN	Surface quality retention (%)
T	Temperature (°C)
T_c	Center temperature (°C)
T_s	Surface temperature (°C)
$T(t,v)$	Temperature of a volume element at certain time t (°C)
T_{ref}	Reference Temperature (°C)
v_c	Retracted vertex
v_e	Expanded vertex
v_0	The best vertex giving the highest objective function value
v_r	Reflected vertex
v_w	The worst vertex giving the lowest objective function value
V	Volume of a food or geometry (m ³)
VACN	Volume average quality retention (%)
VPTP	Variable process temperature profile
z	Temperature change needed to reduce the D-value one log cycle (°C)

Abstract of Dissertation Presented to the Graduate School
of the University of Florida in Partial Fulfillment of the
Requirements for the Doctor of Philosophy

SIMULTANEOUS OPTIMIZATION OF QUALITY
RETENTION IN CONDUCTION-HEATED
FOODS OF DIFFERENT GEOMETRIES

By

Ferruh Erdoğan

August 2000

Chairperson: Murat Ö. Balaban

Major Department: Agricultural and Biological Engineering

The complex method, a general and flexible optimization algorithm, was used to determine the variable process temperature profile during thermal processing to maximize (optimize) the volume average or surface retention of a nutrient in conduction heated foods of different geometries. The objective functions were the volume average concentration (VACN) and surface retention (SCN) of a nutrient during the process, the implicit constraints were the target lethality at the cold point, and a threshold below which the center temperature must reach at the end of the process. A process temperature range of 5-150°C was used as an explicit constraint. Another explicit constraint was that the process temperature had to reach 5°C at the end of the process. The control variables for the optimization were variable process temperature profiles (VPTP) at equidistant time steps throughout the process for the optimization of thermal processing for a sphere or

finite cylinder for single geometry systems and their combination for a double geometry system. In the double geometry system optimization, a multi-objective optimization problem, the Weighing Method (to connect the objective functions for each geometry) and the Lexicographic Ordering Method (to guarantee the most important objective function preserves its optimal value) were combined with the modified Complex Method. All calculations were performed using a computer program written in Visual Basic V. 6.0. This Windows-based software calculated the optimum variable temperature profiles using the geometry options, objective functions, and constraints chosen by the user. VPTPs for different sizes of individual geometries (sphere, finite cylinder), alone or in combination (sphere and finite cylinder) at different processing conditions, together with their nutrient retentions compared to the constant temperature processes, were presented. Effects of time steps, and reproducibility of the algorithm were shown, and the uniqueness problem of the method was addressed.

The VPTPs resulted in some nutrient retention improvements compared to the constant temperature processes. In a single geometry system, the improvements were less than 1 percentage point in both VACN and SCN for smaller size geometries, while they were up to 2-3 percentage points in VACN and up to 3-4 percentage points in SCN for larger sizes. For double geometry systems, improvements were higher (6 percentage point improvement in both VACN and SCN). This was more obvious in the smaller geometries when the double geometry system consisted of a large and small geometry.

CHAPTER 1 INTRODUCTION AND LITERATURE REVIEW

Thermal Processing

Thermal processing is an important method to extend the shelf life of foods. It has been used extensively, sometimes in combination with other preservation techniques. The desired functions of thermal processing are:

- the reduction of the activity of undesirable biological reactions (e.g., microorganisms and/or enzymes),
- physical changes, mainly cooking of foods, and
- chemical and sensory changes.

However, there are also some undesirable changes, like sensory (e.g., discoloration, flavor and textural changes), physical and chemical changes (e.g., over-cooking, liquefaction, vitamin loss, caramelization, Maillard reactions, etc.) (Lund, 1977; Ramesh, 1995). Thus, the thermal processing of foods has two opposing effects which are both time and temperature dependent. The first is characterized by the desired destruction of unwanted biological reactions, and the second is the undesired reduction of quality factors (e.g., vitamins, pigments, flavors, and some essential nutrients); so it is necessary to achieve optimal processing regarding quality and safety (Ramesh, 1995).

Optimization

Optimization can be defined as the choice of a best alternative from a specified set of alternatives. Achieving optimization, therefore, requires some way of describing the potential alternatives and deciding which of the alternatives is the best (Norback, 1980; Evans, 1982). The formal description of any optimization problem has three parts:

- a set of variables which the optimization method can control and use to specify the alternatives (e.g., process temperature profile during thermal processing),
- a set of requirements (e.g., the differential equations, boundary conditions and the integral equations specifying the biological material concentration at the end of the process) which the optimization method must achieve (constraints) or satisfy, and
- a measure of performance to compare one alternative to another (the objective function; e.g., retention of nutrients) (Norback, 1980).

The objective function, which may be continuous, or in some cases discrete, is the function to be optimized (maximized or minimized). This may be obtained from either a mathematical model or by fitting an equation through the experimental points (Saguy, 1983). The optimization problems are divided into continuous and discrete types, depending on the objective function. Discrete problems usually have a finite number of variables, each of which assumes exactly one value at an optimal solution. In continuous problems, the optimal variable values are functions of some parameter, and a solution to the problem requires the specification of this function over the parameter set. Generally

the continuous optimization problems require numerical methods for a solution (Norback, 1980; Saguy, 1983). Thermal processing can be given as an example for a continuous problem. In this example, the change in retort temperature is one control variable, and the maximization of a nutrient in overall volume or at the surface can be taken as an objective function. The constraints can be given as the lower and higher limits of the retort temperature profile, as well as the coldest point lethality or temperature obtained at the end of the process (Norback, 1980).

Optimization of Thermal Processing

Optimization of thermal processes is possible because inactivation kinetics of microorganisms, enzymes and quality factors (e.g., color, textural changes, nutrient degradation) show different temperature sensitivities. Therefore, thermal processing relies on a mathematical model to ensure the safety of the products and maximization of the nutrients (Lund, 1977). The theoretical basis of this is the combination of the time-temperature distribution of the product as established by heat transfer, and the kinetics of microbial and nutrient destruction (Holdsworth, 1985). In the modeling of thermal processes, the minimum lethality at the slowest heating point is related with the criteria for sterilization. This can be represented by the following, widely used mathematical model:

$$F_0' = \int_0^t 10^{\frac{T_c(t) - T_{ref}}{z}} \cdot dt, \quad 1-1$$

where F_0 is the lethality of the slowest heating point (min), t is processing time (min), $T_c(t)$ is the temperature of the slowest heating point at time t , T_{ref} is the reference temperature, and z -value is the temperature change needed to reduce the D -value (time required to reduce the concentration by 90%) one log cycle. This equation can be used to calculate the F_0 -value of any process when the time-temperature history is calculated using heat transfer equations with the appropriate boundary conditions (Holdsworth, 1985). Other than using the F_0 value at the slowest heating point, an integrated sterility value to represent the volume average survival of microorganisms can also be used where ASM is average survival of microorganisms, V is total volume, $T(t,v)$ is the temperature of the given volume element at time t , and D_{ref} is the decimal reduction time at the reference temperature, T_{ref} (Silva et al., 1992a; 1994a, b):

$$ASM = \frac{1}{V} \cdot \int_0^V \left(10^{-\frac{1}{D_{ref}} \int_0^t \frac{T(t,p) - T_{ref}}{z} dt} \right) \cdot dV. \quad 1-2$$

Since there are infinite number of time-temperature combinations to achieve a specified lethality, the use of an objective function based on other criteria is needed for optimization. The most common objective functions used in the optimization of the thermal processing of foods are:

- minimization of cook value, and
- maximization of a quality attribute retention at the surface or throughout the volume (Silva et al., 1992a; 1994a, b).

The concept of the cook value (C) to compare the thermal processes in terms of quality degradation can be defined similarly to the F_0 value as:

$$C = \int_0^t 10^{\frac{T_c(t) - T_{ref}}{z}} dt \quad 1-3$$

The volume average cook value:

$$C_v = \frac{1}{V} \cdot \int_0^V \int_0^t 10^{\frac{T(t,v) - T_{ref}}{z}} dt \cdot dv \quad 1-4$$

where C is the cook value (min), and C_v is the volume average cook value (min) (Silva et al., 1992a; Ramesh, 1995). The most common reference temperature (T_{ref}) used to calculate the cook-value is 100 °C. For conduction-heated foods, when the objective is to maximize the retention of a nutrient at a given position, maximization of quality attribute retention and minimization of cook value are mathematically equivalent (Silva et al., 1992a, 1994a,b). However, when the objective is to optimize the overall quality retention, it is necessary to integrate over the total volume to take into account the different time-temperature profiles as a function of the position in the food. Therefore, the volume average retention has to be used in the optimization as in Eq. 1-2. The derivation of these equations was given by Hayakawa (1978), Banga et al. (1991), and Silva et al. (1992a; 1994a, b). Depending on the quality parameter, the optimization can also be regarded as maximizing the quality retention at the surface (Ohlsson, 1980a, b) or throughout the volume (Nadkarni and Hatton, 1985; Ohlsson, 1980a, b; Saguy and Karel, 1979; Teixeira et al., 1969a, b; Thijsen et al., 1978). The surface or volume average approach can also be

Table 1-1. Objective functions used to optimize the thermal processing.

References	Objective Function	Constraint	Geometry	Type of solution	Boundary Conditions
Teixeira et al. (1969a)	$(N/N_0)_{ave}$	ASM	Finite cylindrical can	Finite difference 2D, h_u	Step-function
Teixeira et al. (1975a)	$(N/N_0)_{ave}$	ASM	Finite cylindrical can	Finite difference 2D, h_u	Step, sinusoidal function, ramps combination, single square wave, sequence of steps
Thijssen et al. (1978)	$(N/N_0)_{ave}$	ASM	Finite cylinder, sphere, rectangular body	Analytical 1D, 2D, h_u and h_{finite}	Step-function
Saguy and Karel (1979)	$(N/N_0)_{ave}$	ASM	Finite cylindrical can	Finite difference 2D, h_u	Variable process temperature
Ohlsson (1980a)	C_{ave} and C_{surf}	F_c	Infinite slab	Finite difference 1D, h_u	Step function with linear come-up-time
Ohlsson (1980b)	C_{ave}	F_c	Finite cylinder	Finite difference 2D, h_u	Step function with linear come-up-time
Thijssen and Kochen (1980)	$(N/N_0)_{ave}$	ASM	Finite cylinder, sphere, rectangular body	Finite difference 2D, h_u and h_{finite}	Variable process temperature
Nadkarni and Hatton (1985)	$(N/N_0)_{ave}$	ASM	Finite cylindrical can	Numerical solution 2D, h_u	Variable process temperature
Banga et al. (1991)	$(N/N_0)_{ave}$ and $(N/N_0)_{surf}$	ASM and F_c	Finite cylindrical can	Finite difference 2D, h_u	Constant and variable process temperature
Silva et al. (1992b)	C_{surf}	F_c	Infinite cylinder, sphere, infinite slab	Finite difference 2D, h_{finite}	Constant process temperature
Terajima and Nonaka (1996)	C_{ave}	F_c	Retortable pouches	Numerical solution 1D	Variable process temperature

$(N/N_0)_{ave}$, volume average retention of quality; $(N/N_0)_{surf}$, surface retention of quality; ASM, target volume average survival of microorganisms; C_{ave} , volume average cook value; C_{surf} , surface cook value; F_c , target lethality in the coldest spot.

applied using the cook value. Although some other objective functions such as minimization of energy consumption, economic costs and formation of toxic compounds

can also be considered, their use is limited due to the lack of available data. Table 1 describes the most common objective functions used (Lund, 1982; Silva et al., 1994a, b).

The optimization of thermal processing is a continuous optimization problem; retort temperature is the control variable, and the result of the time-temperature distribution as maximization of a quality retention is the objective function. The set of requirements (constraints) includes the differential equations and the boundary conditions used in the solution of time-temperature profiles and the integral equation specifying undesirable biological changes based on given geometries. Norback (1980) used integral expression for the quality attribute as measure of the performance. He also pointed out that the maximization of quality retention can only be done for one nutrient (or quality attribute) since the optimization can be done with respect to one objective function at a time. However, Noronha et al. (1996b) stated that it can be possible to reformulate the objective function in order to optimize more than one quality factor. The most straight forward approach in these kinds of problems is to use the sum of the retentions of the quality attributes with weight factors (Miettinen, 1999).

When the optimization problem is of a continuous type, it requires numerical methods for the solution. This is done by discretizing the container volume and the time interval, changing the differential equations into difference equations and the integrals into sums to yield approximations to the problem. The most common numerical method used in heat transfer is the finite difference method. This is simple to formulate, and can be readily extended to two- or three- dimensional problems (Ozisik, 1993). The method has been used by many researchers in the thermal processing area to find the transient

temperature distribution in foods (Teixeira et al., 1969a; 1969b; 1975a; 1975b; Saguy and Karel, 1979; Ohlsson, 1980 a,b; Chau and Snyder, 1988; Chau and Gaffney, 1990; Noronha et al., 1993; 1996a,b; Erdoğan, 1996; Erdoğan et al., 1998a and b; Lebowitz and Bhowmik, 1989; Tucker and Clark, 1990; Silva et al., 1992a,b; 1994 a,b,c; Hendrickx et al., 1993; Fastag et al., 1996). In the kinetic calculations, the thermal inactivation (degradation) of microorganisms and quality factors were always assumed to follow a first order reaction. These studies have generally assumed the foods in certain geometries such as spherical, cylindrical or slab shapes. The slab or cylindrical shapes were also considered in finite or infinite cases. The reviewed works also focused on the packaged foods in retortable pouches or cylindrical cans. In all studies, the authors assumed that their systems consisted of one type of food product focusing on a quality factor attribute. The technological advances in packaging and retort processing areas have led to the use of retortable trays as reported by Schulz (1978). The trays might have different food systems (e.g., meat, potato puree, peas, and carrots) in different sections of one tray.

In an optimization study of thermal processing, the objective is to find the optimal temperature profile, which can be defined as the processing temperature resulting in a minimum surface cook value or maximum quality attribute retention while also achieving the desired degree of sterility. The optimal temperature profile can be calculated as a function of the product heating rate, surface heat transfer coefficient, initial temperature of the product, heating medium come-up-time, z-value for the quality factor and target F_0 value for a given objective function and a shape of infinite cylinder, infinite slab, or sphere (Silva et al., 1992b).

Teixeira et al. (1969a) published the first paper on the optimization of nutrient retention in the thermal processing of conduction heated foods using a computer program written in FORTRAN. This program was developed using finite difference methods to solve the two-dimensional heat conduction equation for determining the time-temperature distribution within a cylindrical container. This was then used to estimate the effect of the thermal history on microbial destruction and nutrient retention. Thiamine was chosen to find the retention in the system due to the availability of its kinetics data. It was concluded that it was possible to find a thermal process with constant retort temperature which optimizes the nutrient retention while maintaining the required lethality. Teixeira et al. (1969b) also presented numerically calculated distributions of surviving microorganisms in cylindrical containers for various can sizes and processing conditions.

Teixeira et al. (1975a, b) extended their previous model to compare the effects of variable retort temperature profiles (step functions, ramp functions and sinusoidal functions) and different container dimensions. In this procedure, the control variable (retort temperature) was forced to a particular functional form, and the mass average nutrient retention as an objective function was determined. The process was repeated with a new retort temperature profile, and the maximum mass average retention was found. In this study, spores of *Bacillus stearothermophilus* were taken as the food spoilage microorganism with a $D_{121.1}$ -value of 4 min and a z-value of 10 °C. The retention of thiamine was used as an objective function with a reference $D_{121.1}$ -value of 178.6 min and z-value of 25.6 °C. They applied trial-and-error search techniques to determine the best retort temperature profile for improving the thiamine retention in thermally processed

foods. It was concluded that variable retort temperature profiles do not appear to show any significant advantage with respect to increasing thiamine retention in the processed food. They did show, however, that variations in the container geometry can be effective in achieving significant improvement.

Saguy and Karel (1979) used the Pontryagin's maximum principle theory to optimize the thiamin retention during sterilization of a conduction-heated canned food, and investigated this optimization technique with the available kinetic data. Details of this method were explained by Saguy and Karel (1979), Loncin and Merson (1979), and Saguy (1983). They analyzed the thermal processing with three can sizes and *Bacillus starothermophilus* as the spoilage microorganism. The D- and z-values reported by Teixeira et al. (1975a) were used in the calculations. The optimal variable retort temperature profile determined by this procedure for the heating period of the process improved thiamine retention by more than 2%. They claimed that a single solution for the temperature profile existed, without giving any data to support it. Their results showed that complicated time temperature profiles would be required if the nutrient retention is to be optimized.

Ohlsson (1980a, b) calculated the time-temperature distribution in solids in flat and cylindrical containers and used this profile in an optimization study. The objective function was the cook-value for sensory quality with the constraint of volume average survival of target microorganisms. He concluded that the cook-value was a valuable parameter for optimization of the quality retention in sterilization, and evaluated the optimal constant sterilization temperatures to obtain the minimal cook-values.

Banga et al. (1991) developed an optimization algorithm based on non-linear programming. The algorithm applied for the solution of fixed processing time conduction heated thermal processing problems using the objective functions of the maximum retention of a quality factor (thiamine) in overall volume and at the surface using constant and variable retort temperature profiles. This algorithm was also applied to find the minimum processing time for the given objective function. The variable retort temperature profiles were mathematically discretized taking N points for a given process time in linear ramps with variable slopes, origins and given lower and upper bounds. They achieved a significant increase of retention at the surface with a variable retort temperature profile compared to the constant temperature profile (up to 20% compared to the 4-6% increase in volume average retention). The variable retort temperature profile process showed advantages over the constant temperature processes in the case of process time minimization using the retention of quality factor at the surface as a constraint. However, the information about the effects of number of points to discretize the given process time, and more importantly the reproducibility of the method and uniqueness of the solution were not discussed.

Silva et al. (1992a) evaluated the commonly used objective functions of volume average retention and volume average cook value to optimize the overall quality and nutrient retention of heat preserved foods by testing the case studies from the literature for these functions. They calculated the temperature distribution within the solid using an explicit finite difference numerical method with non-capacitance surface nodes. Thermal inactivation kinetics of the microorganisms for the calculation of target F_0 value and

quality factors were described by first order reaction kinetics. For high D_{ref} values, e.g., for vitamins, the objective functions were found to be giving the same results. For low D_{ref} values, such as texture and color, the volume average cook value was found to result in the underestimation of the optimal processing temperature compared to the objective function of volume average retention. Their optimization method was Davis-Swan-Campey method and given in Silva et al (1992b).

Silva et al. (1992b) calculated the optimal constant sterilization temperatures as a function of product heating rate, surface heat transfer coefficient, initial product temperature, heating medium come-up-time, z-value for the quality factor and target F_0 value, considering one-dimensional shapes (infinite slab, sphere and infinite cylinder). An explicit finite difference solution with non-capacitance surface nodes was used to find the time-temperature distributions in the geometries. First order reaction kinetics were assumed for the inactivation (degradation) of microorganisms and quality factors. In their optimization approach, target F_0 value was considered as the optimization constraint, and the objective function was the cook value (Eq. 1-3). The optimization routine used Davis, Swan, Campey method (Saguy, 1983). This method starts with an initial point (e.g., initial guess), then a known step size is taken along the search direction. At this point the objective function is evaluated. The step size is doubled for the next function evaluation until a function value exceeds the previous value. The procedure yields four points equally spaced along the search axis for which the function values have already been calculated. The point further from the one corresponding to the smallest function value is discarded. A quadratic equation is fitted through the three retained best points. The next step

focuses on finding the minimum of the fitted equation. Saguy (1983) gives a detailed description of this method. Using this method, Silva et al. (1992b) developed regression equations relating optimal temperatures with all relevant variables and concluded that the initial temperature and heating medium come-up-time had little influence on the optimal temperatures compared to the other variables: product heating rate, z-value of the quality factor and the coldest point lethality.

Noronha et al. (1993) calculated the optimal variable retort temperature profiles for the sterilization of conduction heated foods. The variable profiles were described by a vector of temperatures equally spaced in time. Intermediate temperatures were calculated by linear interpolation. The thermal destruction of microorganisms as well as nutrients was described by a first order reaction kinetics, and the calculation of the transient temperature distribution in the food was performed using an explicit finite difference model with an infinite heat transfer coefficient. In the optimization of variable retort temperature profiles, two objectives were considered: optimization of the quality retention for a fixed process time, and optimization of the process time with a constraint in the quality retention. The optimization of the quality retention was defined as the maximization of the surface quality subjected to the constraints of microbiological quality and final temperature at the center. When the optimization (minimization) of the process time with a constraint on the surface quality was the objective, the problem was to find the temperature profile that minimized the time while achieving the constraints of microbiological sterility, final temperature at the center, and a minimum acceptable quality surface retention value. They used a quasi-Newton multi variable optimization method to calculate the optimum variable retort

temperature profiles for a fixed process time. This method approximates and updates the inverse of the Hessian matrix without the need for matrix inversion (Saguy, 1983). An increase up to 20% in quality retention was predicted for variable profiles compared to the constant profiles when the objective function was the maximization of surface quality. When the minimization of the total process time was considered, the use of variable profiles allowed reduction up to 45% in the total process time while still providing the same surface quality as optimal constant temperature profiles. Although a broad explanation for this method is given by Avriel (1976) and Saguy (1993), the uniqueness and reproducibility of the method were not addressed.

Hendrickx et al. (1993) developed a computer program to model the heat sterilization of one-dimensional conduction heated foods with negligible surface resistance to heat transfer with the application of first order kinetics of thermal inactivation of microorganisms and enzymes and thermal degradation of quality attributes. The constant optimal sterilization temperature was defined as the processing temperature resulting in a minimum surface cook value in the food product after achieving the desired degree of sterility, and was calculated as a function of the food properties (thermal diffusivity and z -value of the quality factor), processing conditions (dimensions and geometry of the container, initial temperature of the product, and heating medium come-up-time) and processing criteria of target F_0 value.

Silva et al. (1993) reviewed the mathematical methods available to optimize heat sterilization of prepackaged foods and evaluated the different optimization methods (manual graphical methods, Pontryagin's maximum principle, Davis-Swann-Campey

method), objective functions (minimizing quality degradation in terms of surface and volume average, energy consumption or economic costs), constraints (coldest point or volume integrated lethality), and decision variables (constant or variable process temperature profiles). Silva et al. (1994a) developed an experimental procedure to validate the optimal process temperatures giving the maximum retention at the surface of conduction heated foods for a specified level of target lethality constraint for the surface retention of an acid-catalyzed sucrose hydrolysis reaction. They found out that the optimal temperatures calculated using numerical optimization models or regression equations were in the range of experimentally determined conditions. Silva et al. (1994c) developed a mathematical method to optimize the sterilization conditions for conduction heated foods packaged in cylindrical and rectangular containers and retortable pouches, using a finite difference method with non-capacitance surface nodes to describe the heat transfer into the food. They studied the applicability of a generalized formula to predict optimal temperatures for maximizing surface or volume average quality retention. In both cases a target sterility value at the slowest heating point was used as a restriction (Eq. 1-1). They showed that the generalized formula of optimal temperatures were applicable to the above geometries. The optimization routine was based on a quadratic interpolation search of Davies-Swann-Campey method (Saguy, 1983).

Fastag et al. (1996) simulated lethality and thiamine retention using a finite difference model based on Teixeira et al. (1969b) for isothermal, sinusoidal, step and ramp retort temperature profiles. Pea puree was chosen for measurement of nutrient retention because of its high thiamine content and available thiamine destruction rate. They found

out that differences in thiamine retention due to the different heating regimes were significant only for large lethality values and smaller cans. Terajima and Nonaka (1996) used the optimal control theory to determine the optimum constant retort temperature profile for quality retention at a given level of sterilizing value in retortable pouches. The cook value (C-value) was employed to describe the quality changes. Optimization was considered to be constrained optimal control problem with unspecified time, and it was solved numerically using the conjugate gradient minimization method. They determined the optimum constant retort temperature profiles for the volume average and surface cook values for browning reactions.

Noronha et al. (1996a) reported that the variable retort temperature profiles allow a small increase in quality retention when compared to the constant profiles, and when the minimization of the process time was the objective function, the variable profiles result in significant reduction in process times. They presented an empirical formula for the variable processes to generalize their use and to allow an accurate description. The maximization of the surface retention was the objective function with the constraints of the coldest point lethality and the temperature reached at the end of the process. This problem was solved using a quasi-Newton multi-variable optimization routine, and the following equation format was suggested:

$$PT(t) = a_0 + a_1 \cdot t - a_3 \cdot e^{a_2 \cdot t}, \quad 1-5$$

where $PT(t)$ is the process temperature profile, t is the time and a_0 , a_1 , a_2 , and a_3 are the constants.

Complex Method

Mishkin et al. (1982 and 1984) used the methods of Pontryagin's maximum principle and Box's Complex Method to improve ascorbic acid retention in a model system of variable air dryer temperature profiles. These studies proved that the Complex Method is a very reliable and simple approach for solving optimization problems with explicit and implicit constraints. The Complex Method for constrained optimization was first presented by Box (1965), and Umeda et al. (1972) presented the use of the method for solving variational problems with state-variable inequality constraints using a tubular reactor design as an example, and demonstrated its applicability. In the literature, the paper by Kazmierczak (1996) was found to be the best in describing the theory and algorithm of the Complex Method. He gave an example of a pest management problem to illustrate the algorithm. The Complex Method was not commonly used in the optimization of thermal processing problems even though it is an efficient simulation optimization approach, and mathematically very simple compared to the Pontryagin's maximum principle. See Appendix A for detailed information about the Complex Method.

There are not many studies on the simultaneous optimization of thermal processing with different food systems, and these studies use an infinite h-value and the same D-values for the quality attributes (Noronha et al., 1996b) to simplify the models. The optimization of this process regarding quality attribute retention requires the use of different objective functions for each shape. Noronha et al. (1996b) formulated the surface quality optimization during sterilization of packed foods with the constraints of the coldest

point lethality and final temperature using constant and variable retort temperature profiles. The constant retort temperature profiles were determined using the univariate search procedure of Davies-Swan-Campey as described by Saguy (1983). The variable retort temperature profiles were defined as a function of time using the empirical Eq. 1-5. The Complex Method was used for the determination of parameters a_0 to a_3 . The Complex Method was chosen since it allowed the incorporation of the constraints on microbial sterility and final temperature at the coldest point as implicit constraints. This also implied that the initial starting point for the optimization was a feasible one, complying with all the constraints. They also stated that it was possible to reformulate the objective function in order to optimize more than one quality factor using the sum of the retentions of the quality attributes with weight factors as suggested by Miettinen (1999). In their study, it was shown that the simultaneous optimization of more than one quality factor is possible applying their method to the different food systems (System I: chili con carne, white rice, and peach slices in syrup; System II: meat, potatoes, and spinach in a pouch; System III: green beans, peas, corn, and carrots). They used a numerical solution method developed by Noronha et al. (1995) for the calculation of the transient temperature history at the slowest heating point for non-conductive heating systems. It was shown that the use of variable retort temperature profiles can be advantageous in reducing the quality destruction and processing time. As seen in the literature, the simultaneous optimization of one or more quality functions is possible. However, there is a lack of information about how a well-defined or explained optimization method can be modified or applied to this thermal processing problem, and how unique and reproducible it can be.

Objectives

The objectives of this study were to use the heat transfer simulation models for various shapes (finite cylinder and sphere) as tools, to accomplish the following:

- development of suitable objective functions and constraints incorporating temperature-dependent safety and quality attribute limits (e.g., the minimum lethality shall be no less than 3 min at 121.1 ° C, the center temperature at the end of the process shall be lower than the initial temperature, the retention of carotenes shall be maximum, or the color degradation shall be minimum),
- modification of a suitable method for optimizing a given objective function (Complex Method),

The independent variables will be:

Size, shape, and contents of the containers (or the geometries),
Heat transfer characteristics as functions of temperature,
Boundary conditions at the surface,

The dependent variables will be:

Lethality in each container, based on appropriate target organism,
Loss of quality, and/or nutrients,
Final center temperature of the geometry,

The control variable for the optimization will be:

Variable process temperature profile.

The tasks to fulfill these objectives are:

- To modify the previously developed mathematical models of heat transfer to predict the internal temperature of different shaped foods to consider the changes in thermophysical properties during the process time in response to variable retort temperature profiles,
- To calculate the coldest point lethality and nutrient retention based on supplied kinetics for different shapes,
- To use only one shape to develop the methodology to maximize a certain nutrient/quality of known kinetics, using a variable retort temperature with Complex Method.
- To extend and modify the developed objective function to add another shape. This required simultaneous satisfaction of more than one restriction/requirement using the Complex Method.

The optimization part was not experimentally validated, since it required precise information for the degradation kinetics of different quality attributes for each food that were not available.

CHAPTER 2 MATERIALS AND METHODS

The Complex Method (Appendix A) developed by Box (1965), and explained in detail by Kazmierczak (1996) was used to find the variable process temperature profiles during thermal processing for single geometry conduction heated systems with suitable objective functions consisted of maximization of a nutrient in overall volume, and at the surface. Constraints included incorporating temperature dependant safety (the lethality at the slowest heating point) and a threshold temperature that the center temperature had to reach at the end of the process. The extension and modification of the objective function for additional shape(s) were also accomplished using the Complex Method.

In the development of objective function and constraints, the independent variables were:

- Size and shape of the geometries (or the containers),
- Heat transfer characteristics as functions of temperature (constant or temperature dependent thermophysical properties),
- Boundary conditions at the surface (surface convection),
- Initial and final temperatures.

The dependent variables were:

- Lethality at the slowest heating point of each container, based on an appropriate target microorganism,
- Center temperature at the end of the process,
- Loss of quality, and/or nutrients in overall volume or at the surface, with different kinetics of inactivation,

The decision variable for the dependent variables was the variable process temperature profile.

For the evaluation of transient temperature distributions for variable process temperature profiles for one and two dimensional geometries, the explicit finite difference models were implemented using non-capacitance surface nodes (NCSN) and energy balance equations with the minimum time step Δt to prevent any instabilities (Chau and Gaffney, 1990; Welt et al., 1997, Erdoğdu 1996; Erdoğdu et al. 1998a,b). These models were modified for the evaluation of the objective functions, and explicit and implicit constraints as follows:

Objective Functions

Volume average retention (VACN) and surface retention (SCN) of a nutrient (e.g., thiamine) was evaluated and used as objective function in the optimization procedure. The following equations show these functions, respectively:

$$VACN = \frac{1}{V} \int_0^V \left(10^{\frac{-1}{D_{ref}} \int_0^t 10^{\frac{T(t,s)-T_{ref}}{z}} dt} \right) dV, \quad 2-1$$

$$SCN = 10^{\frac{-1}{D_{ref}} \int_0^t 10^{\frac{T(t,s)-T_{ref}}{z}} dt}. \quad 2-2$$

For the evaluation of these functions over the processing time, the following explicit method was used. The general first order rate equation (eq. 2-3) for any order rate process was used to describe the thermal inactivation kinetics of microorganisms and nutrients:

$$-\frac{dC}{dt} = k \cdot C^n, \quad 2-3$$

where C is the concentration, k is $2.303/D$ (D: the decimal reduction time), n is the degree of the reaction. For a first order reaction (n=1), after integration over Δt :

$$C^{t+\Delta t} = C^t \exp(-k \cdot \Delta t) \quad 2-4$$

Eqs. 2-3 and 2-4 were applied to each volume element of the specified geometry throughout the process, and eqs. 2-1 and 2-2 were evaluated by integration. As an integration method, the trapezoidal rule was used. The kinetics of thiamine in a pork puree for the evaluation of the objective functions were (Banga et al., 1991) $D_{121.1^\circ\text{C}} = 178.6 \text{ min}$ ($=10716 \text{ s}$); $z = 25.56^\circ\text{C}$.

The following is the step-by-step description of the modified algorithm of the Complex Method (see Appendix A) for the optimization of single geometry systems with

the given independent variables, and evaluated dependant variables with respect to the variable process temperature profile.

Constraints

Explicit Constraints

A process temperature (PT) range of 5-150°C was used as an explicit constraint. Another explicit constraint was that the process temperature had to reach 5°C at the end of the process.

$$\begin{aligned} PT_L &= 5\text{ }^{\circ}\text{C} \\ PT_H &= 150\text{ }^{\circ}\text{C} \end{aligned} \quad 2-5$$

$$PT|_{t=t_{\max}} = PT_L \quad 2-6$$

The range for the explicit constraints for thermal processing optimization studies were not explained well in the literature. In commercial practice, retort temperature rarely exceeds 125 °C for heating and ambient temperature water ($\approx 20\text{ }^{\circ}\text{C}$) is used for cooling. In the pre-studies, the optimum constant heating temperature of 130 °C was calculated for some small sizes of sphere ($r=15\text{ mm}$) and finite cylinder ($r=15\text{ mm}$, $L=15\text{ mm}$) geometries. Therefore, a somewhat higher temperature (150 °C) was chosen for the higher limit of explicit constraints even though that is beyond normal process range. For the lower limit, a value below the ambient temperature (5 °C) was used to quickly quench the

quality factor degradation even though it is normally not economical to use chilled water for the cooling part of the thermal processing. However, the modified method could be easily changed to apply the different range of explicit constraints whenever desired.

Implicit Constraints

Lethality at the slowest heating point of the container, based on an appropriate target microorganism, and that a threshold below which the center temperature must reach at the end of the process were used as the constraints in the algorithm. The lethality at the center was evaluated as:

$$F_0 = \int_0^t 10^{\frac{T_c(t) - T_{ref}}{z}} dt \quad 2-7$$

$$T_c(t_{max}) \leq T_{threshold} \quad 2-8$$

Bacillus stearothermophilus was chosen as the target organism, and the implicit constraint of eq. 2-7 was to be greater than 8 min, resulting in a 2 log cycle reduction of the target organism. The kinetics of this organism was available in the literature (Teixeira et al., 1975a; Banga et al., 1991), and $D_{121.1}^{\circ C} = 8 \text{ min}$ ($=240 \text{ s}$); $z = 10^{\circ C}$. The threshold temperature for the center temperature to reach at the end of the process was taken as the initial uniform temperature of the product ($20^{\circ C}$).

Decision Variable

The decision variable for the optimization was process temperature profile discretized at equidistant time steps throughout the process. These points as a group must satisfy the explicit constraints of Eqs. 2-5 and 2-6 at any time. Using the evaluated objective functions, explicit and implicit constraints with respect to the decision variable, the algorithm for Complex Method (Appendix A) for the optimization of single and double geometry systems were applied as explained below.

Complex Method Algorithm For A Single Geometry System

The developed algorithm will be explained using an example. To accomplish this, the following objective function, and explicit and implicit constraints will be used:

Objective function: Maximize VACN (Eq. 2-1); Explicit constraints: Eqs. 2-5 and 2-6;

Implicit constraints: Eq. 2-7 ($F_0 > 8$ min) and Eq. 2-8 ($T_c < 20$ °C at $t = t_{\max}$);

Thermophysical properties of the geometry: Sphere ($r = 30$ mm, $k = 0.566$ W/m-K, $c_p = 3660$ J/kg-K, $\rho = 1050$ kg/m³, $h_{\text{heating medium}} = 2000$ W/m²-K, $h_{\text{cooling medium}} = 500$ W/m²-K).

Step 1

The algorithm started by establishing the first initial simplex. In order to do this, the discretization of the variable process temperature profile taking N number of points throughout the given process time was accomplished. The process temperatures at the

discretized time points were evaluated using pseudo-random numbers and low and high limits of the process temperature (eqs. 2-5, 2-6, and 2-9) as follows:

$$PT_i = PT_L + r_i \cdot (PT_H - PT_L) \quad i = 1, \dots, N-1 \quad 2-9$$

$$PT_N|_{t=t_{\max}} = 5 \text{ } ^\circ\text{C} \quad 2-10$$

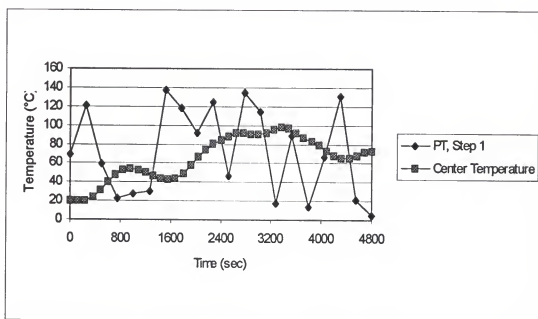


Figure 2-1. The process and center temperature profiles after step 1.

Figure 2-1 shows the obtained process and center temperature profile for a sphere ($r=30$ mm; $N=20$) for a given processing time of 80 min (4800 s).

Step 2

Once the process temperature profile was obtained, the algorithm found the time at which to change the effective heat transfer coefficient value from a heating medium value to a cooling medium value. Starting from the point N-1, the process temperature difference ($T_{N-2}-T_{N-1}$) was checked. If it was higher than 10% of the higher limit (15 C°), and the discretized temperature value at the step (N-2) was higher than 50% of the higher limit (75 C°), that point (N-2) was taken as the h-value break point, and the developed heat transfer model simulated the results for the transient temperature distribution, objective function, and the implicit constraints using the appropriate h-values. These thresholds were chosen based on the judgment of the author and developed by analyzing the errors encountered during the development of the method and running the program. For the given example (Figure 2-1), the h-value break point was N-2, and the calculated F_0 value at the center of the sphere was equal to 1.96 sec. As seen, the first implicit constraint was violated, and the algorithm corrected it as explained in step 3.

Step 3

Since the obtained lethality was not sufficient, and was violating the first implicit constraint of the coldest point lethality, the algorithm moved all the temperatures but the last one half way towards the higher limit (Eq. 2-11):

$$PT_i = \frac{1}{2} \cdot (PT_i + PT_H) \quad 2-11$$

Step 2 was repeated to check the implicit lethality constraint, and the process was repeated until the achieved lethality was higher than the specified lethality ($F_0=8$ min). In the second trial, the lethality value was found to be 18.66 min (Figure 2-2), satisfying this constraint.

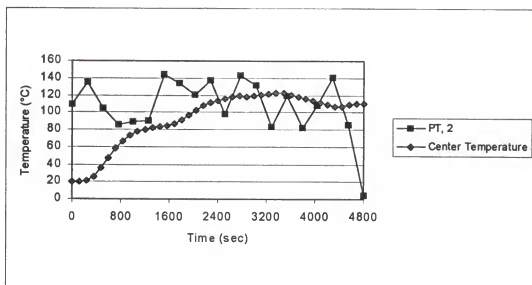


Figure 2-2. The process and center temperature profiles after step 2.

Step 4

Once the violation of the first implicit constraint was corrected, the next step was to satisfy the second implicit constraint ($T_c < 20^\circ\text{C}$ at $t=t_{\max}$). The step 3 resulted in a center temperature of 110.95°C . Therefore, the objective of step 4 was to lower T_c at t_{\max} to the acceptable range. In order to accomplish this, the process temperatures, starting from the point N-1, were moved half way towards the lower limit one by one. The criteria to jump to the next point (e.g. from N-1 to N-2) was: the difference between $PT_{N-1}-PT_L$ is

to be less than $1\text{ }^{\circ}\text{C}$ to prohibit big jumps during cooling. At each move, the step 2 and simulation of the process was accomplished. The stopping criteria to end step 4 was so chosen that the center temperature being less than 75% of the threshold center temperature ($=15\text{ }^{\circ}\text{C}$). Since the decreasing of the temperatures towards the end of the process might cause the violation of the first implicit constraint, the temperatures were moved up using the Eq. 2-11 starting from the point where step 4 ended until the first implicit constraint was again achieved. Of course, that would again affect the center temperature. Therefore, a safe limit of 25% of the threshold center temperature ($=5\text{ }^{\circ}\text{C}$) was used. This safe limit was chosen based on the errors and infinite loops encountered during running the program. See figures 2-3 (violating the first implicit constraint while achieving the second; $F_0=3.53\text{ min}$, $T_c=14.99$) and 2-4 (achieving both of the constraints; $F_0=8.00\text{ min}$, $T_c=16.26\text{ }^{\circ}\text{C}$) for the demonstration of step 4. If the adjustment of temperature values reached all the way back to the first point ($N=1$ and $t=0$), and still not satisfied the implicit constraints, the algorithm started over by going back to step 1 and finding a new temperature profile. Even though this is rarely encountered, a small check was added into the program to eliminate infinite loops. This problem might also be caused if the total processing time was not enough to satisfy both implicit constraints. The solution at this point might be to increase the total processing time depending on the user's discretion. The steps 1 to 4 were repeated for $N+1$ times, finding an initial process temperature profile matrix of $(N+1, N)$; with accompanying evaluation of objective functions and implicit constraints. This constituted the initial complex.

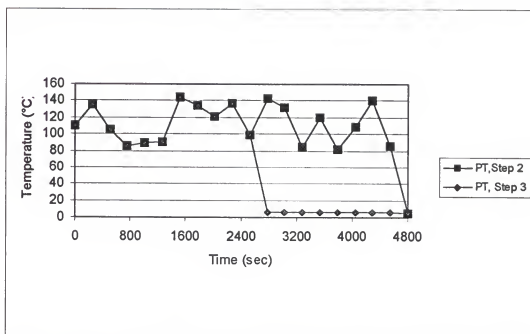


Figure 2-3. The process temperature profiles after steps 2 and 3 (not-achieving the first implicit constraint).

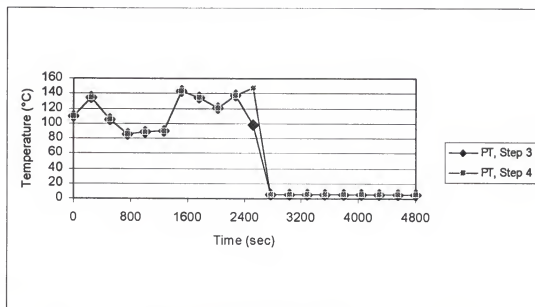


Figure 2-4. The process temperature profiles after steps 3 and 4 (achieving both of the implicit constraints).

Step 5

Up to step 5, the initial vertices for the Complex Method were found, and the objective functions were evaluated at each vertex with the implicit constraints. Each process temperature profile is a vertex of the initial complex. Then, ordering was conducted by ranking the objective function values from the highest to the lowest. Thus the vertices (PT_{ij} , $i=1, \dots, N+1$; $j=1, \dots, N$), $\langle PT_{1j}, PT_{2j}, \dots, PT_{N+1j} \rangle$ show PT_{1j} the best vertex and PT_{N+1j} the worst vertex. The centroid, hyperspace of the non-worst vertices, was evaluated:

$$\overline{PT_j} = \frac{1}{N+1} \sum_{i=1}^N PT_{ij} \quad ; j = 1, \dots, N. \quad 2-12$$

Step 6

The vertex of the worst function value, v_w was reflected by $\alpha=1.4$ times:

$$(PT_{N+1,j})_r = (1 + \alpha) \cdot \overline{PT_j} - \alpha \cdot PT_{N+1,j} \quad j = 1, \dots, N, \quad 2-13$$

and the accompanying implicit constraints were evaluated, and checked for violations. If a violation occurred (e.g. $F_0 < 8$ min), it was handled by using a retraction process where the retracted vertex was given by:

$$(PT_{N+1,j})_e = \beta \cdot PT_{N+1,j} + (1 - \beta) \cdot \overline{PT_j} \quad j = 1, \dots, N, \quad 2-14$$

where $0 < \beta < 1$ is the retraction coefficient. The retraction process was accomplished by systematically decreasing the β (0.9, 0.8, ..., 0.1) until the violated constraint was corrected.

When the retraction process did not accomplish this objective ($\beta=0$), the reflected point was moved towards the best vertex ($PT_{1,j}$) by:

$$PT_{N+1,j} = \frac{1}{2}(PT_{1,j} + PT_{N+1,j}), \quad 2-15$$

again until the violation was corrected.

The retraction method was also applied when the reflected value was inferior to the next-to-worst vertex ($PT_{N,j}$). This meant that there was no advantage of replacing the worst vertex with the reflected one. When the retracted vertex continued to be the inferior, a shrinkage process was applied by moving all the vertices towards the best vertex (Eq. 2-16), checking for violation of the implicit constraints for each move. The shrinkage process resulted in a completely new system, and the method continued with re-ordering and original reflection until the stopping criteria was achieved (Step 5):

$$PT_{i,j} = \frac{1}{2}(PT_{1,j} + PT_{N,j}) \quad i = 2, \dots, N+1; j = 1, \dots, N. \quad 2-16$$

It was also possible to get a reflected value superior than the best vertex ($RT_{1,j}$). In this case, the search continued in the reflection direction by calculating an expanded vertex:

$$(PT_{N+1,j})_e = \gamma \cdot (PT_{N+1,j})_r + (1 - \gamma) \cdot \overline{PT}_j \quad j = 1, \dots, N, \quad 2-17$$

where $\gamma=2$ was the expansion coefficient. If the expanded vertex were found to be superior than the reflected vertex, $RT_{N+1,j}$ was replaced by the expanded vertex. If not,

$RT_{N+1,j}$ was replaced by the reflected vertex, and a new reflected vertex was evaluated after re-ordering and the stopping criteria was checked.

Step 7

Stopping criteria for the algorithm were:

$$\begin{aligned} VACN_1 - VACN_{N+1} &\leq 0.01 \quad or \\ SCN_1 - SCN_{N+1} &\leq 0.01 \end{aligned} \quad 2-18$$

where subscripts “₁” and “_{N+1}” show the results of the best and worst vertices, respectively. Since the small changes at the discretization points of the variable process temperature profile might result in big jumps in the implicit constraints, especially towards the end of the heating part, a very small magnitude for the difference for the objective function (0.01) between the results of the best and worst profile was chosen. With this small magnitude, the differences between the temperature profiles were also very small as well as the implicit constraints and objective functions at the end of the simulation. This made sure that the hyperspace of the variable process temperature profiles were collapsed into a certain point, and it was, from then on, not possible to change the temperatures using reflection, expansion, or retraction. Appendix A shows an example of these steps and applied algorithm for a sphere of $r=15$ mm with the above given thermophysical properties.

Algorithm Testing and Application Systems

The Complex Method algorithm was applied to the following systems simulating homogeneous, isotropic conduction heating for different processing times:

- Sphere ($r=15$ and 30 mm),
- Finite cylinder ($r=15$ mm $2l=15$ mm; $r=30$ mm $2l=60$ mm).

The thermal properties were taken as $k=0.566$ W/m-K, $c_p=3660$ J/kg-K, $\rho=1050$ kg/m³, $h_{\text{heating medium}}=2000$ W/m²-K, $h_{\text{cooling medium}}=500$ W/m²-K since they represent typical food material properties, and typical thermal processing heat transfer coefficient values. The heat transfer coefficient values were used as same for all sizes of the geometries. The first finite cylinder represents a small body or food size while the second one simulated a small can size for processing. The sphere sizes were chosen to be comparable with the finite cylinders. Process temperature profiles for individual shapes at different processing conditions, together with nutrient retentions were calculated. Effects of the number of time steps, and reproducibility data were shown. The results obtained from the use of both objective functions (volume average concentration and surface retention) were compared for single geometries.

All calculations were performed using a computer program written in Visual Basic V. 6.0 (Microsoft, 1994). This Windows-based software calculated the optimum variable temperature profiles using the geometry options, objective functions, and constraints chosen by the user. The algorithm structure of the developed program is given in Fig. 2-5.

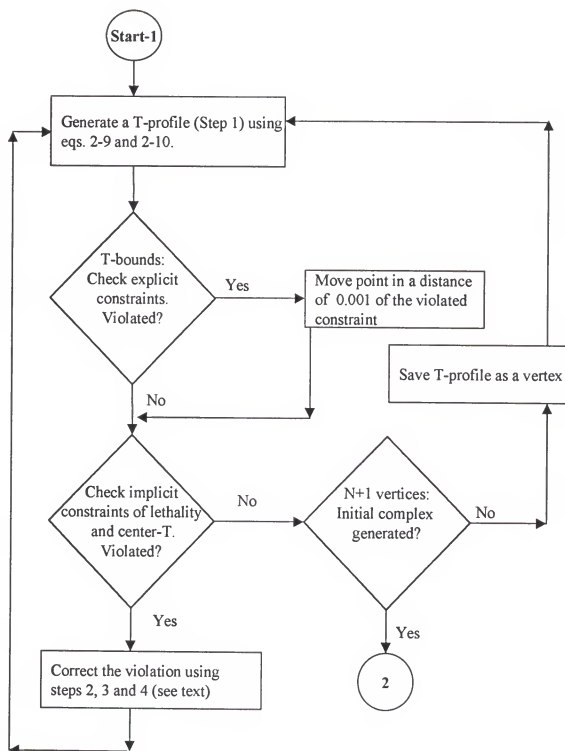


Figure 2-5. The algorithm of the developed program for a single geometry system.

Figure 2.5. Continued.

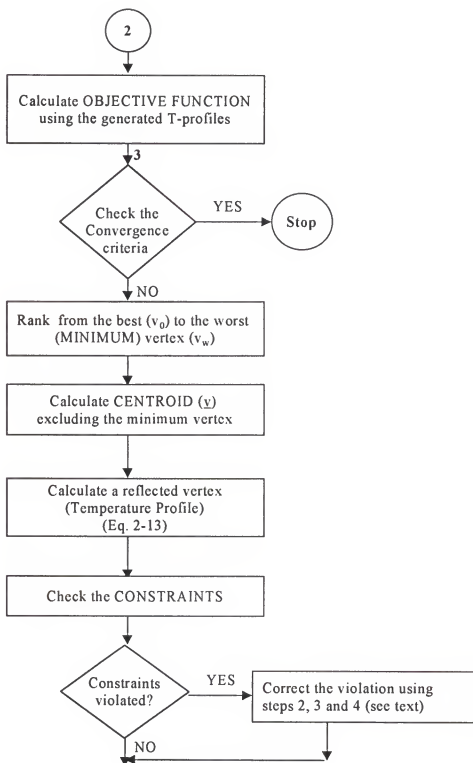


Figure 2.5. Continued.

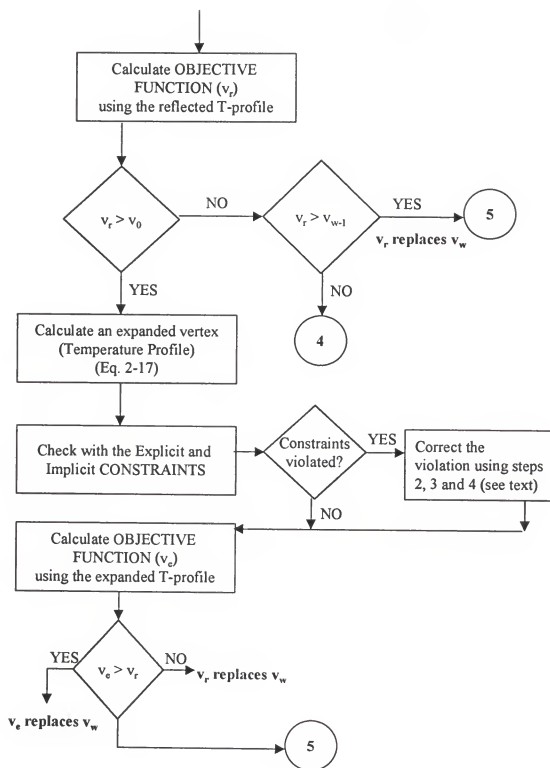


Figure 2.5. Continued.

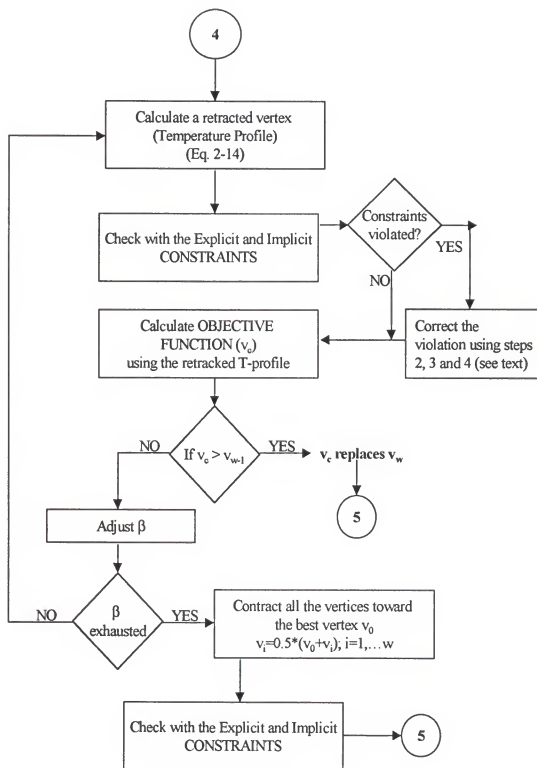
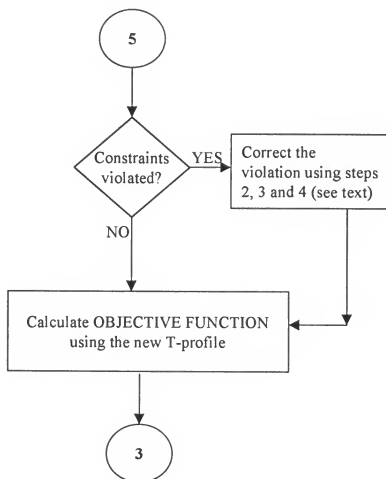


Figure 2.5. Continued.



Algorithm of Complex Method For Double Geometry System

Optimization using the objective functions of VACN and SCN for a double geometry system results in a multi-objective optimization problem, and the goal is to maximize the objective functions for each individual geometry simultaneously. If there is no conflict between the objective functions and constraints, a solution can be found where every objective function attains its maximum (Miettinen, 1999). In a thermal processing problem with a sphere and a finite cylinder, there is a conflict in the constraints since a process temperature profile might violate the lethality constraint in one of the geometries depending on the sizes while maximizing the objective function (nutrient retention) for the other one.

In these optimization problems, there is not a single solution that is optimal with respect to every objective function. Therefore, the first approach for these problems might be to combine the objective functions into a desirable one. The Weighting Method presented by Miettinen (1999) associates each objective function with a weighted coefficient, and then the goal becomes to maximize the weighted sum of the objective function. In this way, the multiple objective functions are transformed into a single objective function (Miettinen, 1999). It is generally assumed that the weighting coefficients w_i are real numbers and normalized. That is;

$$\sum_{i=1}^k w_i = 1,$$

where $w_i \geq 0$, and k is the number of objective functions ($k=2$ in this study). After associating the objective functions for different geometries, the modified Complex Method algorithm can be used for the double geometry system.

Even though the Weighting Method seems to be easier to apply to a double geometry system for thermal processing, there can be some conflicts, especially in the center point lethality and temperature constraints depending on the sizes of the geometries. The optimum profile might maximize the objective function (nutrient retention) while it might be violating the constraints for one of the geometries. Therefore, the algorithm must arrange the objective functions according to their importance. As explained by Miettinen (1999), this ordering means that more important objective function is of the geometry having the constraint that might be violated. After ordering, the most important objective function's constraints is prevented from violation while the algorithm is maximizing the lesser objective function. This prevention guarantees that the other geometry's constraints were also not violated. This method is called "Lexicographic Ordering", and basically it adds another constraint to the problem to guarantee that the most important objective function preserves its optimal value (Miettinen, 1999).

The combination of Weighting and Lexicographic Methods were adapted for the optimization of the double geometry system combined with the Complex Method algorithm as follows:

- The objective functions for a sphere and a finite cylinder were combined using the Weighting Method:

$$VACN = w_1 \cdot VACN_{Sphere} + w_2 \cdot VACN_{FiniteCylinder} \quad (a)$$

$$SCN = w_1 \cdot SCN_{Sphere} + w_2 \cdot SCN_{FiniteCylinder} \quad (b) \quad 2-20$$

where $w_1=w_2=0.5$.

- Then, a process temperature profile was found using the Steps 1 to 4, as explained above. At this point, the algorithm checked the F_0 values of the geometries to decide on the critical object (the lowest F_0 -generating geometry was the critical one), and this chosen critical geometry was used while the algorithm was trying not to violate any constraint. The tracking of the critical object for any constraint to be violated or not took place at each simulation step following the critical object will changing from one to another depending on the generated process temperature profiles and their sizes.
- After the initial complex was generated, the rest of the algorithm followed the original Complex Method with all reflection, expansion, retraction steps, the stopping criteria (Steps 5 to 7), and the addition of Weighting Method and Lexicographic Ordering.

The Software

The developed software was called "Optimization Expert: Optimization of Thermal Processing". Figure 2-6 shows the start-up screen of the software. The following is the step-by-step use of the software.

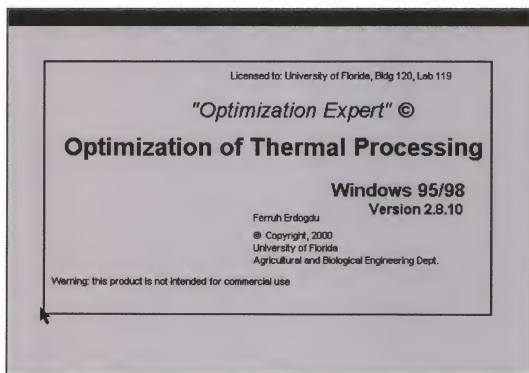


Figure 2-6. The start-up screen of the "Optimization Expert".

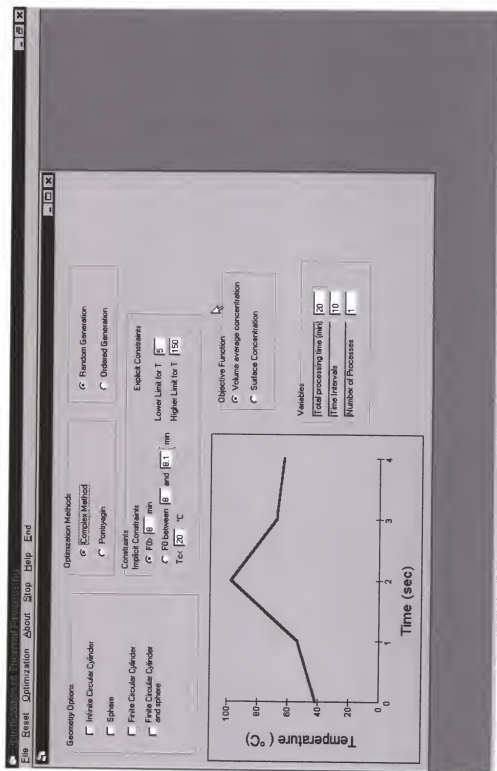


Figure 2-7. Screen of options for the Optimization Expert.

Figure 2-7 shows the screen for the options for the developed program. As seen, Figure 2-7 allowed the user to choose several options required for the program to start the optimization routines. The user had the options of lethality constraint (F_0 to be greater than a certain number, eg., $F_0 \geq 8$ min or in a certain interval, e.g., $8 \leq F_0 \leq 8.1$ min, or objective function (volume average concentration or surface concentration), the initial complex generation method (random or ordered generation), and of course the geometry options (infinite circular cylinder, finite circular cylinder, sphere or finite circular cylinder-sphere combination). Under the title of "Variables", it is possible to enter the total processing time, N number of points to discretize the variable process temperature profile for the given processing time, and the number of runs (showing how many times the program will apply the given conditions to the chosen options to see the uniqueness and reproducibility). Choosing one of the geometry options leads the user to enter the thermal and physical properties of the geometries, and the kinetics of the quality factor and target organism for the lethality constraint. Figure 2-8 shows the screen for the finite circular cylinder-sphere combination. As seen in Figure 2-8, different quality attributes and different microorganism kinetics can be chosen as the different thermophysical properties for each geometry. At this point, the program is ready to start the optimization using the Complex Method. Clicking on the "Go to Calculations" under "Optimization" option as seen in Figure 2-8 starts the optimization routine for the chosen geometries and given properties. Figures 2-9 and 2-10 show the outputs for a sphere geometry of $r=15$ mm, with the given properties in Figure 2-10, in numerical and graphical formats, respectively. This software can be obtained from Dr. M.Ö. Balaban at the U.F.

File Run Optimization About Stop Help End

Free Cycle:

Radius (mm)	15
Length (mm)	15
Thermal Conductivity (W/m ² K)	0.566
Specific Heat (J/gK)	3650
Density (kg/m ³)	1050
Initial (°C)	20

Sphere:

Radius (mm)	15
Thermal Conductivity (W/m ² K)	0.566
Specific Heat (J/gK)	3650
Density (kg/m ³)	1050
Initial (°C)	20

Heat Transfer Coefficient (W/m²K):

HT Heating (W/m ² K)	2000
HT Cooling (W/m ² K)	500

Free Cycle Quality Attribute Kinetics:

Nature	Microorganism
β-value (sec)	10716
z-value (°C)	25.56
Reference Temperature (°C)	121.11

Sphere Quality Attribute Kinetics:

Nature	Microorganism
β-value (sec)	10716
z-value (°C)	25.56
Reference Temperature (°C)	121.11

OK

Figure 2-8. Screen for the thermophysical properties of the geometries and kinetics of the quality attribute and microorganism.

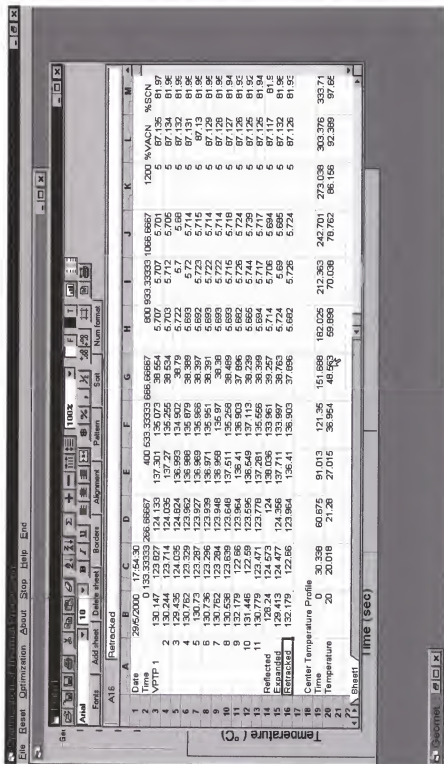


Figure 2-9. Numerical output for a sphere geometry of radius 15 mm with the given physical properties in Figure 2-8.

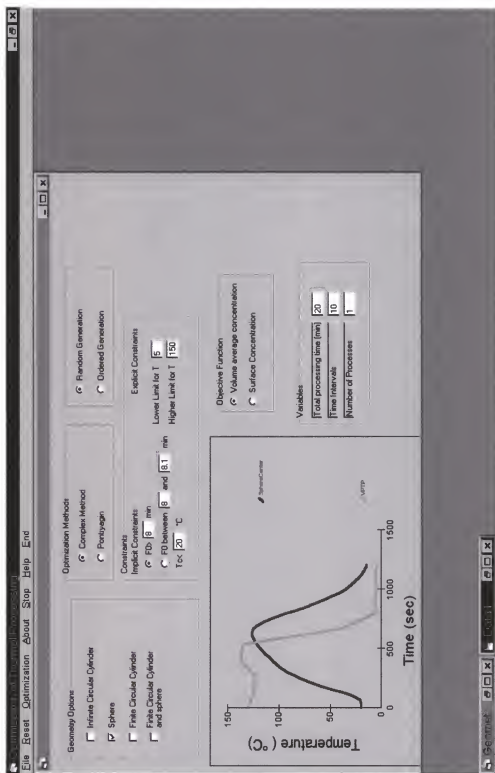


Figure 2-10. Graphical output for a sphere geometry of radius 15 mm with the given physical properties in Figure 2-8.

CHAPTER 3 RESULTS AND DISCUSSION

The Complex Method

Optimization with Single Geometry

Objective function: volume average retention of nutrient

Sphere and finite cylinder shapes having different physical properties were used to see the effects of total processing time and time steps used for discretization on the objective functions and reproducibility of the decision variable (variable process temperature profile; VPTP). The thermophysical properties of the geometries, objective functions, constraints, and the required kinetic parameters for the evaluation of these were given in Chapter 2, Materials and Methods.

Sphere

The spheres of radius 15 (sphere 1) and 30 mm (sphere 2) were chosen as the model geometries to be used in the simulations. Tables 3-1 gives the volume average and surface retention of thiamine to achieve the implicit constraints of target F_0 at the center (≥ 8 min), the threshold final center temperature (< 15 °C) at the end of the processing using optimum constant process temperature profile (CPTP), and required processing time

for sphere. The temperature of 5 °C, lower limit of explicit constraint, was used for the simulation of cooling part, and the heating time and temperature was calculated using trial and error methods: the procedure was initialized with a starting value for the optimum temperature. Then, the heating time and cooling time to obtain the lethality and center temperature constraints were calculated with the VACN value. A new temperature was chosen depending on the results attained and the iterations continued until finding the optimum temperature to maximize the VACN based on the user's discretion. Figures 3-1 and 3-2 show the CPTPs and the resulting center temperatures for each sphere.

Table 3-1. Optimization results using constant process temperature profile (CPTP) for model spheres.

	Sphere-1	Sphere-2
Radius (mm)	15	30
Optimum Constant Heating Temperature (°C)	130	125
Total Processing Time (min)	20	80
VACN (%) (thiamine)	86.57	71.36
SCN (%) (thiamine)	81.36	60.45
F ₀ (min) (<i>B. Stearothermophilus</i>)	8.06	8.04

All the simulation conditions (total processing times, discretized time steps and physical properties of the model geometries of sphere and finite cylinder) were based on the CPTP optimization results given in Table 3-1, in Figures 3-1 and 3-2, and summarized in Table 3-2 for the model spheres. The maximum discretized time steps were used as $N=20$ since preliminary runs of the software showed it would take a long time as the processing time and the number of time steps increased (e.g., the total simulation time for a 80 min process for sphere-2 was around 6 hrs on a Pentium III, 450 MHz Intel Processor machine). This was around 24 hrs for the finite cylinder 2 ($r=30$ mm, $L=60$ mm) with total processing time of 90 min and $N=20$. Therefore, 10 replicate runs for the sphere and 6 runs for the finite cylinder were applied to see the uniqueness and reproducibility with the 50% extended processing times to see if the extension results in improvements.

Table 3-2. Simulation conditions for sphere.

Case #s	Radius (mm)	Total Processing Time (min)	N (# of time steps)
1	15	20	10
2			20
3		30	10
4			20
5	30	80	10
6			20
7		120	10
8			20

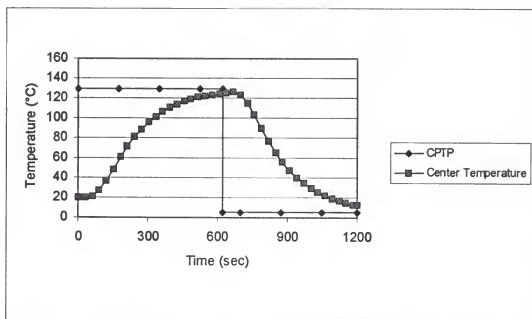


Figure 3-1. Constant optimum temperature profile for sphere 1 ($r=15$ mm) with the resulting center temperature profile.

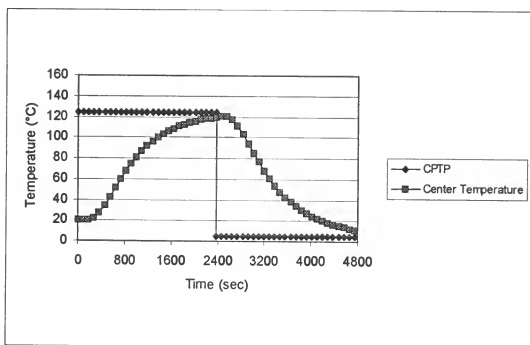


Figure 3-2. Constant optimum temperature profile for sphere 2 ($r=30$ mm) with the resulting center temperature profile.

The processing times of 20 and 30 min for sphere 1, and 80 and 120 min for sphere 2 with two different discretized time steps ($N=10$ and $N=20$) were selected to see the effects of extended processing times and time steps on the results of the variable temperature processes. Tables 3-3 and 3-4 show the calculated VPTPs for model sphere 1 when the total processing time of 20 min with 10 and 20 time steps were used. Table 3-5 shows the volume average (VACN) and surface concentration of thiamine (SCN) at the end of the process with the resulting F_0 value. Different VPTPs were obtained at each run for both time steps used ($N=10$ and 20). However, each VPTP gave a similar VACN, SCN, and F_0 value. The standard deviations of the different runs were less than 1%. While the VACN values (87.14% for $N=10$ and 87.28% for $N=20$) were almost same with the ones obtained by using the CPTPs (86.57%), the SCN values seemed to increase around 1.5 percentage points (81.98% for $N=10$; 82.62% for $N=20$ compared to 81.36% for CPTP) when 20 min of processing time was applied (Table 3-5). Total processing time of 30 min (50% extended) was then applied to the model sphere 1 to see the effect of extended time with the time steps of $N=10$ and 20. Tables 3-6 to 3-8 show the calculated VPTPs and resulting objective function and constraint values. The extended time (30 min) also did not increase the objective function value of VACN (87.10% for $N=10$; 86.29% for $N=20$ compared to 86.57% for CPTP). However, the increase in SCN values were around 2.5 percentage points compared to a CPTP process (83.95% for $N=10$; 82.64% for $N=20$ compared to 81.36% for CPTP; Table 3-8). Figures 3-3 and 3-4 show comparisons of the CPTP and VPTP, the one giving the highest %VACN value, and the resulting center temperature profiles for the used discretized time steps of $N=10$ (Trial 9,

Table 3-5. The VACN (%), SCN(%), and F_0 (min) results of the calculated VPTPs of the model sphere 1 ($r=15$ mm) for the processing time of 20 min and two different discretized time steps of $N=10$ and $N=20$ (Objective Function: VACN).

Trials	N=10			N=20		
	VACN (%)	SCN (%)	F_0 (min)	VACN (%)	SCN (%)	F_0 (min)
1	87.15	81.98	8.00	87.36	82.71	8.00
2	87.07	81.74	8.00	86.62	81.37	8.00
3	87.18	82.16	8.00	87.47	83.03	8.01
4	87.12	81.89	8.01	87.27	82.48	8.00
5	87.15	81.93	8.01	87.27	82.50	8.00
6	87.16	81.98	8.02	87.38	82.83	8.00
7	87.16	82.00	8.02	87.02	82.34	8.00
8	87.17	82.06	8.00	87.47	83.02	8.00
9	87.22	82.17	8.01	87.47	83.00	8.02
10	87.03	81.91	8.01	87.44	82.98	8.00
Average	87.14 ± 0.05	81.98 ± 0.13	8.01	87.28 ± 0.27	82.62 ± 0.51	8.00

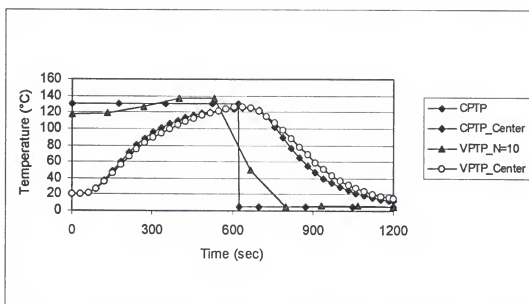


Figure 3-3. Comparison of the CPTP and the best VPTP with resulting center temperature profiles (Sphere-1, $r=15$ mm, $t=20$ min, $N=10$, Objective Function: VACN).

Table 3-8. The VACN (%), SCN(%), and F_0 (min) results of the calculated VPTPs of the model sphere 1 ($r=15$ mm) for the processing time of 30 min and two different discretized time steps of $N=10$ and $N=20$ (Objective Function: VACN).

Trials	N=10			N=20		
	VACN (%)	SCN (%)	F_0 (min)	VACN (%)	SCN (%)	F_0 (min)
1	87.41	85.14	8.01	84.95	80.34	8.00
2	87.61	84.16	8.02	85.40	83.03	8.00
3	85.06	82.86	8.01	87.43	83.93	8.20
4	86.72	84.29	8.04	86.32	82.46	8.00
5	86.80	81.51	8.00	87.44	84.71	8.00
6	87.73	84.61	8.04	84.77	80.26	8.00
7	86.81	83.96	8.00	87.44	84.53	8.14
8	87.70	84.04	8.00	86.45	81.49	8.00
9	86.47	83.89	8.00	87.29	83.23	8.01
10	87.71	85.04	8.00	85.37	81.96	8.00
Average	87.10 ± 0.86	83.95 ± 1.07	8.01	86.29 ± 1.09	82.64 ± 1.52	8.04

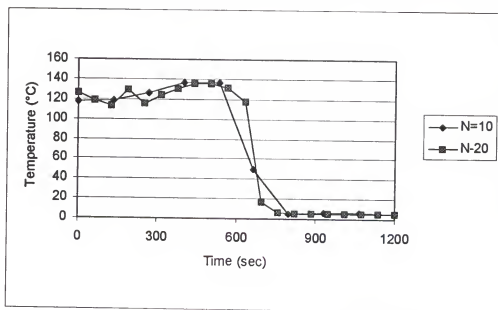


Figure 3-5. Comparison of the best calculated VPTPs of $N=10$ and $N=20$ for sphere 1 ($r=15$ mm, $t=20$ min, Objective Function: VACN).

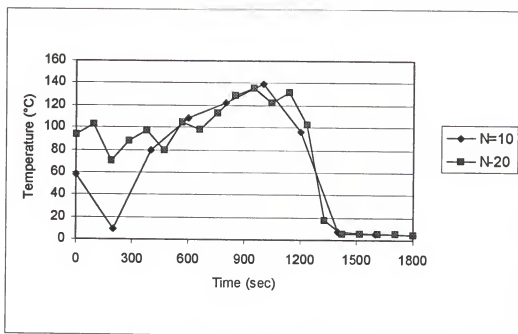


Figure 3-6. Comparison of the best calculated VTPs of $N=10$ and $N=20$ for sphere 1 ($r=15$ mm, $t=30$ min, Objective Function: VACN).

The radius of the model sphere 1 was then doubled to see the effects of size on the optimization results with respect to uniqueness and reproducibility of the objective function and the variable temperature profiles. It was also important to see if the variable temperature profiles result in the significant improvements in the objective function values.

The optimization using CPTPs found the optimum VACN value as 71.36% and SCN value of 60.45% resulting from a processing time of around 80 min (Fig. 3-2). Therefore, the processing times of 80 min, and 50% longer 120 min with time steps $N=10$ and 20 were applied to the model sphere 2. Tables 3-9 to 3-11 show the results for $t=80$ min, and 3-12 to 3-14 for $t=120$ min. Figures 3-7 and 3-8 show comparisons of the CPTP

Table 3-10. The calculated variable process temperature profiles (VPTP) of the model sphere-2 ($r=30$ mm) for processing time of 80 min and the discretized time steps of $N=20$ (Objective Function: VACN).

[illegible]

Table 3-11. The VACN (%), SCN(%), and F_0 (min) results of the calculated VPTPs of the model sphere 2 ($r=30$ mm) for the processing time of 80 min and two different discretized time steps of $N=10$ and $N=20$ (Objective Function: VACN).

Trials	N=10			N=20		
	VACN (%)	SCN (%)	F_0 (min)	VACN (%)	SCN (%)	F_0 (min)
1	72.49	62.17	8.00	72.80	63.67	8.00
2	73.01	63.59	8.02	72.79	62.94	8.00
3	73.22	64.43	8.01	72.99	64.01	8.02
4	72.65	62.51	8.00	73.30	64.76	8.01
5	73.06	63.76	8.00	72.96	63.95	8.00
6	73.03	63.85	8.01	72.58	63.34	8.00
7	72.75	62.89	8.00	72.78	63.13	8.00
8	73.11	63.94	8.00	73.20	64.67	8.02
9	72.91	63.18	8.00	72.90	63.84	8.00
10	73.07	63.76	8.00	73.18	64.39	8.01
Average	72.93 ± 0.23	63.41 ± 0.70	8.01	72.95 ± 0.62	63.87 ± 0.62	8.01

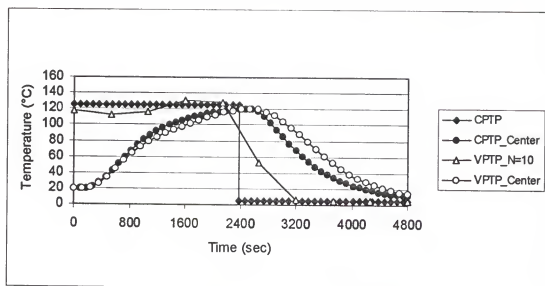


Figure 3-7. Comparison of the CPTP and the best VPTP with resulting center temperature profiles (Sphere-2, $r=30$ mm, $t=80$ min, $N=10$, Objective Function: VACN).

Table 3-13. The calculated variable process temperature profiles (VPTP) of the model sphere-2 ($r=30$ mm) for processing time of 120 min and the discretized time steps of $N=20$ (Objective Function: VACN).

Time (sec)	Variable Process Temperature Profiles ($^{\circ}\text{C}$)									
	1	2	3	4	5	6	7	8	9	10
0.0	106.0	82.4	95.8	120.6	32.1	136.8	142.5	107.5	141.2	112.8
378.9	109.6	89.7	84.4	78.1	71.3	84.3	99.4	79.6	89.9	80.4
757.9	83.4	102.6	62.6	120.4	98.4	73.5	102.3	112.8	87.2	78.2
1136.8	99.4	103.4	129.5	106.2	115.6	75.0	77.7	99.3	92.3	77.2
1515.8	81.0	66.9	62.2	67.6	94.4	93.4	78.3	97.2	96.2	66.5
1894.7	68.8	85.6	62.7	95.7	62.1	98.2	101.2	100.4	92.2	117.6
2273.7	99.1	80.7	70.8	73.2	104.4	101.1	85.7	89.3	110.9	108.3
2652.6	90.7	101.2	109.8	91.1	72.2	95.9	101.2	108.3	114.8	114.6
3031.6	119.7	98.7	126.9	98.6	93.8	113.0	94.7	105.9	109.7	112.3
3410.5	118.6	77.7	91.5	119.6	127.2	119.3	97.7	113.5	134.7	109.4
3789.5	130.3	146.7	106.8	116.3	101.4	119.2	125.7	124.9	114.3	121.9
4168.4	126.2	112.6	141.2	137.4	127.3	120.1	126.4	115.7	119.6	116.7
4547.4	99.5	133.6	123.9	115.3	122.2	135.2	139.5	137.0	93.3	133.0
4926.3	91.5	122.5	114.6	112.5	140.7	69.9	81.5	82.2	75.5	89.9
5305.3	32.3	13.9	7.5	17.7	33.8	21.7	12.6	11.5	18.7	15.9
5684.2	5.8	5.6	5.6	5.8	5.5	7.0	5.5	5.7	10.0	5.7
6063.2	5.7	5.9	5.9	5.6	5.6	5.7	5.7	5.8	10.1	5.7
6442.1	5.7	6.0	5.9	5.8	5.6	5.7	5.7	5.8	6.1	5.7
6821.1	5.7	5.4	5.8	5.8	5.9	5.7	5.9	5.7	10.5	5.4
7200.0	5.0	5.0	5.0	5.0	5.0	5.0	5.0	5.0	5.0	5.0

As seen in the tables above, 10 different VPTPs were found, each giving a similar VACN, SCN and F_0 values. Figures 3-9 (Trial 8 in Table 3-9 and Trial 4 in Table 3-10) and 3-10 (Trial 10 in Table 3-12 and Trial 1 in Table 3-13) show the comparison of the best calculated VPTPs of $N=10$ $N=20$ with respect to the objective function of VACN for the processing times of 80 and 120 min, respectively for sphere 2.

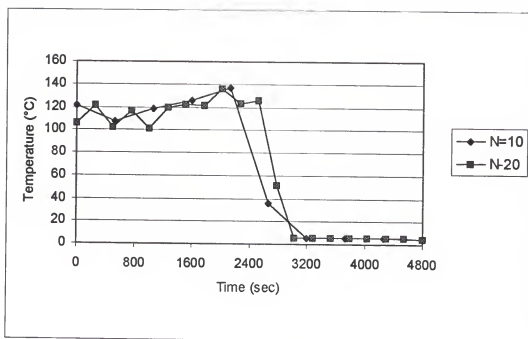


Figure 3-9. Comparison of the best calculated VPTPs of N=10 and N=20 for sphere 2 ($r=30$ mm, $t=80$ min, Objective Function: VACN).

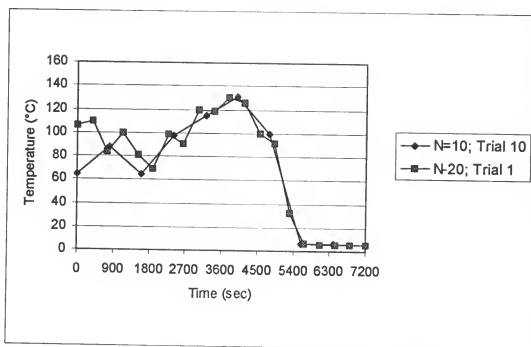


Figure 3-10. Comparison of the best calculated VPTPs of N=10 and N=20 for sphere 2 ($r=30$ mm, $t=120$ min, Objective Function: VACN).

Table 3-14. The VACN (%), SCN(%), and F_0 (min) results of the calculated VPTPs of the model sphere 2 ($r=30$ mm) for the processing time of 120 min and two different discretized time steps of $N=10$ and $N=20$ (Objective Function: VACN).

Trials	N=10			N=20		
	VACN (%)	SCN (%)	F_0 (min)	VACN (%)	SCN (%)	F_0 (min)
1	71.99	67.60	8.00	72.79	66.82	8.00
2	73.40	66.88	8.01	70.41	59.76	8.00
3	72.09	64.10	8.00	70.57	60.38	8.00
4	72.90	67.69	8.00	71.66	64.22	8.02
5	71.11	64.91	8.01	70.67	61.51	8.00
6	72.46	65.45	8.00	72.16	66.47	8.00
7	73.22	68.39	8.00	71.31	62.06	8.00
8	71.41	62.42	8.00	70.81	65.06	8.00
9	73.54	68.99	8.00	71.78	67.02	8.00
10	73.72	68.59	8.01	70.87	65.90	8.00
Average	72.58 \pm 0.92	66.50 \pm 2.18	8.00	71.30 \pm 0.78	63.92 \pm 2.77	8.00

The processing time of 80 min did not increase the objective function value of VACN significantly (around 1.5 percentage points) compared to a CPTP process (72.93% for $N=10$ and 72.95% for $N=20$ compared to 71.36% of CPTP; Table 3-11). However, the change in the SCN was up to 3 percentage points (63.41% for $N=10$ and 63.87% for $N=20$ compared to 60.45% of CPTP; Table 3-11). Similar results for VACN were obtained by extending process time to 120 min. The increase in SCN was around 3-6 percentage points compared to CPTP (Table 3-14). The results showed that the use VPTPs was not significantly advantageous over CPTPs with small sized objects compared to the larger sized ones with respect to the objective function of VACN. The only

explanation for this can be given as the shorter processing time and that the temperature's coming equilibrium in the object very fast. When the size was increased the effect of VPTPs became more obvious. Even though the increase of 1-3 percentage points with respect to VACN seems insignificant, 3-6 percentage points difference in SCN was found compared to CPTP. This result raised the question of whether this might be more obvious if the SCN were used as the objective function instead of VACN with the same constraints and processing conditions. The use of different geometries of larger sizes with VPTPs might also result in better retention, especially at the surface, because of the longer processing times to achieve the implicit constraints. The difference between the results obtained by $N=10$ and $N=20$ were not significant. The center temperature profiles of the model systems with respect to the calculated VPTPs are given in Appendix B.

Finite cylinder

The finite cylinders of radius 15 mm, total length 15 mm (finite cylinder 1) and radius 30 mm, total length 60 mm (finite cylinder 2) were chosen to be used as model geometries in the simulations. Table 3-15 presented the VACN and SCN values for thiamine retention to satisfy the implicit constraints of target F_0 at the center (≥ 8 min), and the final center temperature (<15 °C) at the end of the CPTP process for model finite cylinders 1 and 2, respectively while figures 3-11 and 3-12 show the CPTPs and the resulting center temperature. Using the results of the CPTP optimization, the simulation set up for the model finite cylinders, given in Table 3-16, was used.

Table 3-15. Optimization results using constant retort temperature profile for model finite cylinders.

	Finite Cylinder-1	Finite Cylinder-2
Radius (mm)	15	30
Half-Length (mm)	7.5	30
Optimum Constant Heating Temperature (°C)	130	125
Total Processing Time (min)	16	90
VACN (%) (thiamine)	90.86	68.06
SCN (%) (thiamine)	83.61	49.20
F ₀ (min) (<i>B. Stearothermophilus</i>)	8.02	8.04

Table 3-16. Simulation setup for finite cylinder.

Case #s	Radius (mm)	Total Length (mm)	Total Processing Time (min)	N (# of time steps)
1	15	15	16	10
2				20
3			24	10
4				20
5	30	60	90	10
6				20
7			135	10

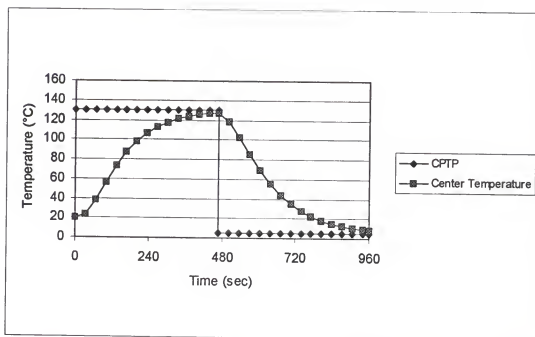


Figure 3-11. Constant optimum temperature profile for finite cylinder 2 ($r=30$ mm, $L=60$ mm) with the resulting center temperature profile.

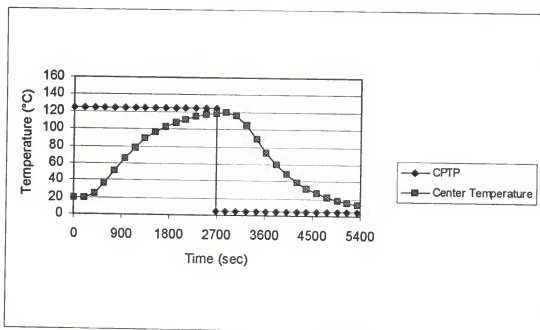


Figure 3-12. Constant optimum temperature profile for finite cylinder 2 ($r=30$ mm, $L=60$ mm) with the resulting center temperature profile.

Tables 3-17 to 3-22 show the calculated VPTPs and resulting VACN, SCN and target F_0 values for the model finite cylinder 1 ($r=15\text{mm}$; $L=15\text{ mm}$) for a total processing time of 16 min and 24 min (50% extended), with two different time steps ($N=10$; $N=20$). As in the sphere case, the different temperature profiles gave similar values for the objective function. The standard deviations of the results were less than 1%, and the difference between the results obtained by CPTPs and VPTPs with respect to the objective function of VACN was around 1 percentage points (91.89% for $N=10$ and 91.62% for $N=20$, compared to 90.86% of CPTP; Table 3-19). This difference was up to 3 percentage points in the case of SCN (86.54% for $N=10$ and 86.00% for $N=20$ compared to 83.61% of CPTP; Table 3-19). When the longer processing time was applied with the same processing conditions, there could not also be found any significant improvements compared to the CPTP as in the sphere case.

Table 3-17. The calculated variable process temperature profiles (VPTP) of the model finite cylinder 1 ($r=15\text{ mm}$, $L=15\text{ mm}$) for processing time of 16 min and the discretized time steps of $N=10$ (Objective Function: VACN).

Time (sec)	Variable Process Temperature Profiles ($^{\circ}\text{C}$)					
	1	2	3	4	5	6
0.0	102.7	131.3	94.1	101.8	128.9	97.6
106.7	127.1	92.4	90.9	92.5	116.2	101.7
213.3	114.3	111.2	115.3	106.7	109.5	104.8
320.0	119.4	128.7	124.4	124.0	134.8	127.3
426.7	136.0	133.9	135.6	137.7	128.5	134.7
533.3	128.0	127.7	129.4	128.5	124.2	130.5
640.0	22.7	19.6	27.9	44.4	21.0	31.0
746.7	6.0	5.5	5.7	5.5	5.8	5.6
853.3	5.9	5.8	5.8	5.4	5.8	5.9
960.0	5.0	5.0	5.0	5.0	5.0	5.0

Table 3-18. The calculated variable process temperature profiles (VPTP) of the model finite cylinder 1 ($r=15$ mm, $L=15$ mm) for processing time of 16 min and the discretized time steps of $N=20$ (Objective Function: VACN).

Time (sec)	Variable Process Temperature Profiles (°C)					
	1	2	3	4	5	6
0.0	130.0	115.0	119.2	100.6	90.8	109.0
50.5	116.0	115.1	111.0	112.4	134.0	93.0
101.1	104.2	106.8	104.5	106.2	104.9	103.0
151.6	93.9	120.6	110.9	123.2	90.7	122.8
202.1	122.4	120.3	121.2	89.9	118.5	118.8
252.6	116.1	112.5	70.2	120.0	115.3	117.0
303.2	109.1	104.6	122.6	119.1	129.1	116.3
353.7	135.8	131.0	125.0	125.0	110.2	133.6
404.2	131.1	120.0	130.6	135.4	140.6	128.7
454.7	132.5	129.7	134.1	127.1	128.7	137.8
505.3	129.2	129.2	136.3	137.6	130.6	118.7
555.8	130.5	133.0	132.2	125.8	134.7	133.1
606.3	56.6	101.6	95.8	74.6	77.2	72.3
656.8	5.9	8.3	7.7	6.6	7.3	8.4
707.4	5.8	5.7	6.0	5.6	6.1	5.7
757.9	5.7	5.7	5.2	5.7	5.4	5.9
808.4	5.6	5.7	5.6	5.7	5.9	5.4
858.9	5.8	5.6	5.6	6.0	5.9	5.9
909.5	5.7	5.8	5.7	5.9	5.8	5.8
960.0	5.0	5.0	5.0	5.0	5.0	5.0

Figures 3-13 and 3-14 show comparisons of the CPTP and VPTP, giving the highest %VACN value, and the resulting center temperature profiles for the discretized time steps of $N=10$ (Trial 3, Table 3-19), and $N=20$ (Trial 4; Table 3-19), respectively for a processing time of 16 min, and Figures 3-15 (Trial 3 in Table 3-17 and Trial 4 in Table 3-18) and 3-16 (Trial 3 in Table 3-30 and Trial 2 in Table 3-21) show the comparison of

the best calculated VPTPs of $N=10$ $N=20$ with respect to the objective function of VACN for the processing times of 16 and 24 min, respectively for finite cylinder 1.

Table 3-19. The VACN (%), SCN(%), and F_0 (min) results of the calculated VPTPs of the model finite cylinder 1 ($r=15$ mm, $L=15$ mm) for the processing time of 16 min and two different discretized time steps of $N=10$ and $N=20$ (Objective Function: VACN).

Trials	N=10			N=20		
	VACN (%)	SCN (%)	F_0 (min)	VACN (%)	SCN (%)	F_0 (min)
1	91.49	85.95	8.00	91.78	86.22	8.00
2	92.02	86.71	8.03	91.32	85.60	8.02
3	92.09	86.90	8.00	91.67	85.73	8.02
4	92.05	86.67	8.01	91.84	86.44	8.01
5	91.62	86.23	8.01	91.53	85.60	8.00
6	92.08	86.82	8.01	91.60	86.40	8.21
Average	91.89 ± 0.27	86.54 ± 0.37	8.02	91.62 ± 0.19	86.00 ± 0.40	8.04

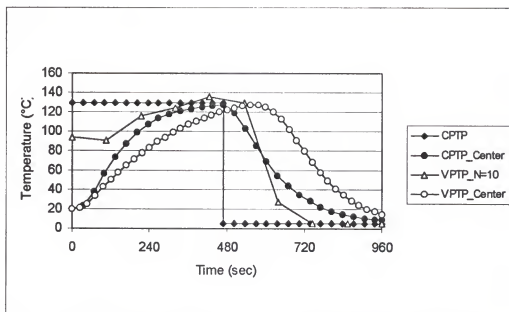


Figure 3-13. Comparison of the CPTP and the best VPTP with resulting center temperature profiles (Finite Cylinder-1, $r=15$ mm, $L=15$ mm, $t=16$ min, $N=20$, Objective Function: VACN).

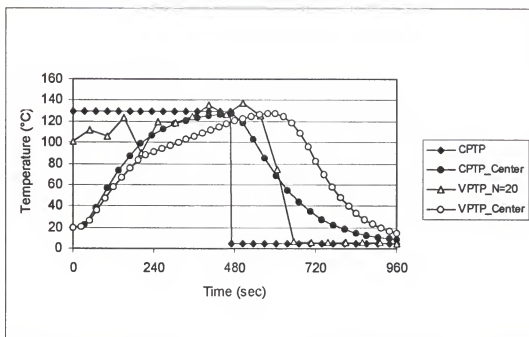


Figure 3-14. Comparison of the CPTP and the best VPTP with resulting center temperature profiles (Finite Cylinder-1, $r=15$ mm, $L=15$ mm, $t=16$ min, $N=20$, Objective Function: VACN).

Table 3-20. The calculated variable process temperature profiles (VPTP) of the model finite cylinder 1 ($r=15$ mm, $L=15$ mm) for processing time of 24 min and the discretized time steps of $N=10$ (Objective Function: VACN).

Time (sec)	Variable Process Temperature Profiles (°C)					
	1	2	3	4	5	6
0.0	116.4	116.7	119.7	111.6	91.5	105.4
160.0	110.4	82.0	102.5	110.7	107.2	82.7
320.0	70.6	138.0	108.4	100.8	89.0	109.1
480.0	116.9	127.6	145.3	96.1	86.1	107.8
640.0	105.7	107.6	95.9	90.1	136.3	111.8
800.0	146.3	48.3	87.0	129.8	112.3	116.3
960.0	89.7	46.6	111.4	139.5	142.5	144.3
1120.0	26.3	28.7	28.3	18.5	18.0	37.2
1280.0	6.1	10.8	5.6	5.6	5.8	5.7
1440.0	5.0	5.0	5.0	5.0	5.0	5.0

Table 3-21. The calculated variable process temperature profiles (VPTP) of the model finite cylinder 1 ($r=15$ mm, $L=15$ mm) for processing time of 24 min and the discretized time steps of $N=20$ (Objective Function: VACN).

Time (sec)	Variable Process Temperature Profiles (°C)					
	1	2	3	4	5	6
0.0	120.3	149.2	79.8	73.5	130.0	101.5
75.8	113.1	67.7	96.3	109.2	96.9	137.0
151.6	86.8	88.3	118.7	117.3	87.2	109.5
227.4	93.1	75.4	87.6	64.3	118.9	94.0
303.2	92.1	142.0	90.5	142.4	124.2	143.8
378.9	105.8	101.4	104.7	136.6	99.3	134.3
454.7	95.8	101.6	97.5	136.9	91.2	127.1
530.5	116.4	96.6	90.6	118.5	141.6	109.2
606.3	118.6	94.5	88.6	44.5	122.7	84.1
682.1	114.2	90.7	111.8	135.1	139.0	95.4
757.9	90.4	131.3	128.9	25.9	114.1	95.7
833.7	100.4	125.8	133.2	44.6	90.3	113.2
909.5	124.7	143.2	133.4	110.3	88.3	99.3
985.3	145.0	118.8	119.9	52.0	115.8	97.9
1061.1	141.9	86.1	72.2	94.7	99.4	115.0
1136.8	11.5	9.9	7.3	18.5	21.5	12.4
1212.6	5.9	6.4	5.6	15.5	5.7	6.0
1288.4	5.6	5.7	6.1	5.9	5.8	5.5
1364.2	5.9	5.6	5.9	6.0	5.7	5.9
1440.0	5.0	5.0	5.0	5.0	5.0	5.0

Table 3-22. The VACN (%), SCN(%), and F_0 (min) results of the calculated VPTPs of the model finite cylinder 1 ($r=15$ mm, $L=15$ mm) for the processing time of 24 min and two different discretized time steps of $N=10$ and $N=20$ (Objective Function: VACN).

Trials	N=10			N=20		
	VACN (%)	SCN (%)	F_0 (min)	VACN (%)	SCN (%)	F_0 (min)
1	90.52	84.18	8.00	88.21	79.83	8.00
2	91.09	85.72	8.00	89.94	82.72	8.00
3	90.56	84.53	8.00	91.27	86.23	8.00
4	90.47	84.43	8.00	90.39	82.23	8.00
5	89.46	83.53	8.00	89.59	82.92	8.00
6	90.03	84.74	8.04	89.19	81.88	8.07
Average	90.36 ± 0.55	84.52 ± 0.72	8.01	89.75 ± 1.05	82.75 ± 2.12	8.01

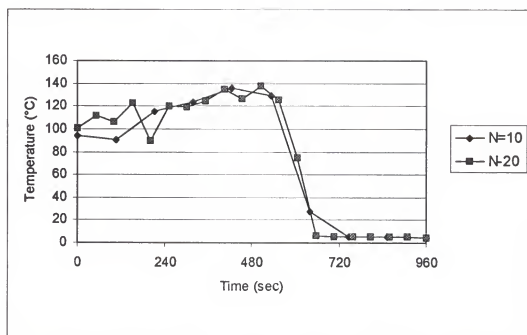


Figure 3-15. Comparison of the best calculated VPTPs of $N=10$ and $N=20$ for finite cylinder 1 ($r=15$ mm, $L=15$ mm, $t=16$ min, Objective Function: VACN).

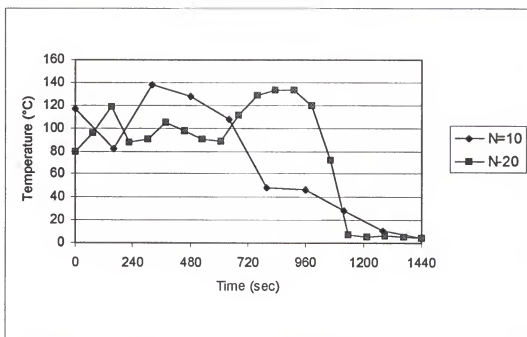


Figure 3-16. Comparison of the best calculated VPTPs of $N=10$ and $N=20$ for finite cylinder 1 ($r=15$ mm, $L=15$ mm, $t=24$ min, Objective Function: VACN).

Table 3-23. The calculated variable process temperature profiles (VPTP) of the model finite cylinder 2 ($r=30$ mm, $L=60$ mm) for processing time of 90 min and the discretized time steps of $N=10$ (Objective Function: VACN).

Time (sec)	Variable Process Temperature Profiles (°C)					
	1	2	3	4	5	6
0	120.7	104.0	110.9	107.3	137.4	124.5
600	112.0	117.1	115.9	113.0	108.6	102.9
1200	124.2	123.8	122.6	123.5	129.9	123.9
1800	128.7	126.9	131.0	128.6	124.7	129.7
2400	128.9	132.6	126.4	131.2	129.2	130.7
3000	36.2	30.3	36.0	35.0	32.3	43.1
3600	5.8	8.5	5.6	5.7	5.7	5.6
4200	5.8	5.6	5.9	5.7	5.6	5.8
4800	5.7	5.7	5.6	5.8	5.7	5.9
5400	5.0	5.0	5.0	5.0	5.0	5.0

Since the improvement of VACN and SCN values for the model finite cylinder-1 did not seem to be significant, model finite cylinder-2 was chosen in bigger dimensions. The processing times for this cylinder was also decided using the CPTP optimization results given in Table 3-15 and Figure 3-4. The simulation set up was given in Table 3-16. Tables 3-23 to 3-27 show the calculated VPTPs with resulting VACN, SCN and target F_0 values for the model finite cylinder 2 ($r=30\text{mm}$; $L=60\text{ mm}$) with total processing time of 90 and 135 min (50% extended) and two different time steps ($N=10$; $N=20$). The processing time was around 90 min with the CPTP (Fig. 3-12). As seen in the following tables, the standard deviations of the results were less than 1 percentage points. The CPTP resulted in 68.06% VACN, and 49% SCN while the values of 69.77% VACN and 53% SCN for $N=10$, and 70.54% VACN and 55.34% SCN for $N=20$ were obtained for the processing time of 90 min. Even though the improvements for VACN using the VPTP processes were 1.7 to 2.5 percentage points compared to the CPTP processes, up to 4 to 6.3 percentage points improvement was obtained with respect to the SCN values.

Applying 50% increase in total processing time (135 min; $N=10$) did not improve the VACN results, similar to the smaller size case. However, the SCN value was up to 59%, and this resulted in an improvement of around 10 percentage points in the surface concentration of nutrient. Figures 3-17 and 3-18 show comparisons of the CPTP and VPTP giving the highest %VACN value, and the resulting center temperature profiles for the discretized time steps of $N=10$ (Trial 1, Table 3-25), and $N=20$ (Trial 2; Table 3-25), respectively for the processing time of 90 min, and Figure 3-19 (Trial 1 in Table 3-23 and Trial 2 in Table 3-24) shows the comparison of the best calculated VPTPs of $N=10$ $N=20$

with respect to the objective function of VACN for the processing times of 90 min for finite cylinder 2. The change of center temperatures of the model systems with respect to the VPTPs are given in Appendix C.

Table 3-24. The calculated variable process temperature profiles (VPTP) of the model finite cylinder 2 ($r=30$ mm, $L=60$ mm) for processing time of 90 min and the discretized time steps of $N=20$ (Objective Function: VACN).

Time (sec)	Variable Process Temperature Profiles (°C)					
	1	2	3	4	5	6
0.0	116.5	107.8	108.2	113.2	123.0	116.2
284.2	120.8	110.2	106.7	119.8	118.3	110.6
568.4	99.0	110.8	116.7	114.1	112.8	111.6
852.6	96.7	117.5	111.0	111.2	109.0	112.7
1136.8	124.9	112.4	120.2	112.1	119.0	116.0
1421.1	119.7	119.2	119.6	127.8	123.6	112.7
1705.3	123.9	128.1	124.3	125.4	128.0	126.1
1989.5	131.0	126.8	126.4	130.1	120.9	133.5
2273.7	122.4	129.6	131.7	132.8	135.9	127.9
2557.9	137.2	123.7	120.1	116.3	122.9	127.7
2842.1	105.1	113.3	119.2	86.1	89.9	101.9
3126.3	10.3	14.4	13.5	9.3	9.6	12.6
3410.5	5.8	5.7	5.8	5.7	5.6	5.7
3694.7	5.7	5.7	6.0	5.7	5.8	5.8
3978.9	5.6	5.9	5.5	5.7	5.8	5.7
4263.2	5.6	5.8	5.9	5.7	5.7	5.7
4547.4	5.7	5.9	5.7	5.6	5.8	5.7
4831.6	5.8	5.7	5.7	5.8	5.7	5.7
5115.8	5.7	5.9	5.6	5.7	5.7	5.8
5400.0	5.0	5.0	5.0	5.0	5.0	5.0

The results from the sphere and finite cylinder showed that the VPTPs can improve the nutrient retention, especially at the surface, when the larger sizes of the geometries were

used. The higher improvements in the SCN case raises the question of using SCN as objective function instead of VACN with the same constraints and processing conditions.

The following shows the results for the use of SCN values as objective function for the defined sphere and finite cylinder geometries.

Table 3-25. The VACN (%), SCN(%), and F_0 (min) results of the calculated VPTPs of the model finite cylinder 1 ($r=30$ mm, $L=60$ mm) for the processing time of 90 min and two different discretized time steps of $N=10$ and $N=20$ (Objective Function: VACN).

Trials	N=10			N=20		
	VACN (%)	SCN (%)	F_0 (min)	VACN (%)	SCN (%)	F_0 (min)
1	69.96	53.74	8.01	70.06	53.69	8.01
2	69.67	53.27	8.00	70.98	56.93	8.00
3	69.91	53.80	8.01	70.92	56.94	8.00
4	69.88	53.75	8.00	70.37	54.53	8.00
5	69.26	51.08	8.00	70.29	54.40	8.00
6	69.92	53.41	8.00	70.65	55.56	8.01
Average	69.77 ± 0.27	53.17 ± 1.05	8.00	70.54 ± 0.37	55.34 ± 1.37	8.00

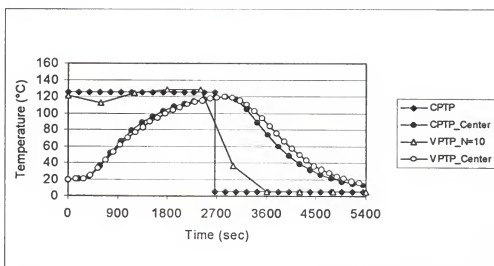


Figure 3-17. Comparison of the CPTP and the best VPTP with resulting center temperature profiles (Finite Cylinder-2, $r=30$ mm, $L=60$ mm, $t=90$ min, $N=10$, Objective Function: VACN).

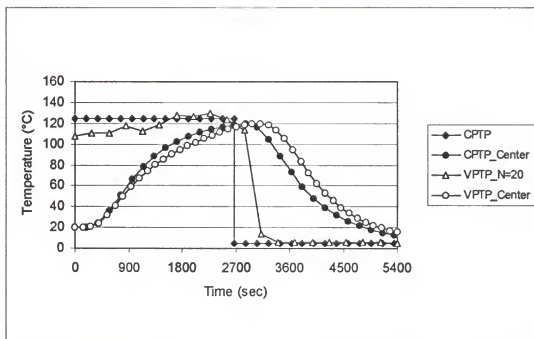


Figure 3-18. Comparison of the CPTP and the best VPTP with resulting center temperature profiles (Finite Cylinder-2, $r=30$ mm, $L=60$ mm, $t=90$ min, $N=20$)

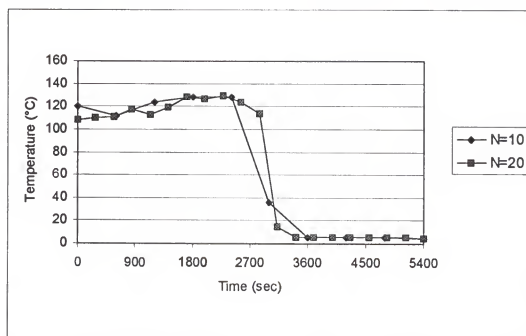


Figure 3-19. Comparison of the best calculated VPTPs of $N=10$ and $N=20$ for finite cylinder 2 ($r=30$ mm, $L=60$ mm, $t=90$ min, Objective Function: VACN).

Table 3-26. The calculated variable process temperature profiles (VPTP) of the model finite cylinder 2 ($r=30$ mm, $L=60$ mm) for the applied processing time of 135 min and the discretized time steps of $N=10$ (Objective Function: VACN).

Time (sec)	Variable Process Temperature Profiles (°C)					
	1	2	3	4	5	6
0	94.2	52.6	44.1	73.5	65.6	118.2
900	101.8	88.9	51.5	88.0	83.9	101.8
1800	127.3	88.6	122.5	95.5	75.7	106.3
2700	121.6	133.7	113.8	113.3	85.6	137.0
3600	98.7	124.1	135.0	122.3	124.0	93.7
4500	107.8	50.9	62.6	118.5	135.0	84.9
5400	56.0	55.0	54.2	80.8	50.2	67.1
6300	6.2	13.3	16.4	6.5	6.7	8.6
7200	5.7	6.5	6.1	5.6	6.1	5.9
8100	5.0	5.0	5.0	5.0	5.0	5.0

Table 3-27. The VACN (%), SCN(%), and F_0 (min) results of the calculated VPTPs of the model finite cylinder 1 ($r=30$ mm, $L=60$ mm) for the processing time of 135 min and two different discretized time steps of $N=10$ (Objective Function: VACN)

Trials	N=10		
	VACN (%)	SCN (%)	F_0 (min)
1	68.11	58.81	8.00
2	70.87	57.25	8.00
3	70.67	57.61	8.00
4	71.60	65.10	8.00
5	70.89	57.08	8.00
6	69.65	57.08	8.00
Average	70.30 ± 1.24	58.82 ± 3.15	8.00

Objective function: surface retention of nutrient

Sphere

The processing times of 20 min for sphere 1, and 80 min for sphere 2 with two different discretized time steps ($N=10$; $N=20$) were used to see the improvements in the SCN and VACN values as a result of the VPTPs compared to the CPTP processes. As seen in Table 3-1, the CPTP process gave the VACN and SCN values of 86.57% and 81.36% for sphere-1, and 71.36% and 60.45% for sphere-2, respectively. When the VACN values was used as objective function in the optimization with VPTPs, there was no significant improvement in sphere-1, and up to 3 percentage points improvement in SCN values was obtained for sphere-2. Extending processing times did not improve these results.

Table 3-29. The calculated variable process temperature profiles (VPTP) of the model sphere 1 ($r=15$ mm) for processing time of 20 min and the discretized time steps of $N=20$ (Objective Function: SCN).

Time (sec)	Variable Process Temperature Profiles ($^{\circ}\text{C}$)									
	1	2	3	4	5	6	7	8	9	10
0.0	142.1	124.1	119.9	124.4	126.8	131.1	121.5	124.5	129.1	113.7
63.2	106.5	121.0	132.2	127.0	127.3	129.3	118.8	123.0	129.1	130.0
126.3	127.2	116.2	120.8	106.9	119.5	123.2	122.3	123.4	133.1	109.9
189.5	120.4	122.7	123.1	120.6	125.6	124.0	124.1	130.0	129.6	124.7
252.6	122.9	124.5	127.0	124.9	122.2	119.2	121.8	122.4	127.0	125.0
315.8	124.9	129.4	128.6	127.1	132.7	129.5	129.5	132.5	126.7	123.0
378.9	130.9	126.0	125.9	131.1	129.0	132.6	124.7	127.7	126.4	130.9
442.1	134.6	134.9	135.0	133.3	132.6	128.5	129.7	135.4	130.6	134.4
505.3	130.6	138.5	132.3	134.0	131.6	134.7	134.5	129.3	129.8	134.2
568.4	139.7	125.3	128.1	132.7	134.3	136.6	139.6	133.1	134.1	133.0
631.6	108.5	119.5	123.8	119.0	107.3	103.3	119.2	105.6	120.8	116.8
694.7	12.2	18.8	20.2	10.0	8.0	10.3	11.9	10.8	10.5	10.8
757.9	5.9	5.8	5.7	6.1	5.8	5.8	5.7	5.6	5.7	5.9
821.1	5.9	5.7	5.8	5.9	5.7	5.8	5.7	5.8	5.7	5.7
884.2	5.6	5.7	5.8	5.7	5.9	5.7	5.7	5.8	5.8	5.8
947.4	5.7	5.8	5.6	5.3	5.7	5.8	5.8	5.7	5.7	6.0
1010.5	5.6	5.7	5.8	5.9	5.8	5.7	5.7	5.5	5.8	5.9
1073.7	5.8	5.7	5.6	5.8	5.7	5.7	5.7	5.6	5.7	5.8
1136.8	5.7	5.7	5.8	5.7	5.8	5.8	5.8	5.8	5.8	5.8
1200.0	5.0	5.0	5.0	5.0	5.0	5.0	5.0	5.0	5.0	5.0

Figures 3-20 and 3-21 show comparisons of the CPTP and VPTP giving the highest %SCN value, and the resulting center temperature profiles for the discretized time steps of $N=10$ (Trial 8, Table 3-30), and $N=20$ (Trial 4; Table 3-30), respectively, for the processing time of 20 min.

Table 3-30. The VACN (%), SCN(%), and F_0 (min) results of the calculated VPTPs of the model sphere 1 ($r=15$ mm) for the processing time of 20 min and two different discretized time steps of $N=10$ and $N=20$ (Objective Function: SCN).

Trials	N=10			N=20		
	VACN (%)	SCN (%)	F_0 (min)	VACN (%)	SCN (%)	F_0 (min)
1	87.17	82.16	8.00	87.35	82.81	8.00
2	87.21	82.26	8.01	87.44	83.08	8.01
3	87.09	81.89	8.00	87.27	82.93	8.00
4	87.34	82.91	8.04	87.47	83.12	8.01
5	87.05	81.91	8.00	87.30	82.88	8.00
6	87.19	82.11	8.00	87.22	82.58	8.00
7	87.20	82.23	8.00	87.17	82.52	8.00
8	87.58	83.81	8.03	87.23	82.76	8.01
9	87.31	82.62	8.00	86.73	81.90	8.03
10	87.02	81.78	8.12	87.44	83.03	8.00
Average	87.22 \pm 0.16	82.37 \pm 0.61	8.02	87.26 \pm 0.21	82.77 \pm 0.36	8.01

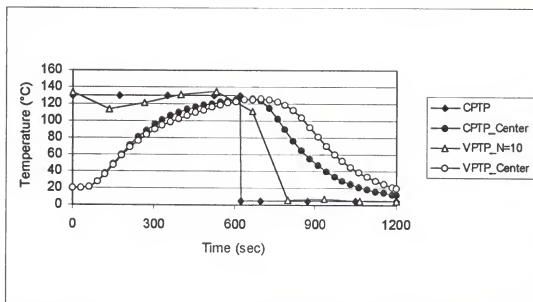


Figure 3-20. Comparison of the CPTP and the best VPTP with resulting center temperature profiles (Sphere-1, $r=15$ mm, $t=20$ min, $N=10$, Objective Function: SCN).

Table 3-33. The VACN (%), SCN(%), and F_0 (min) results of the calculated VPTPs of the model sphere 1 ($r=30$ mm) for the processing time of 80 min and two different discretized time steps of $N=10$ and $N=20$ (Objective Function: SCN).

Trials	N=10			N=20		
	VACN (%)	SCN (%)	F_0 (min)	VACN (%)	SCN (%)	F_0 (min)
1	72.99	63.73	8.01	73.05	64.86	8.06
2	73.01	63.93	8.01	72.80	63.54	8.00
3	73.40	65.94	8.00	73.33	65.17	8.00
4	72.90	64.37	8.29	72.98	64.47	8.02
5	72.98	63.71	8.00	73.27	65.29	8.05
6	73.52	66.22	8.03	73.46	65.51	8.01
7	73.11	64.59	8.00	73.17	65.07	8.03
8	73.16	65.53	8.20	73.51	65.60	8.00
9	72.81	63.22	8.01	72.63	64.61	8.00
10	73.03	63.66	8.00	73.52	65.51	8.00
Average	73.09 \pm 0.22	64.49 \pm 1.05	8.06	73.17 \pm 0.30	64.96 \pm 0.63	8.02

Tables 3-31 to 3-33 show the calculated VPTP results and resulting VACN, SCN, and F_0 values for sphere-2 for processing times of 80 min with the use of $N=10$ and $N=20$ and the SCN value as objective function. As seen in Table 3-33, the use of SCN as objective function improved the SCN (64.49% for $N=10$ and 64.96% for $N=20$, compared to 60.45% result of CPTP) and VACN values (73.09% for $N=10$ and 73.17% for $N=20$ compared to 71.36% result of CPTP) around 4 percentage points and 2 percentage points compared to the CPTP process, respectively compared to the improvements of 2 percentage points and 1.5 percentage points for SCN and VACN values, respectively when the VACN was used as the objective function.

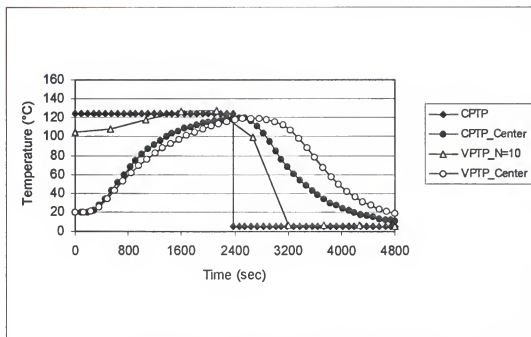


Figure 3-22. Comparison of the CPTP and the best VPTP with resulting center temperature profiles (Sphere-1, $r=30$ mm, $t=80$ min, $N=10$, Objective Function: SCN).

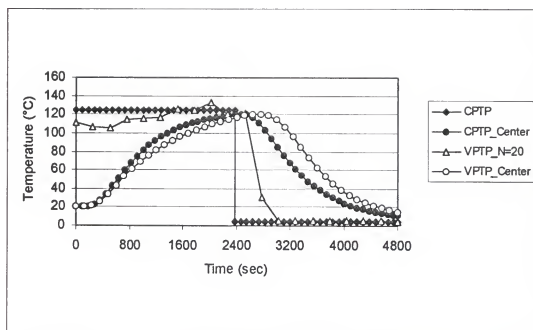


Figure 3-23. Comparison of the CPTP and the best VPTP with resulting center temperature profiles (Sphere-1, $r=30$ mm, $t=80$ min, $N=20$, Objective Function: SCN).

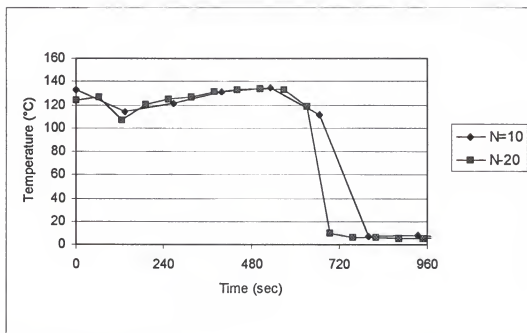


Figure 3-24. Comparison of the best calculated VPTPs of N=10 and N=20 for sphere 1 ($r=15$ mm, $t=20$ min, Objective Function: SCN).

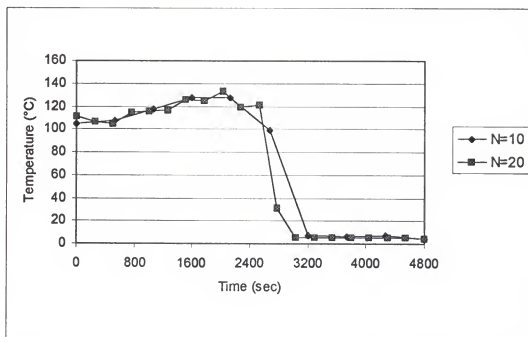


Figure 3-25. Comparison of the best calculated VPTPs of N=10 and N=20 for sphere 2 ($r=30$ mm, $t=80$ min, Objective Function: SCN).

Figures 3-22 and 3-23 show comparisons of the CPTP and VPTP giving the highest %VACN value, and the resulting center temperature profiles for the used discretized time steps of $N=10$ (Trial 6, Table 3-33), and $N=20$ (Trial 10; Table 3-33), respectively, for the processing time of 20 min. These results showed that the use of the two objective functions (VACN and SCN) in model spheres did not cause significant differences and improvements in the resulting VACN values (maximum of 2 percentage points). However, the use of VPTPs caused some improvements on the surface retention compared to the CPTPs (maximum of 6 percentage points) even though the overall retention did not change significantly. Figures 3-24 (Trial 8 in Table 3-28 and Trial 4 in Table 3-29) show and 3-25 (Trial 6 in Table 3-30 and Trial 10 in Table 3-32) the comparison of the best calculated VPTPs of $N=10$ $N=20$ with respect to the objective function of SCN for the processing times of 20 min for sphere 1. The change of center temperatures of the model systems with respect to the VPTPs are given in Appendix D.

Finite Cylinder

The processing times of 16 min for finite cylinder-1, and 90 min for finite cylinder-2 with discretized time step of $N=10$ were used to see the improvements in the SCN and VACN values as a result of the VPTPs compared to the CPTP processes using the SCN as objective function. As seen in Table 3-15, the CPTP process gave the VACN and SCN values of 90.86% and 83.61% for finite cylinder-1, and 68.06% and 49.20% for finite cylinder-2, respectively. When the VACN values were used as objective function in the optimization with VPTPs, there was around 1 to 2.5 percentage points improvement for both cylinders in VACN. However, up to 4 to 6.3 percentage points improvement in SCN

values were obtained. Extending processing times did not improve these results. Tables 3-34 and 3-35 show the calculated VPTP results and resulting VACN (91.78%), SCN (86.59%), and F_0 values for finite cylinder-1 for the processing times of 16 min for $N=10$, using SCN as objective function, compared to 90.86% VACN and 83.61% SCN results of CPTP. This showed that the use of SCN as objective function did not result in significant changes in SCN and VACN values compared to the objective function of VACN. The improvement in SCN and VACN values were around 3 and 1 percentage points, respectively compared to the CPTP process. Figure 3-26 shows the comparisons of the CPTP and VPTP giving the highest %SCN value, and the resulting center temperature profiles for the used discretized time steps of $N=10$ (Trial 3, Table 3-35) for the processing time of 16 min.

Table 3-34. The calculated variable process temperature profiles (VPTP) of the model finite cylinder 1 ($r=15$ mm, $L=15$ mm) for processing time of 16 min and the discretized time steps of $N=10$ (Objective Function: SCN).

Time (sec)	Variable Process Temperature Profiles ($^{\circ}\text{C}$)					
	1	2	3	4	5	6
0.0	112.6	108.6	113.5	128.6	107.2	119.4
106.7	124.7	118.0	105.1	118.7	101.9	96.3
213.3	125.8	113.0	119.1	112.8	117.5	117.4
320.0	126.5	120.7	127.3	125.4	115.5	127.5
426.7	130.7	135.3	134.2	133.5	137.8	132.7
533.3	115.2	129.8	121.1	126.2	132.1	127.6
640.0	24.6	25.5	22.5	22.3	23.7	26.4
746.7	5.7	5.7	5.6	5.9	5.9	5.9
853.3	5.7	5.4	6.3	5.8	5.8	5.6
960.0	5.0	5.0	5.0	5.0	5.0	5.0

Table 3-35. The VACN (%), SCN(%), and F_0 (min) results of the calculated VPTPs of the model finite cylinder 1 ($r=15$ mm, $L=15$ mm) for time of 16 min and discretized time steps of $N=10$ (Objective Function: SCN).

Trials	VACN (%)	SCN (%)	F_0 (min)
1	91.29	86.12	8.00
2	91.80	86.56	8.00
3	92.01	87.14	8.00
4	91.66	86.30	8.00
5	91.87	86.36	8.01
6	92.03	87.07	8.00
Average	91.78 ± 0.27	86.59 ± 0.42	8.00

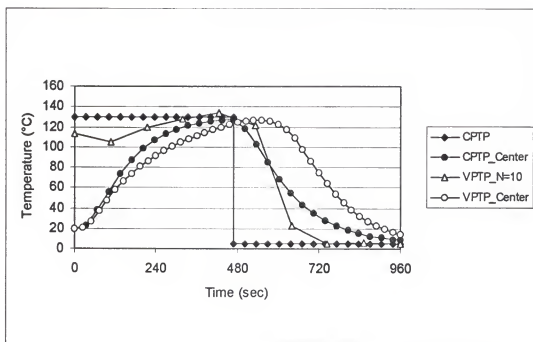


Figure 3-26. Comparison of the CPTP and the best VPTP with resulting center temperature profiles (Finite Cylinder-1, $r=15$ mm, $L=15$ mm, $t=16$ min, $N=10$, Objective Function: SCN).

Tables 3-36 and 3-37 show the calculated VPTP results and resulting VACN, SCN, and F_0 values for finite cylinder-2 for the processing times of 90 min with $N=10$ when SCN value was used as objective function. As seen in Table 3-37, the use of SCN as objective function improved the SCN and VACN values around 5 and 2 percentage points compared to the CPTP process, respectively. The improvements, when the VACN was used as objective function, were around 4 and 1.7 percentage points for SCN and VACN values, respectively. Therefore, there was no significant improvement with respect to the use of different objective functions Figure 3-27 shows the comparisons of the CPTP and VPTP giving the highest %SCN value, and the resulting center temperature profiles for the discretized time steps of $N=10$ (Trial 4, Table 3-36) for the processing time of 90 min. The change of center temperatures of the model systems with respect to the VPTPs are given in Appendix E.

Table 3-36. The calculated variable process temperature profiles (VPTP) of the model finite cylinder 1 ($r=30$ mm, $L=60$ mm) for processing time of 90 min and the discretized time steps of $N=10$ (Objective Function: SCN).

Time (sec)	Variable Process Temperature Profiles ($^{\circ}\text{C}$)					
	1	2	3	4	5	6
0	106.8	114.9	112.8	119.5	117.4	126.9
600	115.3	110.8	114.8	111.5	114.7	112.8
1200	122.8	124.0	121.7	119.4	122.7	125.8
1800	129.0	129.2	130.2	127.8	129.8	127.9
2400	129.0	129.3	127.9	130.7	130.7	127.2
3000	47.7	40.9	45.5	73.7	31.5	37.6
3600	5.6	5.6	5.9	5.0	5.9	5.9
4200	5.6	5.8	5.6	6.0	5.8	5.8
4800	5.9	5.6	5.7	6.8	5.6	5.8
5400	5.0	5.0	5.0	5.0	5.0	5.0

Table 3-37. The VACN (%), SCN(%), and F_0 (min) results of the calculated VPTPs of the model finite cylinder 1 ($r=30$ mm, $L=60$ mm) for the processing time of 90 min and discretized time steps of $N=10$ (Objective Function: SCN).

Trials	VACN (%)	SCN (%)	F_0 (min)
1	70.09	54.46	8.00
2	70.02	54.06	8.01
3	70.11	54.32	8.00
4	70.18	55.25	8.36
5	69.85	53.54	8.06
6	69.82	53.23	8.00
Average	70.01 ± 0.15	54.14 ± 0.72	8.07

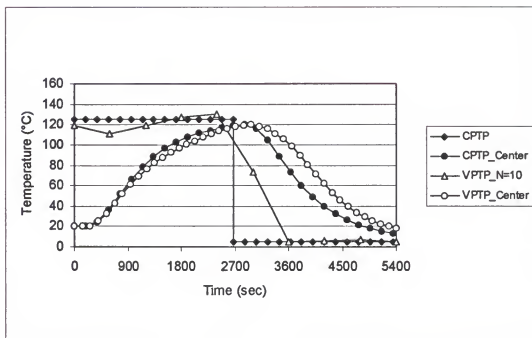


Figure 3-28. Comparison of the CPTP and the best VPTP with resulting center temperature profiles (Finite Cylinder-2, $r=30$ mm, $L=60$ mm, $t=90$ min, $N=10$, Objective Function: SCN).

Optimization with double geometry

Four combinations of sphere and finite cylinder geometries were used for the double geometry systems (A: sphere 1 - finite cylinder 1; B: sphere 2 - finite cylinder 1; C: sphere 1 - finite cylinder 2; D: sphere 2 - finite cylinder 2) to evaluate the VPTPs and test the reproducibility using the objective function of VACN (Eq. 20a). The total processing times were chosen based on the single geometry system (20 min for system A; 80 min for B; 90 min for C; and 90 min for D), and the resulting VACN and SCN results were compared with the results of the CPTP process applied to the system. The

processing times were chosen as the minimum time required for the satisfaction of implicit constraints for both geometries when the CPTP processes were used individually.

Table 3-38 shows the calculated VPTPs for the double geometry system A with a total processing time of 20 min and $N=10$. Table 3-39 shows the weighted objective function, and VACN, SCN, and F_0 values for each geometry. As seen in Table 3-39 the VACN and SCN values are 87.09% and 81.85% for the sphere 1 and 84.38 and 77.82 for the finite cylinder 1, respectively. Table 3-1 gave the optimization results using CPTP for sphere 1 as 86.57% and 81.36% for VACN and SCN, respectively. When the CPTP obtained for sphere 1 was applied on the system A, imagining both geometries are in the same medium and having the same process, this resulted in 83.87% VACN and 76.91% SCN with a F_0 value of 25.55 min for the finite cylinder 1. The weighted objective function value for the CPTP process was 85.22% compared to the 85.74% value of the VPTP process. Table 3-39 shows the advantage of the VPTP process in all aspects compared to the CPTP process. Figures 3-28 and 3-29 show the comparisons of the CPTP and VPTP (trial 6; Table 3-39), giving the highest weighted objective function value, with respect to the resulting center temperature profiles. The results for double geometry system B are given in Tables 3-40 and 3-41 for a total processing time of 20 min and $N=10$. As seen in Table 3-41 the VACN and SCN values are 72.93% and 63.71% for the sphere 2 and 58.88 and 56.14 for the finite cylinder 1, respectively. Table 3-1 gave the optimization results using CPTP for sphere 2 as 71.36% and 60.45% for VACN and SCN, respectively. When the CPTP for sphere 2 was applied to the system B, this resulted in 52.86% VACN and 49.58% SCN with an F_0 value of 79.46 min in finite cylinder 1. The

weighted objective function value for the CPTP process was 62.11% compared to the 65.91% value of the VPTP process. Table 3-41 shows the advantage of the VPTP process compared to the CPTP process, and Figures 3-29 and 3-30 show the comparisons of the CPTP and VPTP (trial 5; Table 3-41).

Table 3-38. The calculated variable process temperature profiles (VPTP) for double geometry system consisting of a sphere ($r=15$ mm) and a finite cylinder ($r=15$ mm, $L=15$ mm) for the processing time of 20 min and discretized time steps of $N=10$ (Objective Function: VACN).

Time (sec)	Variable Process Temperature Profiles (°C)					
	1	2	3	4	5	6
0.0	119.1	141.2	131.3	126.3	127.3	123.5
133.3	122.3	106.1	118.0	122.4	126.0	120.1
266.7	126.1	131.5	127.9	127.1	125.6	124.8
400.0	134.4	130.9	135.8	137.8	135.9	136.2
533.3	140.2	143.9	136.6	132.8	135.7	138.2
666.7	32.0	37.3	33.8	36.2	34.2	42.4
800.0	5.7	6.0	5.9	5.7	6.0	6.3
933.3	6.2	5.9	6.1	5.9	5.2	5.9
1066.7	5.6	6.1	5.6	5.8	5.9	5.1
1200.0	5.0	5.0	5.0	5.0	5.0	5.0

Table 3-39. The VACN (%), SCN(%), and F_0 (min) results of the calculated VPTPs of double geometry system consisting of a sphere ($r=15$ mm) and a finite cylinder ($r=15$ mm, $L=15$ mm) for the processing time of 20 min and discretized time steps of $N=10$ (Objective Function: VACN).

VPTP Trials	Weighted Objective Function	Sphere ($r=15$ mm)			Finite Cylinder ($r=15$ mm, $L=15$ mm)		
		VACN (%)	SCN (%)	F_0 (min)	VACN (%)	SCN (%)	F_0 (min)
1	85.70	87.05	81.79	8.00	84.33	77.88	32.88
2	85.55	86.94	81.39	8.00	84.16	76.92	32.97
3	85.81	87.15	82.00	8.01	84.46	78.03	32.68
4	85.78	87.16	82.04	8.01	84.41	78.09	32.88
5	85.83	87.10	81.92	8.00	84.37	77.82	31.25
6	85.84	87.15	81.99	8.02	84.53	78.18	32.82
VPTP Average	85.74 ± 0.11	87.09 ± 0.09	81.85 ± 0.25	8.01	84.38 ± 0.13	77.82 ± 0.46	32.58
CPTP	85.22	86.57	81.36	8.06	83.87	76.91	25.55

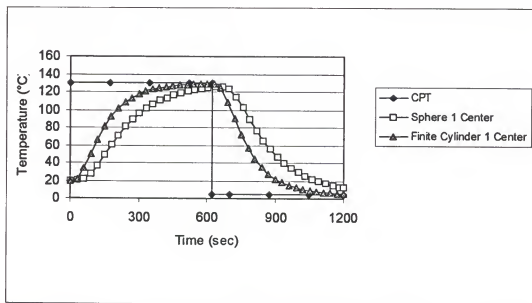


Figure 3-28. Comparison of the sphere 1 ($r=15$ mm) and finite cylinder 1 ($r=15$ mm, $L=15$ mm) center temperature profiles, subjected to the CPTP for sphere 1 ($r=15$ mm, Objective Function: VACN).

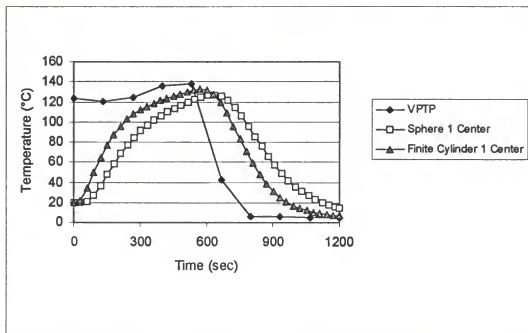


Figure 3-29. Comparison of the sphere 1 ($r=15$ mm) and finite cylinder 1 ($r=15$ mm, $L=15$ mm) center temperature profiles, subjected to the optimum VPTP for this double geometry system (Objective Function: VACN).

Table 3-40. The calculated variable process temperature profiles (VPTP) for double geometry system consisting of a sphere ($r=30$ mm) and a finite cylinder ($r=15$ mm, $L=15$ mm) for the processing time of 80 min and discretized time steps of $N=10$ (Objective Function: VACN).

Time (sec)	Variable Process Temperature Profiles (°C)					
	1	2	3	4	5	6
0.0	120.6	110.6	112.8	131.0	116.9	78.4
533.3	112.0	115.3	113.5	119.6	112.7	112.5
1066.7	113.6	116.3	120.0	115.0	120.2	121.9
1600.0	127.4	128.9	130.0	127.6	130.4	125.9
2133.3	135.2	132.2	128.6	128.7	126.9	135.3
2666.7	59.4	51.8	44.7	71.7	52.6	55.8
3200.0	6.0	5.8	5.7	6.6	5.9	5.4
3733.3	5.7	5.6	5.8	5.8	5.7	5.7
4266.7	5.7	5.7	5.7	5.6	5.7	5.7
4800.0	5.0	5.0	5.0	5.0	5.0	5.0

Table 3-41. The VACN (%), SCN(%), and F_0 (min) results of the calculated VPTPs of double geometry system consisting of a sphere ($r=30$ mm) and a finite cylinder ($r=15$ mm, $L=15$ mm) for the processing time of 80 min and discretized time steps of $N=10$ (Objective Function: VACN).

VPTP Trials	Weighted Objective Function	Sphere ($r=30$ mm)			Finite Cylinder ($r=15$ mm, $L=15$ mm)		
		VACN (%)	SCN (%)	F_0 (min)	VACN (%)	SCN (%)	F_0 (min)
1	65.86	72.93	63.51	8.00	58.79	55.82	90.36
2	66.10	72.99	63.74	8.02	59.20	56.68	90.73
3	66.16	73.04	63.86	8.03	59.29	56.85	83.63
4	65.35	72.75	63.91	8.00	57.95	54.29	65.32
5	66.35	73.12	64.19	8.00	59.59	57.06	79.33
6	65.61	72.93	63.71	8.00	58.47	56.14	103.48
VPTP Average	65.91 ± 0.37	72.93 ± 0.15	63.71 ± 0.40	8.01	58.88 ± 0.60	56.14 ± 1.02	85.48 ± 12.83
CPTP	62.11	71.36	60.45	8.04	52.86	49.58	79.76

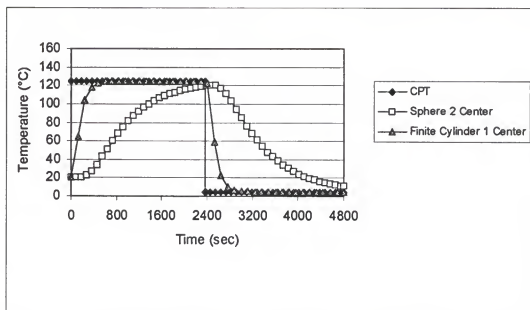


Figure 3-30. Comparison of the sphere 2 ($r=30$ mm) and finite cylinder 1 ($r=15$ mm, $L=15$ mm) center temperature profiles, subjected to the CPTP for sphere 2 ($r=30$ mm, Objective Function: VACN).

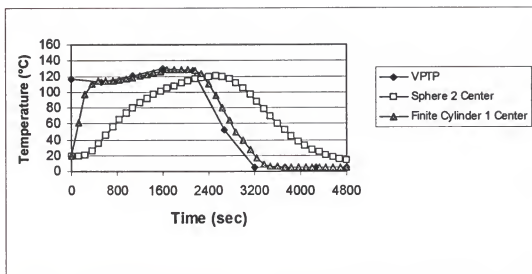


Figure 3-31. Comparison of the sphere 2 ($r=30$ mm) and finite cylinder 1 ($r=15$ mm, $L=15$ mm) center temperature profiles, subjected to the optimum VPTP for this double geometry system (Objective Function: VACN).

Table 3-42. The calculated variable process temperature profiles (VPTP) for double geometry system consisting of a sphere ($r=15$ mm) and a finite cylinder ($r=30$ mm, $L=60$ mm) for the processing time of 90 min and discretized time steps of $N=10$ (Objective Function: VACN).

Time (sec)	Variable Process Temperature Profiles (°C)					
	1	2	3	4	5	6
0	127.1	107.6	114.0	103.6	111.7	126.3
600	111.1	117.7	116.4	116.9	114.2	108.9
1200	122.7	120.1	120.6	121.3	123.3	124.8
1800	127.4	130.1	129.6	127.3	127.0	128.2
2400	130.5	131.0	130.2	133.5	133.1	130.3
3000	50.2	24.5	33.0	38.5	30.7	30.7
3600	6.5	5.4	5.8	5.9	5.7	5.9
4200	5.6	6.1	5.8	5.8	5.6	5.9
4800	5.4	5.8	5.7	5.8	5.7	5.9
5400	5.0	5.0	5.0	5.0	5.0	5.0

Table 3-42 shows the calculated VPTPs for the double geometry system C with a total processing time of 90 min and $N=10$. Table 3-43 shows the weighted objective function, and VACN, SCN, and F_0 values for each geometry. As seen in Table 3-43 the VACN and SCN values are 53.10% and 51.67% for the sphere 1 and 69.85% and 53.44% for the finite cylinder 2, respectively. The optimization results using CPTP for finite cylinder 2, given in Table 3-15 was 68.06% and 49.21% for VACN and SCN, respectively. When the CPTP for finite cylinder 2 was applied to the system C, this resulted in 49.04% VACN and 46.95% SCN with a F_0 value of 82.30 min in sphere 1. The weighted objective function value for the CPTP process was 58.55% compared to the 61.47% value of the VPTP process. Table 3-43 shows the advantage of the VPTP process in all aspects compared to the CPTP process. Figures 3-32 and 3-33 show the comparisons of the CPTP and VPTP (trial 1; Table 3-43) and the resulting center temperature profiles. The results for double geometry system D are given in Tables 3-44 and 3-45 for a total processing time of 90 min and $N=10$. As seen in Table 3-44 the VACN and SCN values are 67.04% and 58.22% for the sphere 2 and 70.12 and 54.01 for the finite cylinder 2, respectively. The optimization results using CPTP for finite cylinder 2 was 68.06% and 49.20% for VACN and SCN, respectively. When the CPTP for finite cylinder 2 was applied on the system D, this resulted in 65.04% VACN and 54.57% SCN with a F_0 value of 15.26 min in sphere 2. The weighted objective function value for the CPTP process was 66.55% compared to the 68.58% value of the VPTP process. Table 3-45 shows the advantage of the VPTP compared to the CPTP process, and Figures 3-34 and 3-33 show the comparisons of the CPTP and VPTP (trial 6; Table 3-45).

Table 3-43. The VACN (%), SCN(%), and F_0 (min) results of the calculated VPTPs of double geometry system consisting of a sphere ($r=15$ mm) and a finite cylinder ($r=30$ mm, $L=60$ mm) for the processing time of 90 min and discretized time steps of $N=10$ (Objective Function: VACN).

VPTP Trials	Weighted Objective Function	Sphere ($r=15$ mm)			Finite Cylinder ($r=30$ mm, $L=60$ mm)		
		VACN (%)	SCN (%)	F_0 (min)	VACN (%)	SCN (%)	F_0 (min)
1	62.03	53.96	52.32	82.57	70.10	53.91	8.01
2	61.13	52.54	51.24	105.37	69.71	53.13	8.00
3	61.48	53.07	51.75	96.69	69.89	53.58	8.01
4	61.40	53.00	51.71	100.03	69.80	53.55	8.00
5	61.33	52.91	51.55	97.88	69.75	53.35	8.01
6	61.46	53.09	51.46	93.90	69.84	53.12	8.00
VPTP Average	61.47 ± 0.30	53.10 ± 0.47	51.67 ± 0.47	96.07 ± 7.65	69.85 ± 0.14	53.44 ± 0.30	8.01
CPTP	58.55	49.04	46.95	82.30	68.06	49.20	8.04

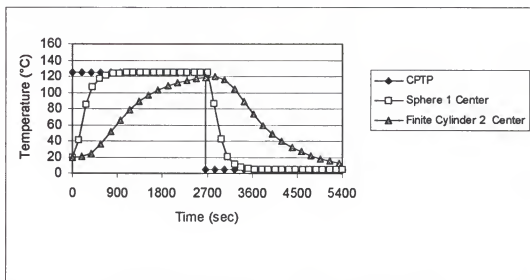


Figure 3-32. Comparison of the sphere 1 ($r=15$ mm) and finite cylinder 2 ($r=30$ mm, $L=60$ mm) center temperature profiles, subjected to the CPTP for finite cylinder 2 ($r=30$ mm, $L=60$ mm, Objective Function: VACN).

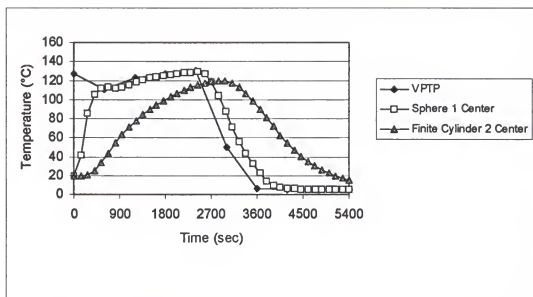


Figure 3-33. Comparison of the sphere 1 ($r=15$ mm) and finite cylinder 2 ($r=30$ mm, $L=60$ mm) center temperature profiles, subjected to the optimum VOTP for double geometry system (Objective Function: VACN).

Table 3-44. The calculated variable process temperature profiles (VOTP) for double geometry system consisting of a sphere ($r=30$ mm) and a finite cylinder ($r=30$ mm, $L=60$ mm) for the processing time of 90 min and discretized time steps of $N=10$ (Objective Function: VACN).

Time (sec)	Variable Process Temperature Profiles (°C)					
	1	2	3	4	5	6
0	110.5	117.9	119.7	134.4	119.1	122.5
600	116.3	116.2	117.1	108.1	118.4	97.0
1200	124.1	119.1	118.9	122.5	118.0	108.8
1800	129.8	130.1	132.5	129.2	131.3	124.1
2400	126.7	129.7	125.9	129.5	128.5	133.0
3000	38.0	39.9	36.7	39.0	32.8	111.0
3600	5.6	5.8	5.7	5.8	5.7	9.4
4200	5.7	5.7	5.7	5.8	5.2	5.7
4800	5.8	5.8	5.4	5.7	5.7	5.2
5400	5.0	5.0	5.0	5.0	5.0	5.0

Table 3-45. The VACN (%), SCN(%), and F_0 (min) results of the calculated VPTPs of double geometry system consisting of a sphere ($r=30$ mm) and a finite cylinder ($r=30$ mm, $L=60$ mm) for the processing time of 90 min and discretized time steps of $N=10$ (Objective Function: VACN).

VPTP Trials	Weighted Objective Function	Sphere ($r=30$ mm)			Finite Cylinder ($r=15$ mm, $L=15$ mm)		
		VACN (%)	SCN (%)	F_0 (min)	VACN (%)	SCN (%)	F_0 (min)
1	68.19	66.57	57.64	16.15	69.82	53.79	8.08
2	68.42	66.86	57.83	15.83	69.98	53.69	8.00
3	68.29	66.73	57.57	16.02	69.86	53.24	8.01
4	68.36	66.87	57.73	15.75	69.85	52.54	8.00
5	68.25	66.70	57.42	15.92	69.86	53.26	8.00
6	69.94	68.47	61.13	14.37	71.42	57.75	8.00
VPTP Average	68.58 ± 0.67	67.04 ± 0.71	58.22 ± 1.43	15.67 ± 0.65	70.12 ± 0.64	54.01 ± 1.89	8.02
CPTP	66.55	65.04	54.27	15.26	68.06	49.20	8.04

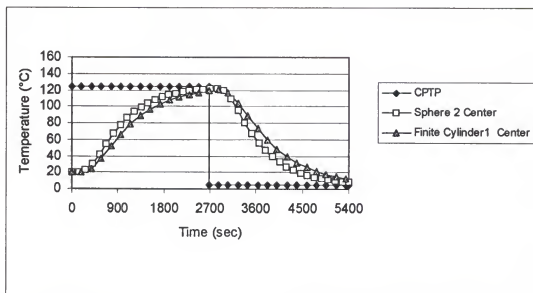


Figure 3-34. Comparison of the sphere 2 ($r=30$ mm) and finite cylinder 2 ($r=30$ mm, $L=60$ mm) center temperature profiles, subjected to the CPTP for finite cylinder 2 ($r=30$ mm, $L=60$ mm, Objective Function: VACN).

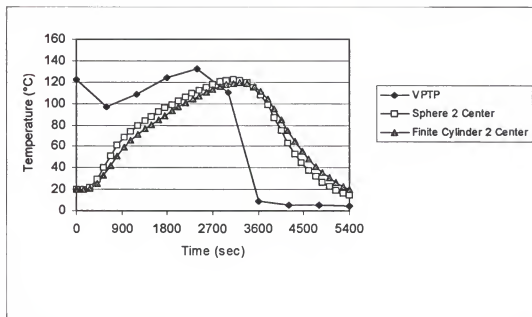


Figure 3-35. Comparison of the sphere 2 ($r=30$ mm) and finite cylinder 2 ($r=30$ mm, $L=60$ mm) center temperature profiles, subjected to the optimum VPTP for double geometry system (Objective Function: VACN)

As seen in the tables and figures above, the VPTPs resulted in better VACN and SCN results in the double geometry systems compared to the CPTPs. The improvements were more obvious when the VPTP was applied to the system containing a larger and a smaller geometry (like systems B and C). The improvements in VACN and SCN were 6 and 7 percentage points in system B, and 3 and 4 percentage points in system C in the smaller geometries (finite cylinder 1 in B and sphere 1 in C). The center temperature profiles for each geometry in each system with the VPTPs are given in Appendix F.

The critical objects were sphere-1 for system A, sphere-2 for system B, and finite cylinder-2 for systems C and D. Therefore, the following figures 3-36 to 3-39 show a comparison of the best VPTPs of double geometry systems and critical objects for $N=10$ for the objective function of VACN.

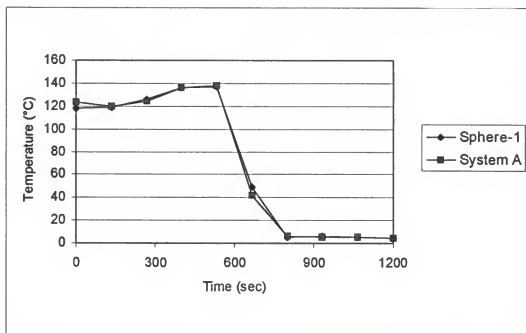


Figure 3-36. Comparison of the best VPTPs for sphere 1 ($r=15$ mm) and system A (sphere 1: $r=15$ mm; finite cylinder 1: $r=15$ mm, $L=15$ mm) for $N=10$ (Objective Function: VACN).

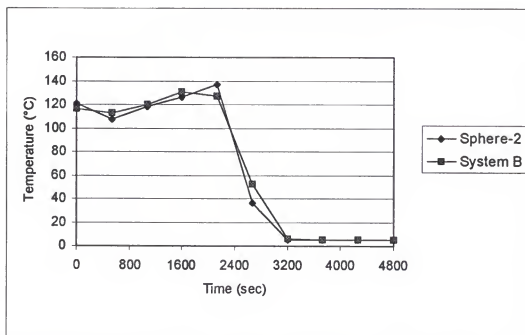


Figure 3-37. Comparison of the best VPTPs for sphere 2 ($r=15$ mm) and system B (sphere 2: $r=30$ mm; finite cylinder 1: $r=15$ mm, $L=15$ mm) for $N=10$ (Objective Function: VACN).

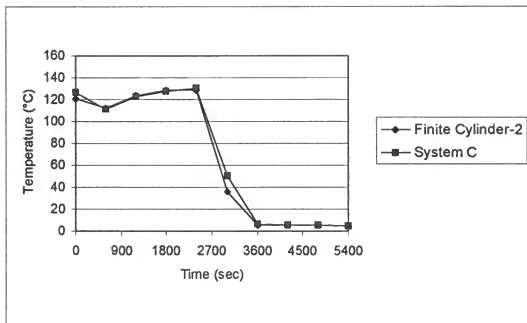


Figure 3-38. Comparison of the best VPTs for finite cylinder 2 ($r=30$ mm, $L=60$ mm) and system C (sphere 1: $r=15$ mm; finite cylinder 2: $r=30$ mm, $L=60$ mm) for $N=10$ (Objective Function: VACN).

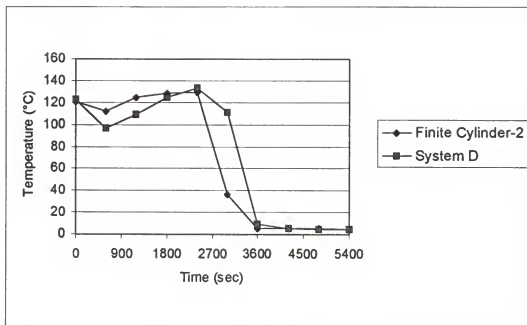


Figure 3-39. Comparison of the best VPTs for finite cylinder 2 ($r=30$ mm, $L=60$ mm) and system D (sphere 2: $r=30$ mm; finite cylinder 2: $r=30$ mm, $L=60$ mm) for $N=10$ (Objective Function: VACN).

There were big differences in the optimum results of the single smaller geometries when they combined with the larger geometries to make a double geometry system. For example, the optimum result for sphere 1 when optimized alone was (86.57% VACN for CPTP and 87.14% VACN for VPTP). The VACN objective function value for sphere 1 in system C (when optimized in combination with a larger body) dropped to 53.10%. Similarly, the optimum result for finite cylinder 1 when optimized alone was from 90.86% for CPTP and 91.89% for VPTP, and dropped to 58.88% in system B when optimized in combination with a larger body. These big drops were the result of the larger geometries being the critical objects in the double geometry systems and that the method was required to satisfy the implicit constraints for them.

As seen in the Figures 3-36 to 3-39, the optimum VPTPs were very similar for system A (87.10% VACN for sphere 1) and sphere 1 alone (87.22% VACN), for system B (73.12% VACN for sphere 2) and sphere 2 alone (73.54% VACN), and for system C (70.10% VACN for finite cylinder 2) and finite cylinder 2 alone (71.65% VACN) both graphically and with respect to their objective function values. However, for system D, these values were 71.42% versus 71.65% in the case of system D, and the best VPTPs were not similar graphically even though they resulted in similar VACN values. All these results showed that, the different VPTPs all tend to result in very similar objective function values for single or double geometry systems. Therefore, it can be thought that the resulting objective function value may be a true maximum for these systems. All the calculated profiles for single or double geometry systems were similar to the profiles reported by Teixeira et al. (1975b), Saguy and Karel (1979), and Noronha et al. (1996b).

Uniqueness and Reproducibility Issues

Literature review showed that none of the studies regarding the optimization of thermal processing for single or multi-geometry systems addressed the uniqueness or the reproducibility of the methods in terms of the calculated process temperature profile or the resulting objective function.

Saguy and Karel (1979) used the Pontryagin's maximum principle to optimize the thiamin retention in conduction-type heating of canned foods. They concluded that a unique retort temperature profile to optimize the nutrient retention existed. However, there was no data, proof or discussion to support this claim strongly. Banga et al. (1991) used a nonlinear programming algorithm for the maximization of a quality factor in conduction-heated canned foods. The advantages of the variable process temperature processes over the constant temperature processes, and the unconditional convergence of the algorithm were discussed. Noronha et al. (1993 and 1996b) used the quasi-Newton optimization algorithm and the complex method to determine the variable process temperature profile for the infinite geometries (infinite cylinder, infinite slab, sphere) and for packed foods of different systems, respectively without giving any information on the reproducibility of the method and uniqueness of the result.

When the calculated variable process temperature profiles given in Appendices B to F were carefully observed, one can see similar trends even though none of them is exactly the same as the other. For example, for the figures for sphere 1 ($r=15$ mm, $t=20$

min, $N=10$) in Appendix B, If the initial trajectory of the profiles were discarded, it will be easy to see that all of them follows very similar paths, increasing up to 140 °C (not more than that) and rapidly cooling to the lower temperature limit of (5 °C). All these profiles produced very similar objective function values, which differed no more than 1-2%. These differences can be claimed to be the result of the randomly calculated starting variable temperature profiles. Including some more explicit constraints, e.g., putting an initial heating period to the process as it was done for the end of the process, might help reduce these differences occurring especially at the beginning of the process. As seen in Appendix F, the calculated VPTPs for the double geometry systems for different runs were more similar to each other compared the single geometry systems. Therefore, making the objective functions more complex might be resulting in more unique VPTPs. In the future studies, a more complex objective function, e.g., combination of VACN and SCN for the same system can be tried to see whether more unique profiles can be obtained, or not.

According to all the results obtained for both single and double geometry systems, it might be claimed that there is a unique solution with regard to the objective function and the calculated process temperature profile, and the modified Complex Method can reproduce the result. However, there are small differences in the results. These might be the result of the accumulation of truncation errors in the finite numerical procedures used for the transient temperature distribution calculation of the geometries and in the integration methods used for the calculation of the objective functions and the implicit constraints.

Hager (1988) gave a graph for the function:

$$y = 10^6 \cdot (x^6 - 6x^5 + 15x^4 - 20x^3 + 15x^2 - 6x + 1) \quad 3-1$$

where y was evaluated near $x=1$, and the computed points on the graph are connected with straight line segments. This equation is theoretically equal to the following:

$$y = 10^6 \cdot (x - 1)^6 \quad 3-2$$

which is always positive for $x \neq 1$. However, Figure 3-40 shows a fuzzy region where y might be even negative when x is around 1. This is basically due to the rounding error during the calculation procedure for graphing. It is to be thought that if even a small calculation might result in such a fuzzy region, then the series of numerical finite difference calculations and integrations might cause the accumulation of the truncation or rounding errors in the optimization routine, and it might not be possible to find the same exact result for each run since the result lies in a fuzzy region, as seen in Figure 3-40.

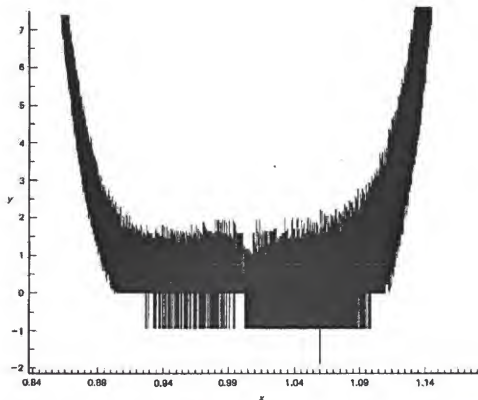


Figure 3-40. The computed graph of y versus x for equation 3-1.

Comparison With the Literature Results

Noronha et al. (1993) used quasi-Newton multivariable optimization algorithm to find the optimal variable retort temperature profiles for the sterilization of conduction heated foods of the different geometries (infinite cylinders, infinite slabs and infinite cylinders). The modified Complex Method was compared with a selected sphere case of their studies. The thermal and physical properties for these cases were given as follows:

	Case I.	Case II
Radius (mm)	16	16
F_0 (min)	6	9
z_{ref} for microbial lethality ($^{\circ}\text{C}$)	10	10
z_{ref} for quality factor ($^{\circ}\text{C}$)	30	30
D_{ref} for quality factor (s)	10716	10716
Total process time (min)	19.17	18.04
Initial Temperature ($^{\circ}\text{C}$)	40	40
Thermal diffusivity (m^2/s)	1.54×10^{-7}	1.54×10^{-7}
h ($\text{W}/\text{m}^2\text{-K}$)	∞	∞ in both heating and cooling
Surface retention (%)	85.1	83.5

The modified Complex Method was run for each case for 4 times. Since there was no information about the explicit constraints and the reached center temperature at the end of the process, the explicit constraints (the lower and higher limits of the variable profile) were used as they are, with the requirement that the center temperature would reach lower than the initial temperature. The surface retention was found as 85.1 ± 0.1 and 83.8 ± 0.1 per cent which are very similar to the values reported by Noronha et al. (1993). The calculated variable temperature profiles with resulting center temperature profiles by using the modified Complex Method developed in this study were given in Appendix G for the above two cases of Noronha et al. (1993). The similar results found by Noronha et al. (1993) and this might result in a conclusion that there is a unique and optimum profile which gives that result for the thermal processing optimization problems.

Among all the studies in the literature, the one published by Noronha et al. (1996b) seemed to be better than the others in the concept of showing that the optimization of multi geometry systems is possible. However, there were deficiencies like:

- To force the variable retort temperature profile into a certain function given in eq. 1-5 is simplistic. The random profiles could be described by a vector of temperatures equally spaced in time and generated using pseudo-random numbers, and some explicit constraints, e.g. lower and upper boundaries, for the variable temperature profile could be easily given.
- The lack of explanations about how the complex method was applied to the system and the decision criteria to end the optimization process.
- The lack of tracking the coldest point lethality during the application of optimization routine (the use of different variable temperature profiles might result in the change of the coldest point lethality for the critical product from one to another depending on the size and thermo-physical properties of the objects in the system).
- the lack, as seen in all the other studies, of discussion about the reproducibility and uniqueness of the resulting variable temperature profile and its associated results.

The modified complex method developed here eliminates the above mentioned assumptions, and gives the researcher an easy to apply method for the thermal processing of single and multi geometry systems. This method is also easy to modify for the multi-geometry systems, and for more restrictive objective functions and constraints.

CHAPTER 4 CONCLUSIONS AND RECOMMENDATIONS

Conclusions

- The developed algorithm for the modified Complex Method can be satisfactorily used for the optimization of thermal processing of conduction heated foods consisting of single or multi geometries.
- Simultaneous optimization of more than one quality factor is possible when the independent objective functions were associated into one function with the Weighted Method, and the violation of the constraints were followed by Lexicographic Ordering.
- The use of variable process temperature profiles can result in some increases in the objective functions of volume average and surface concentrations of nutrients compared to constant temperature profile processes.
- There was no significant difference between the applied objective functions of surface and volume average retentions for any variable profile.
- Improvements were more obvious in the larger size shapes and in the double geometry systems consisting of uneven sizes, e.g. one large and one small size of each geometry.

- Optimization of thermal processing is possible when variable temperature profiles are used as the decision variables for the maximization of nutrient retention. This is true for both single body alone and more than one body of different sizes and geometries.
- Since the mathematical manipulation of the Complex Method is easy, compared especially to the Pontryagin's maximum principle, this method gives an advantage of choosing the explicit and implicit constraints in any restrictive or non-restrictive way. Even though the examples of the center temperature and the coldest point lethality were used for the implicit constraints in the algorithm, for our case, it is easy to change these constraints into other forms, e.g. the surface or overall lethality. The implicit constraints can even be chosen in more restrictive ways, e.g. the maximum color degradation at the surface shall not be higher than 25%, or the minimum retention of thiamin shall not be lower than 70% at the surface.
- The application of the calculated profiles in classic retort systems does not seem practical since the temperature of the environment is controlled by steam pressure, and the sudden changes in pressure might result in bulges or breakages on the seals of the containers. However, the completely automated systems which may follow a prescribed time-temperature profile might be used to apply the calculated profiles although it does not seem to be practical for just few percentage point increases in the overall nutrient retention.

Recommendations

- The developed algorithm can also be adapted to find the minimum processing time required to comply with all the implicit constraints. It is also easy to add other shapes to the algorithm to make a triple or quadruple geometry system. In the way that the algorithm was developed, optimization for any shape or any food such as a conical shape, shrimp, or elliptical cylinders can be accomplished with the adjustment of minor details in the developed program (e.g. transient temperature distribution calculation program for the shape in question).
- The variable profiles can also be used to reduce the total processing times with the same lethality values resulting in economical advantages. At this point, the economical calculations have to be done to compare the results with the constant profiles, and this might trigger the use of variable profiles in the commercial practice.
- It might also be interesting to see how the variable thermal properties, the different reaction kinetics for the quality degradation and microbial reduction will affect the optimization results for the same processing conditions. With the developed software, it is easy to test these various conditions on the optimization problem.
- This software can be used easily in the thermal processing field to study the effects of constant and variable process temperature profiles on the implicit constraints and objective functions, and it can be easily used for educational purposes.

APPENDIX A THE COMPLEX METHOD

The Complex Method is a general and powerful optimization algorithm that arose from the idea of applying simplexes to find the maximum (or minimum) of a general non-linear function of several variables within a constrained region (Box, 1965; Umeda et al., 1972; Kazmierczak, 1996). Compared to Pontryagin's maximum principle, the Complex Method does not require gradients of the objective function, and it operates with information about the objective function associated with constraints (control levels) (Kazmierczak, 1996).

The Complex Method is based on a simplex algorithm where a simplex can be geometrically defined as a convex hull of $n+1$ points, or vertices, in R^n , where n denotes the number of controllable variables (Box, 1965; Kazmierczak, 1996). Therefore, it can be called the constrained simplex method. The method searches for the maximum (or minimum) value of a function:

$$f(x_1, \dots, x_n) \tag{1}$$

subject to m constraints of the form:

$$g_k \leq x_k \leq h_k, \quad k = 1, \dots, m \tag{2}$$

where

$$\begin{aligned}
x_k &= f(x_1, \dots, x_n) \\
g_k &= c_k \\
h_k &= d_k \\
g_k &= f(x_1, \dots, x_n) \\
h_k &= f(x_1, \dots, x_n)
\end{aligned}
\tag{3}$$

where c_k and d_k are constants. The method assumed that an initial point x_1^0, \dots, x_n^0 satisfied all the m available constraints (Box, 1965).

The method consists of six basic parts: initialization, ordering, reflection, expansion, retraction, and shrinkage (Kazmierczak, 1996). For the initialization, at least $n+1$ points (feasible vertices), each constant or consisting of specific time paths for each control variable must be identified and used to define the initial simplex. The first vertex is a given one satisfying all the explicit and implicit constraints. The further n vertices, required to set up the initial complex, may be found using variety of methods including the use of pseudo-random numbers and ranges for each of the independent variables:

$$x_i = g_i + r_i \cdot (h_i - g_i) \tag{4}$$

where r_i is a pseudo-random number over the interval $(0,1)$.

After the initial set of vertices are chosen, the objective function is evaluated at each vertex. Then, the ordering is conducted ranking the function values, then thus the vertices, $\langle v_0, v_1, \dots, v_w \rangle$ showing v_0 the best vertex and v_w the worst vertex, by comparison (Kazmierczak, 1996). Once the initial ordering is accomplished, the vertex of least function value, v_w is replaced by a point $\alpha > 0$ times as far from the centroid, the hyperspace center of the non-worst vertices, of the remaining points, where α is a reflection

coefficient determining how far away from the centroid the reflected vertex will be located. Calculating the centroid with the following eq. 5;

$$\bar{v} = \frac{1}{w} \sum_{i=0}^{w-1} v_i \quad 5$$

a reflected vertex v_r can be obtained as:

$$v_r = (1 + \alpha) \bar{v} - \alpha \cdot v_w \quad 6$$

If the new vertex results in violation of explicit and/or implicit constraints, it has to be systematically retracted until it enters back into the feasible region (Box, 1965). If the function value of v_r is superior to the next-to-worst vertex v_{w-1} , then v_r replaces the worst vertex changing the shape of the simplex as a new member. Then, the stopping criteria are tested (generally checking the difference between the best and the worst response). If not satisfied, the vertices are re-ranked, and the process begins again (Kazmierczak, 1996).

It is possible to get a reflected value superior than the best vertex. If this happens, it will be better and faster to continue the search in the direction of reflection, and this is accomplished by calculating an expanded vertex:

$$v_e = \gamma \cdot v_r + (1 - \gamma) \bar{v} \quad 7$$

where $\gamma > 1$ is the expansion coefficient. If v_e is superior than v_r , the v_w is replaced by v_e . If not, v_w is replaced by v_r , and a new v_r is calculated after re-ordering and the stopping criteria is checked (Kazmierczak, 1996).

If the reflected value is inferior to v_{w-1} , a retraction process is used to move the reflected vertex back to the projection path towards v_w . The retracted vertex is given by:

$$v_c = \beta \cdot v_w + (1 - \beta) \bar{v} \quad 8$$

where $0 < \beta < 1$ is the retraction coefficient. The retraction process is accomplished by systematically decreasing β until v_c is superior to v_{w-1} . Then, re-ordering is initiated, and the stopping criteria is checked (Kazmierczak, 1996). If v_c continues to be inferior to v_{w-1} , then a shrinkage process is used by moving all the vertices towards the best vertex, resulting in a completely new system evaluation, which is computationally expensive (Kazmierczak, 1996).

$$v_i = \frac{1}{2}(v_0 + v_i) \quad 9$$

After the shrinkage is accomplished, the method continues with re-ordering, and original reflection of the next-to-worst point until stopping criteria is achieved. The following is a real example to find the optimum variable retort temperature profile (VPTP) for the sphere 1 ($r=15$ mm) with the given thermal and physical properties in Chapter 2 ($N=10$, and Objective function: VACN). Applying the steps 1 to 4 constituted the initial complex as given in the following Table 1:

Table 1. The initial complex to find the optimum variable retort temperature profile (VPTP) for the sphere 1 ($r=15$ mm) with respect to the objective function of VACN.

Time (sec)	Variable Temperature Profiles (VPTP)										
	1	2	3	4	5	6	7	8	9	10	11
0	148.1	136.8	149.5	148.6	96.2	121.2	132.4	119.0	106.3	146.1	129.4
133.3	118.6	117.2	145.7	118.6	104.7	135.7	120.3	140.8	93.3	122.5	145.2
266.7	142.4	130.5	135.3	133.8	116.1	141.7	120.1	139.8	120.5	115.3	124.2
400.0	135.8	133.1	118.3	129.2	149.2	118.0	137.1	128.4	149.1	148.5	124.0
533.3	131.4	149.2	146.1	142.9	149.3	145.3	142.1	140.2	149.4	125.0	146.5
666.7	39.4	40.0	35.7	33.0	70.6	35.1	38.8	32.7	39.6	34.6	37.2
800.0	5.9	5.9	5.6	5.9	6.0	5.6	5.5	5.5	5.5	5.8	5.9
933.3	5.9	5.5	5.6	5.5	5.9	5.9	5.9	5.9	5.6	5.5	6.0
1066.7	6.0	5.5	5.9	5.5	5.5	5.6	5.9	5.9	5.8	5.8	5.5
1200.0	5.0	5.0	5.0	5.0	5.0	5.0	5.0	5.0	5.0	5.0	5.0
VACN (%)	83.1	83.2	81.9	85.7	78.9	84.5	86.4	82.1	79.9	86.3	85.0
SCN (%)	76.2	76.1	72.1	79.8	68.3	77.1	80.5	74.1	68.8	79.7	77.4
F_0 (sec)	947.3	941.5	667.3	592.2	1507	533.6	544.4	946.7	1168	501.7	502.1

At this point, the initial vertices (each VPTP represented a vertex, v) for the Complex Method was found, the ordering with respect to the objective function (VACN), and the centroid of the non-worst vertices were calculated (step 5). Vertex #11 here showed the worst vertex (v_w). Then, the vertex of v_w was reflected by $\alpha=1.4$ times, and a reflected vertex of v_r was calculated with its resulting objective function and implicit constraints values (step 6). Since the resulting objective function value of the reflected vertex (79.1%) was lower than the objective function value of the v_w (85%), v_r was systematically retracked until its resulting objective function value was higher than that of the next-to-worst vertex (v_{w-1}) (step 6). The reflected and retracked vertices with

their resulting objective function values were given in Table 2, and Table 3 and showed the changes in the initial complex after several steps.

Table 2. The reflected (v_r) and retracted (v_e) vertices for the initial complex.

Time (sec)	The reflected vertex (v_r)	The retracted vertex (v_e)
0	149.9	101.3
133.3	149.9	107.0
266.7	148.8	117.0
400.0	110.0	143.7
533.3	132.1	145.6
666.7	5.0	63.2
800.0	5.4	5.8
933.3	5.5	5.8
1066.7	6.0	5.5
1200.0	5.0	5.0
VACN (%)	79.1	83.8
SCN (%)	65.3	76.1
F_0 (sec)	698.9	781.3

Table 3. The complex to find the optimum variable retort temperature profile (VPTP) for the sphere 1 ($r=15$ mm) with respect to the objective function of VACN several steps after the initial complex.

Time (sec)	Variable Temperature Profiles (VPTP)										
	1	2	3	4	5	6	7	8	9	10	11
0	126.7	131.8	126.6	132.0	128.9	128.8	129.3	131.3	130.9	143.1	130.8
133.3	122.2	120.0	123.3	120.1	121.7	121.8	121.8	121.6	121.6	119.1	121.5
266.7	116.2	119.9	122.9	120.0	120.0	120.4	120.7	120.6	121.0	128.0	121.5
400.0	141.0	136.6	139.1	136.7	138.9	138.7	138.5	138.9	138.6	131.9	138.3
533.3	137.6	141.5	135.5	141.7	138.6	138.7	138.8	138.3	138.5	142.0	138.7
666.7	40.8	38.7	40.1	38.7	39.8	39.8	39.6	39.0	39.2	34.6	39.3
800.0	5.4	5.5	5.8	5.5	5.6	5.6	5.6	5.6	5.6	5.7	5.7
933.3	5.9	5.9	5.8	5.9	5.9	5.9	5.9	5.8	5.8	5.7	5.8
1066.7	6.0	5.9	5.7	5.9	5.8	5.8	5.8	5.8	5.8	5.7	5.8
1200.0	5.0	5.0	5.0	5.0	5.0	5.0	5.0	5.0	5.0	5.0	5.0
VACN (%)	86.9	86.9	86.8	86.7	86.7	86.7	86.7	86.6	86.6	86.6	86.6
SCN (%)	81.2	81.3	81.4	81.0	81.1	81.1	81.1	81.1	81.0	81.1	81.0
F_0 (sec)	485.3	491.7	519.3	508.2	515.9	518.7	521.9	524.6	529.6	520.9	535.7

After this step, when the resulting objective function value of the reflected vertex was superior than the best vertex (v_1), the search continued by calculating an expanded vertex (v_e) and its resulting objective function value. Table 4 showed a reflected and the following expanded vertices with their objective function and implicit constraints values:

Table 4. The reflected (v_r) and expanded (v_e) vertices for the the complex.

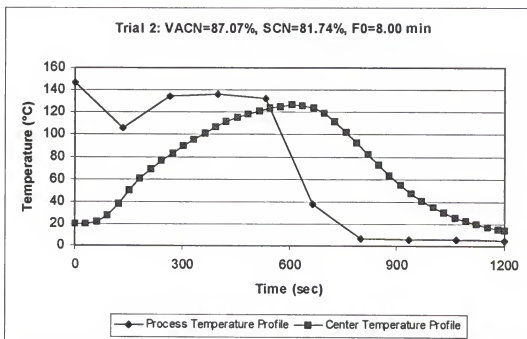
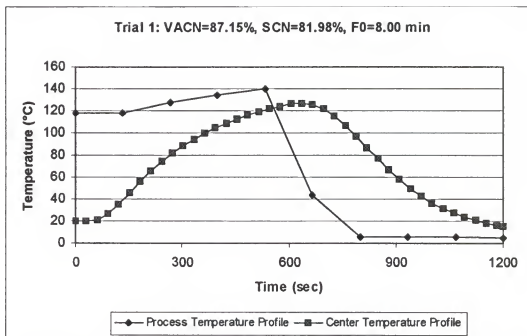
Time (sec)	The reflected vertex (v_r)	The expanded vertex (v_e)
0	131.1	129.3
133.3	121.0	127.8
266.7	120.2	121.0
400.0	137.3	138.3
533.3	139.7	138.8
666.7	38.7	39.6
800.0	5.5	5.6
933.3	5.9	5.8
1066.7	5.9	5.8
1200.0	5.5	5.0
VACN (%)	87.0	86.6
SCN (%)	81.5	81.1
F_0 (sec)	483.7	524.8

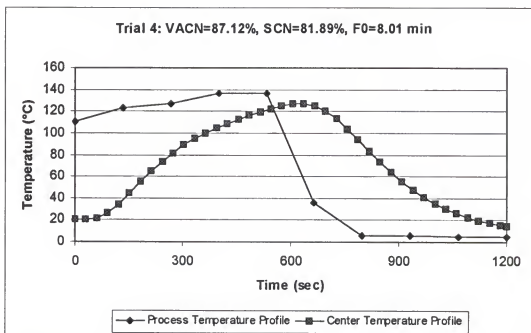
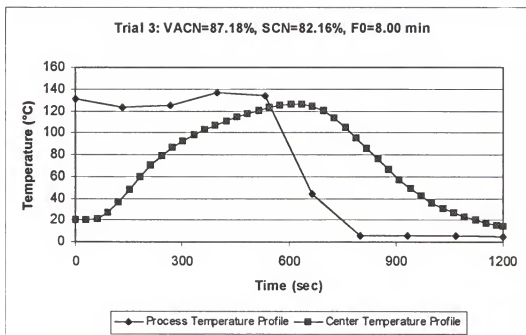
This example concluded with the results given in Table 5. At this point, using a small magnitude of 0.01 (step 7) for stopping criteria, the differences between the temperature profiles were very small as well as the objective functions and implicit constraints. This made the hyperspace collapse into a certain point, and from then on, it was not possible to change the temperature profiles by using reflection, expansion or retraction. The objective function values were not exactly same as seen in Table 5. The rounding to one digital point showed them as same.

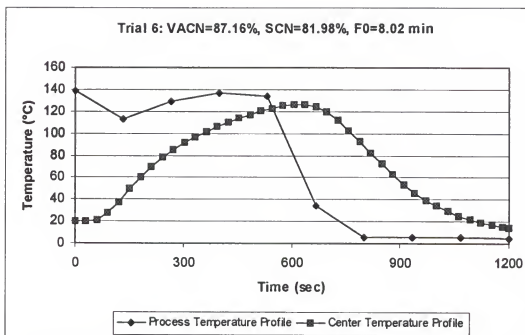
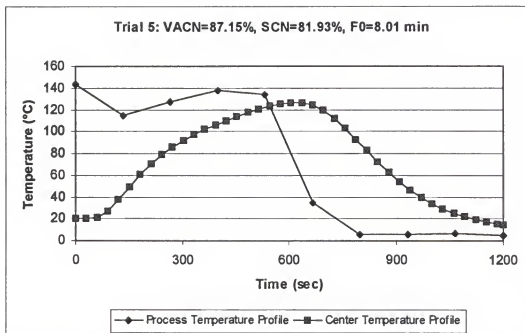
Table 5. The final complex finding the optimum variable retort temperature profile (VPTP) for the sphere 1 ($r=15$ mm) with respect to the objective function of VACN.

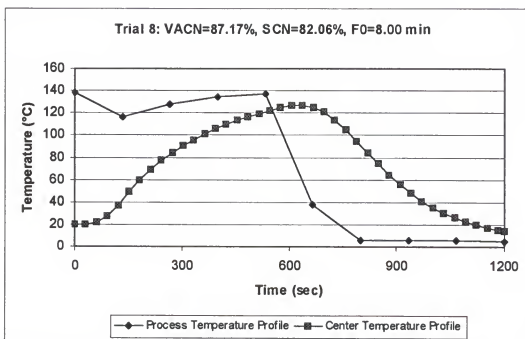
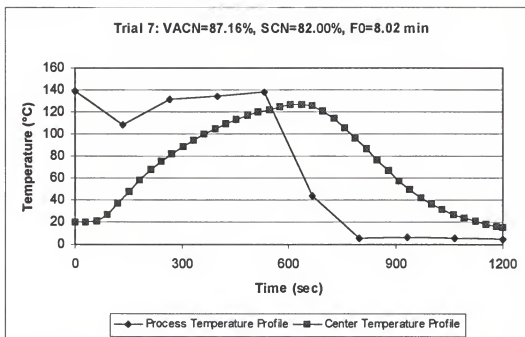
Time (sec)	Variable Temperature Profiles (VPTP)										
	1	2	3	4	5	6	7	8	9	10	11
0	130.1	130.2	129.4	130.8	130.7	130.7	130.8	130.5	132.2	131.4	130.8
133.3	123.8	123.7	124.0	123.3	123.3	123.3	123.3	123.6	122.7	122.6	123.5
266.7	124.1	124.0	124.8	124.0	123.9	123.9	123.9	123.6	124.0	123.6	123.8
400.0	137.3	137.3	137.0	137.0	137.0	137.0	137.0	137.5	136.4	136.5	137.3
533.3	135.1	135.3	134.9	135.9	136.0	136.0	136.0	135.3	136.9	137.1	135.6
666.7	38.6	38.5	38.8	38.4	38.4	38.4	38.4	38.5	37.9	38.2	38.4
800.0	5.7	5.7	5.7	5.7	5.7	5.7	5.7	5.7	5.7	5.7	5.7
933.3	5.7	5.7	5.7	5.7	5.7	5.7	5.7	5.7	5.7	5.7	5.7
1066.7	5.7	5.7	5.7	5.7	5.7	5.7	5.7	5.7	5.7	5.7	5.7
1200.0	5.0	5.0	5.0	5.0	5.0	5.0	5.0	5.0	5.0	5.0	5.0
VACN (%)	87.1	87.1	87.1	87.1	87.1	87.1	87.1	87.1	87.1	87.1	87.1
SCN (%)	82.0	82.0	82.0	82.0	82.0	82.0	82.0	81.9	81.9	81.9	81.9
F_0 (sec)	480.5	480.6	481.4	480.6	480.6	480.8	480.8	480.8	480.1	480.1	481.1

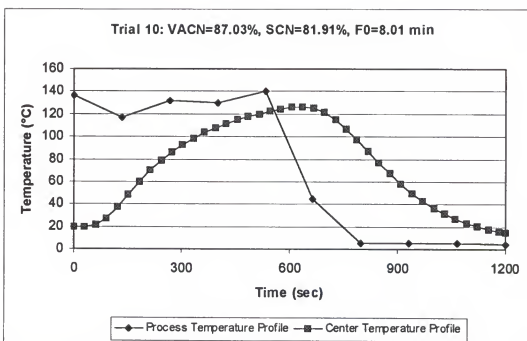
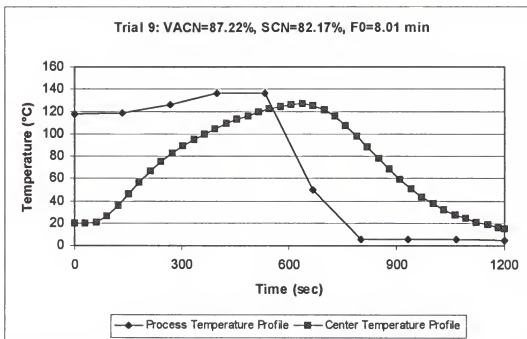
APPENDIX B
PROCESS AND CENTER TEMPERATURE PROFILES FOR A SPHERE
UNDER DIFFERENT PROCESSING CONDITIONS;
OBJECTIVE FUNCTION: VACN

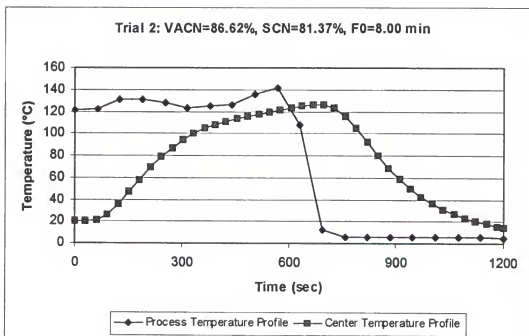
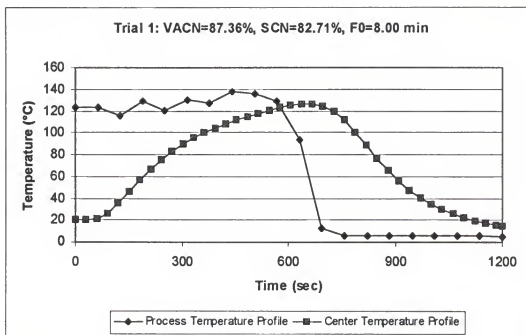
1. Sphere ($r=15\text{mm}$, $t=20\text{ min}$, $N=10$).

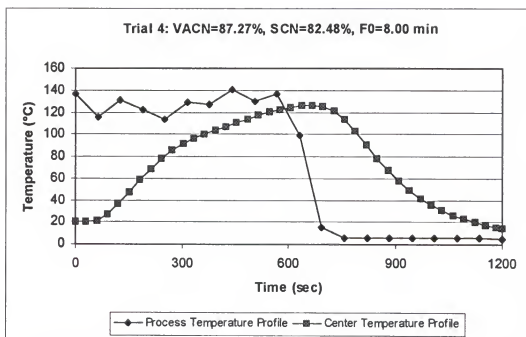
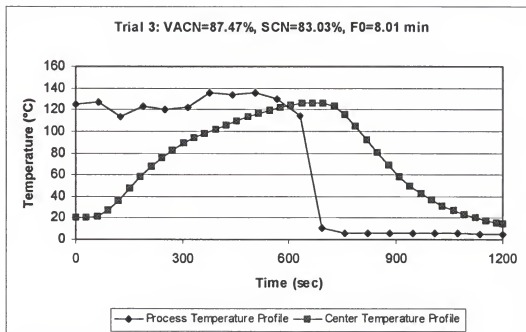


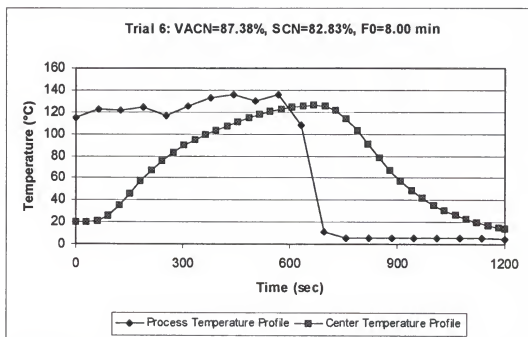
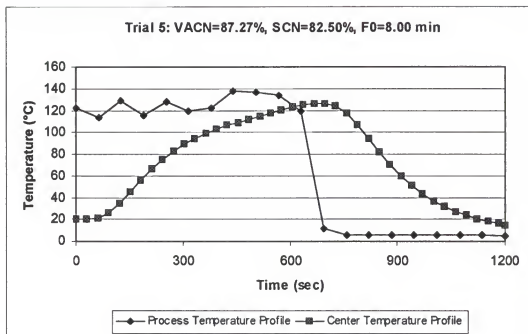


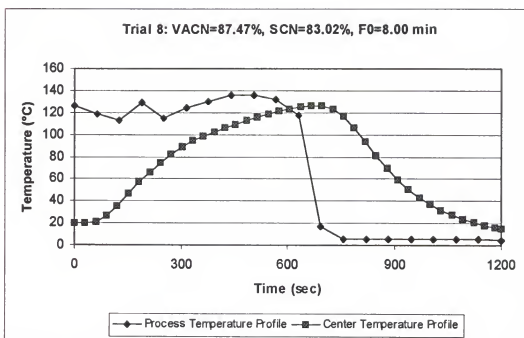
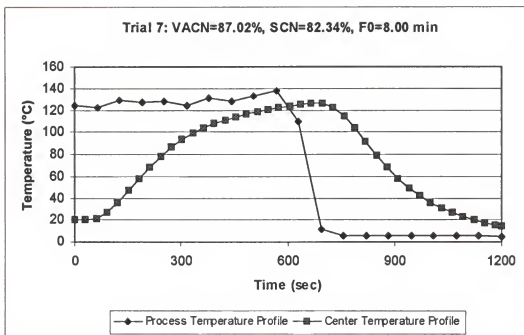


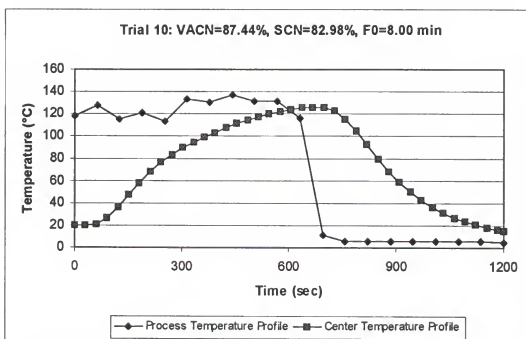
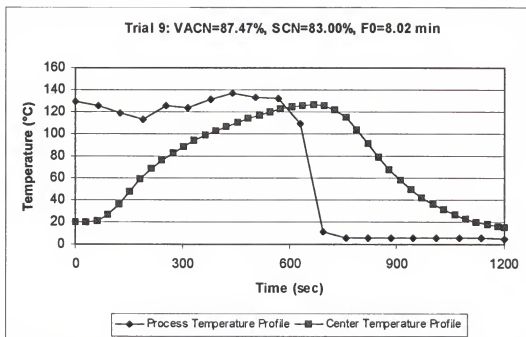


2. Sphere ($r=15$ mm, $t=20$ min, $N=20$).

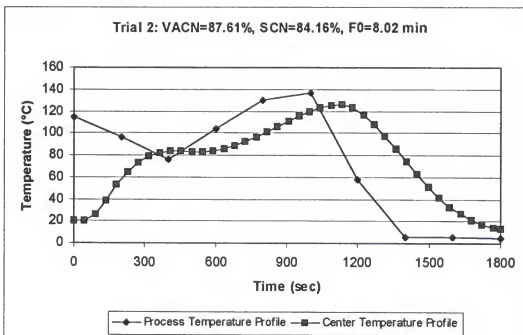
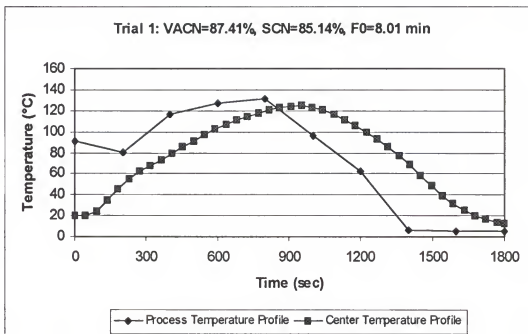


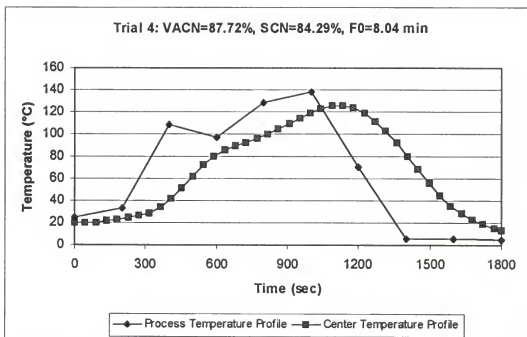
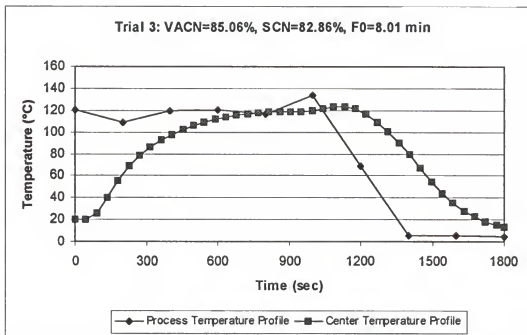


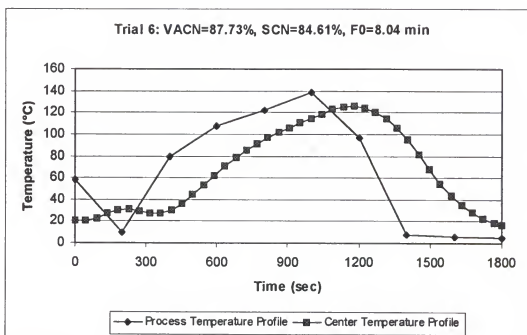
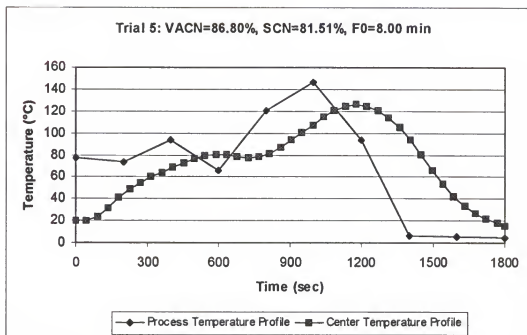




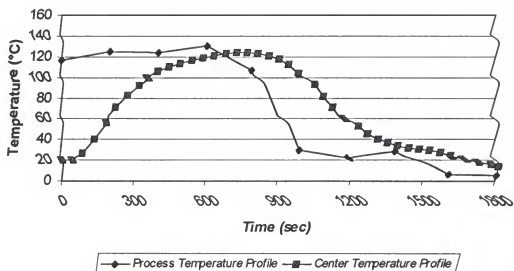
3. Sphere ($r=15$ mm, $t=30$ min, $N=10$).



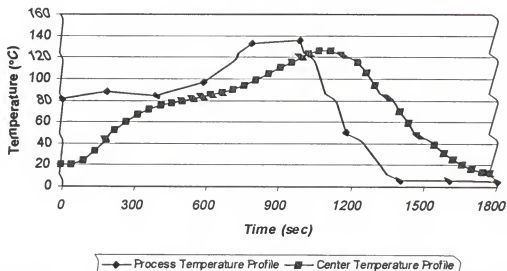


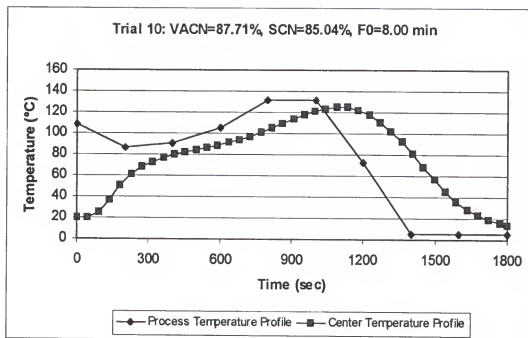
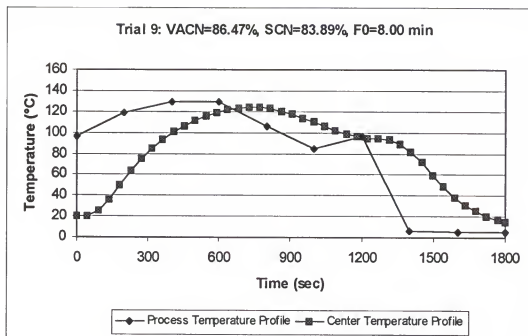


Trial 7: VACN=86.81%, SCN=83.96%, F0=8.00 min

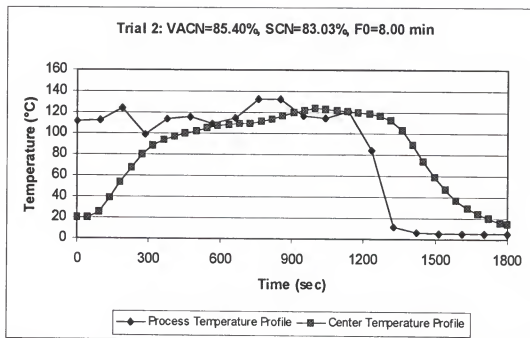
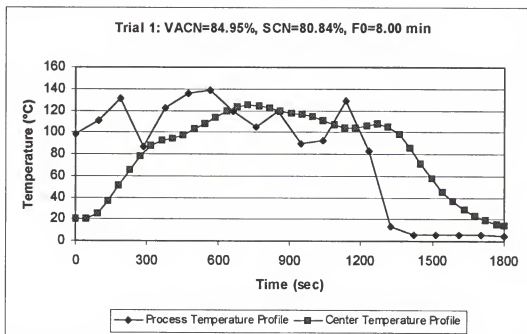


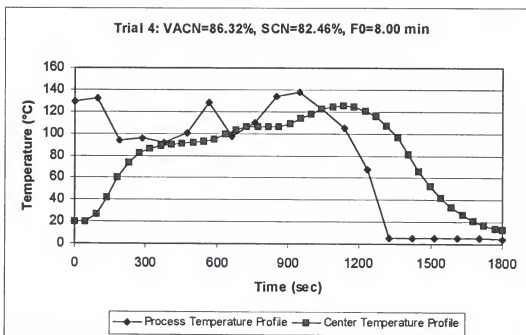
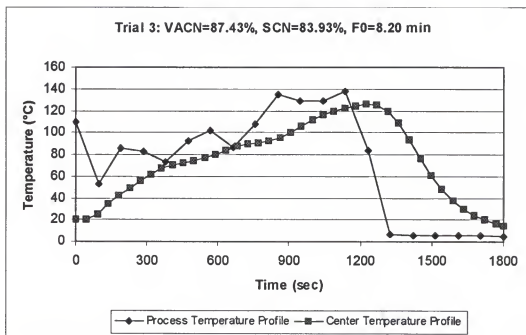
Trial 8: VACN=87.70%, SCN=84.54%, F0=8.00 min

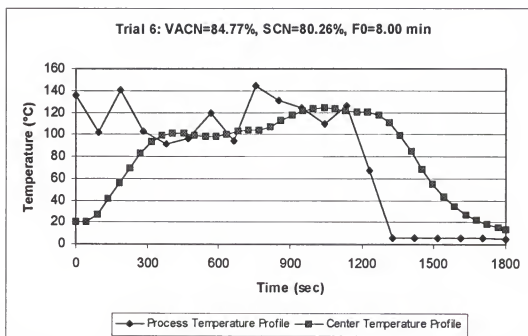
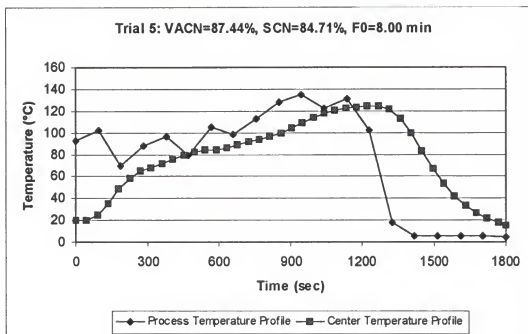


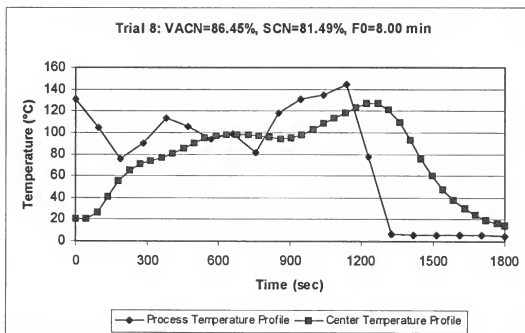
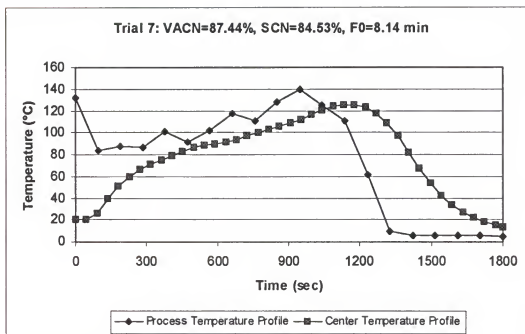


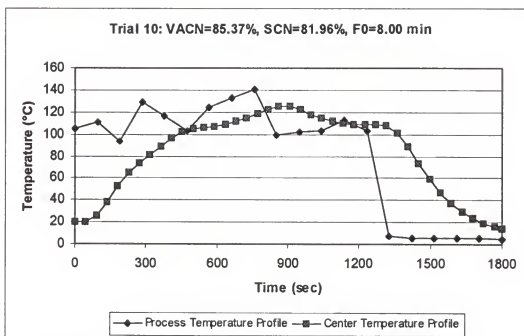
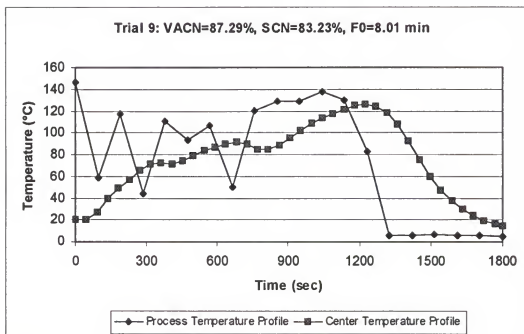
4. Sphere ($r=15$ mm, $t=30$ min, $N=20$).

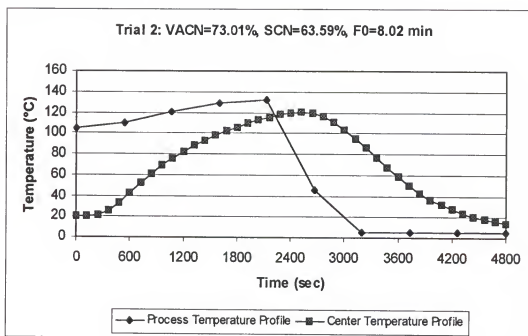
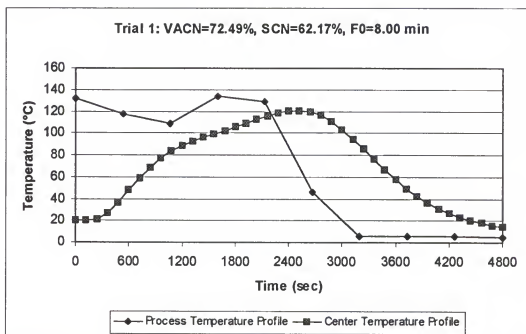


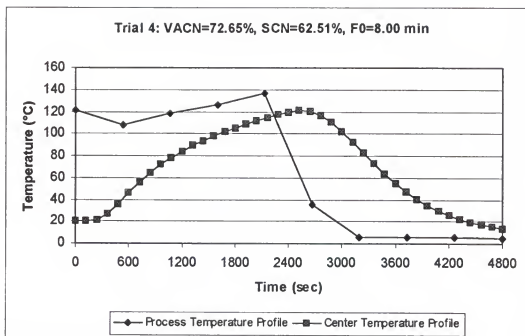
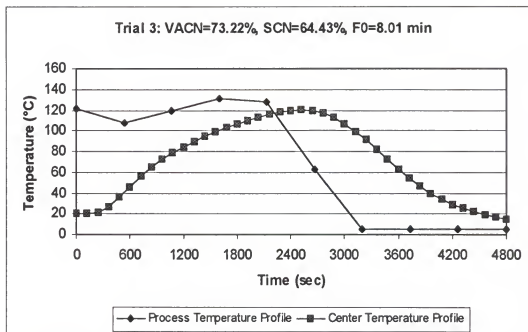




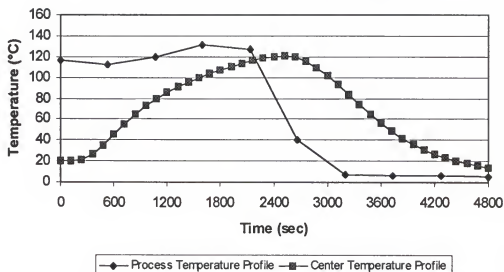




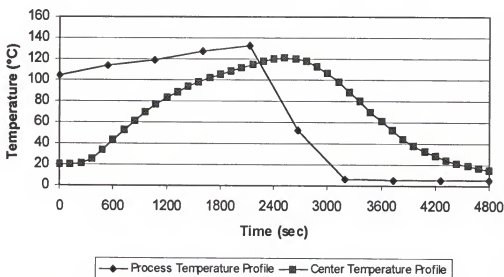
5. Sphere ($r=30$ mm, $t=80$ min, $N=10$).

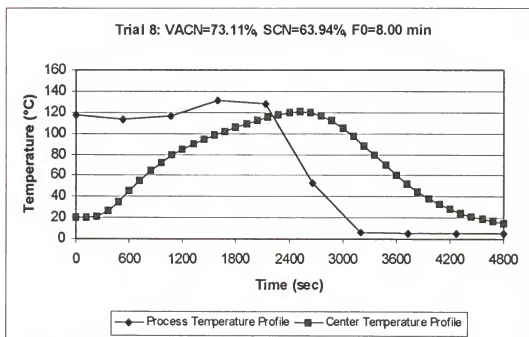
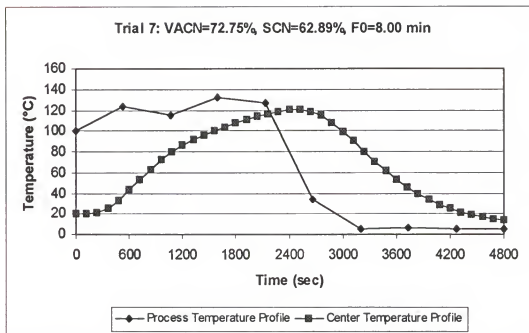


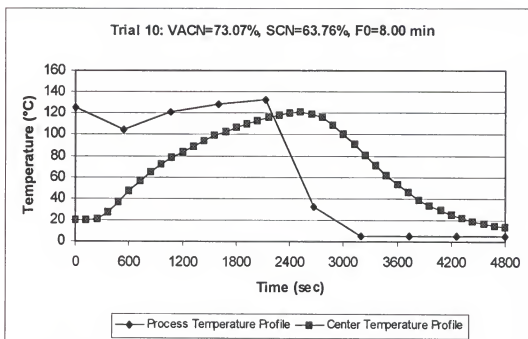
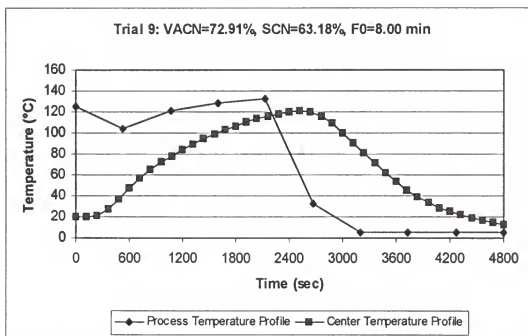
Trial 5: VACN=73.06%, SCN=63.76%, F0=8.00 min

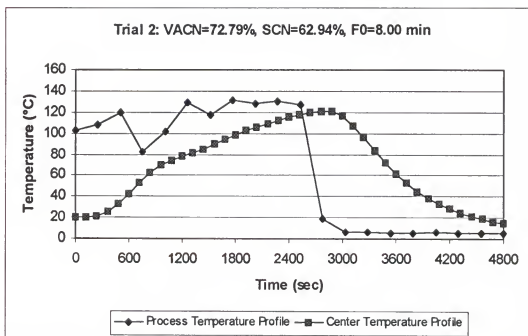
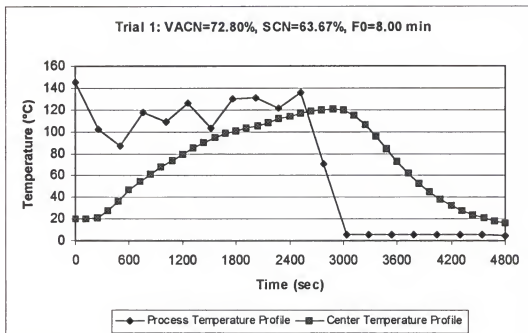


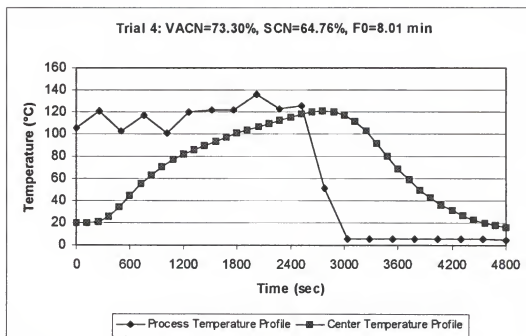
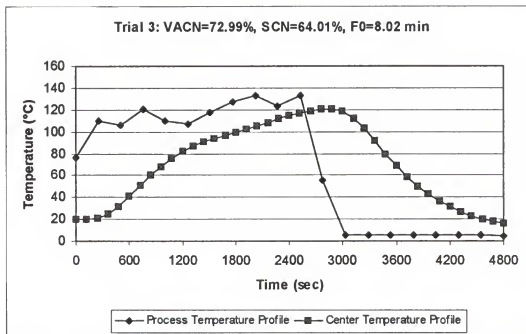
Trial 6: VACN=73.03%, SCN=63.85%, F0=8.00 min

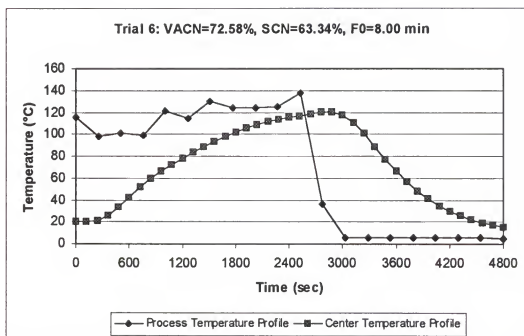
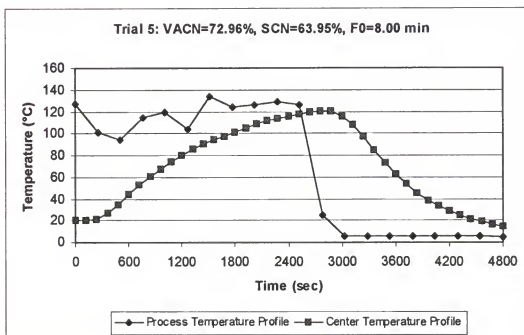


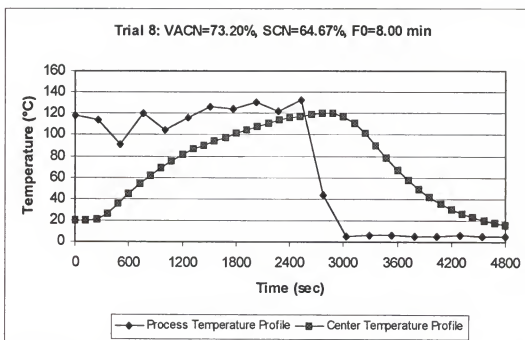
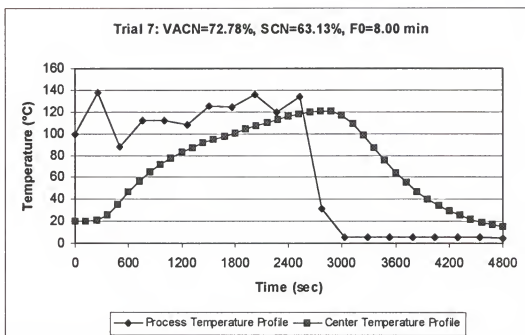


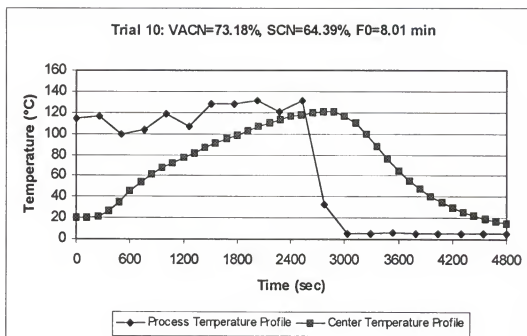
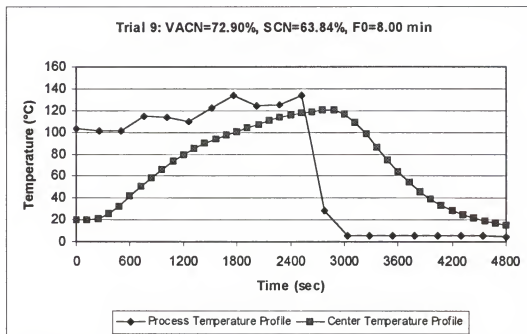


6. Sphere ($r=30$ mm, $t=80$ min, $N=20$).

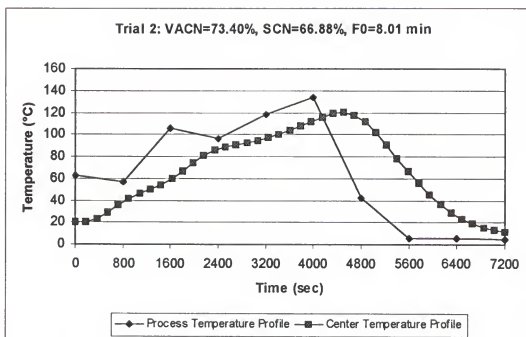
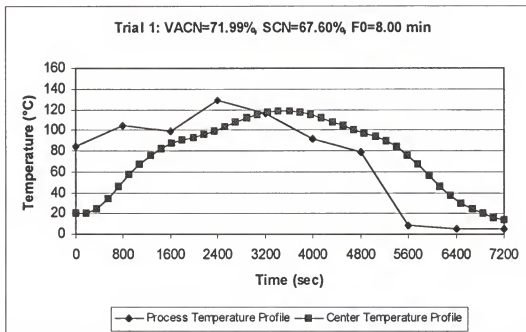


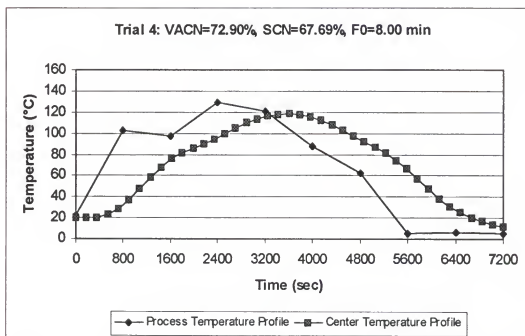
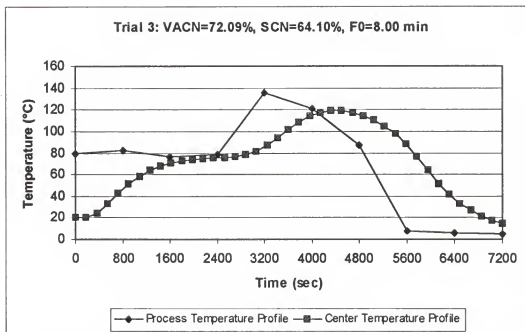




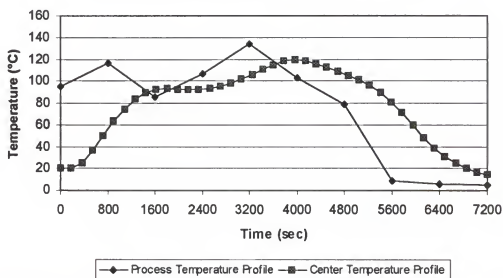


7. Sphere ($r=30$ mm, $t=120$ min, $N=10$).

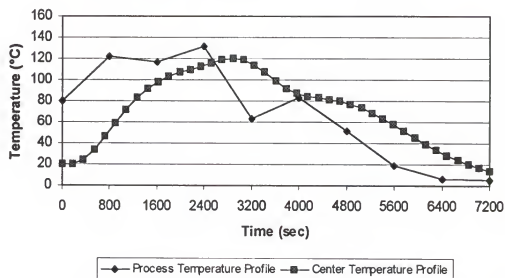


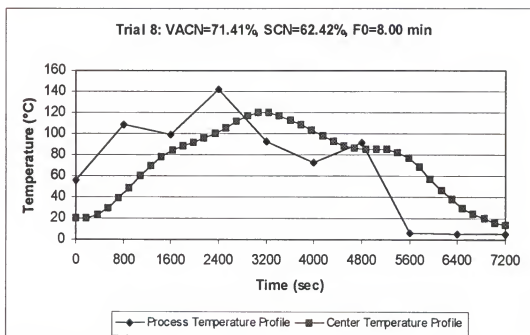
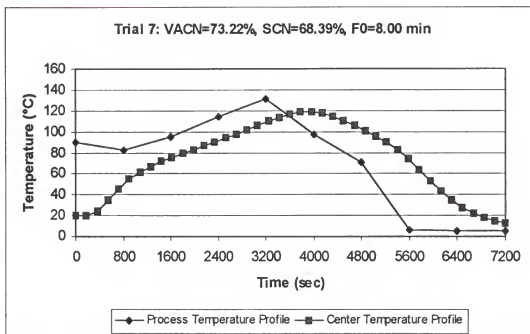


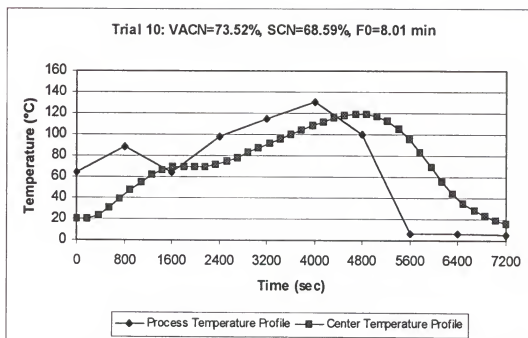
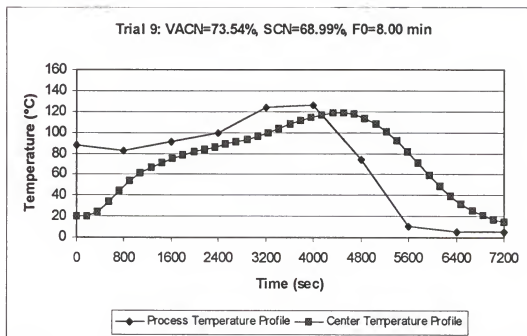
Trial 5: VACN=71.11%, SCN=64.91%, F0=8.00 min



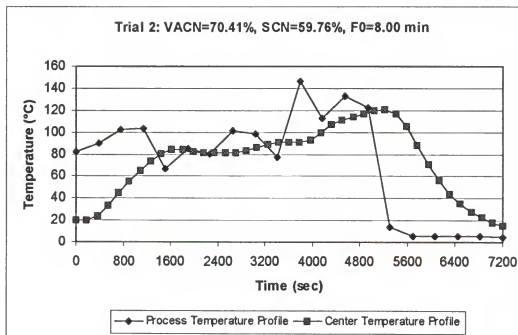
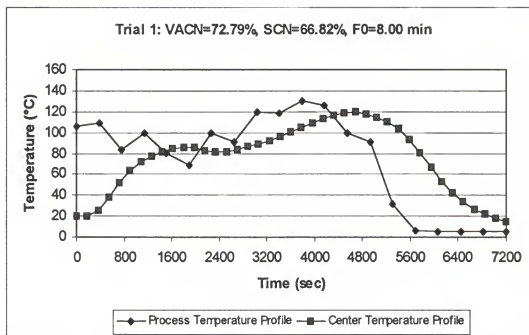
Trial 6: VACN=72.46%, SCN=65.45%, F0=8.00 min



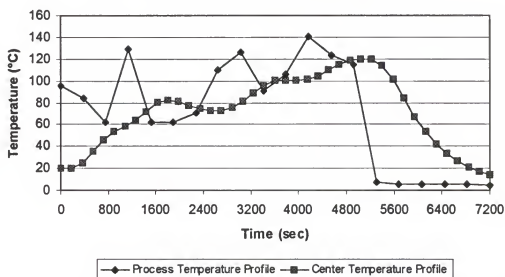




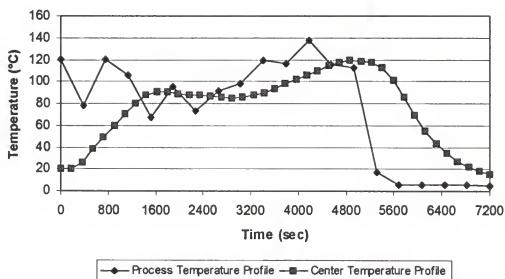
8. Sphere ($r=30$ mm, $t=120$ min, $N=20$).

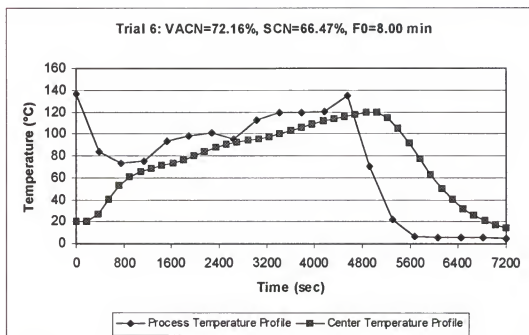
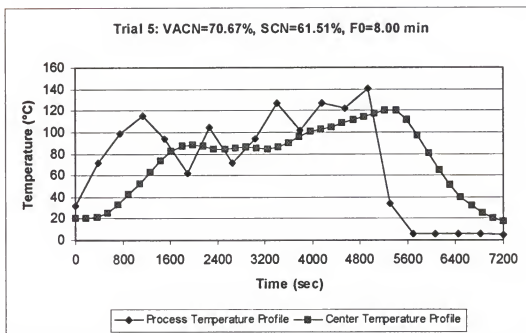


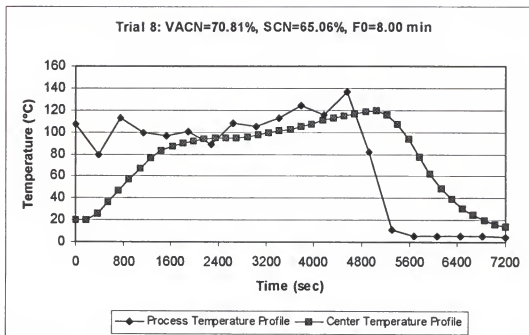
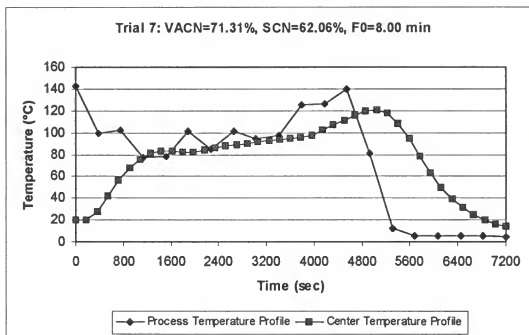
Trial 3: VACN=70.57%, SCN=60.38%, F0=8.00 min

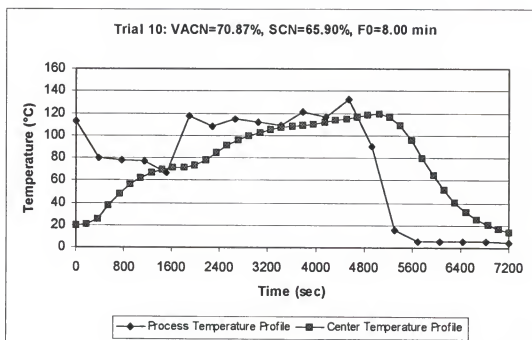
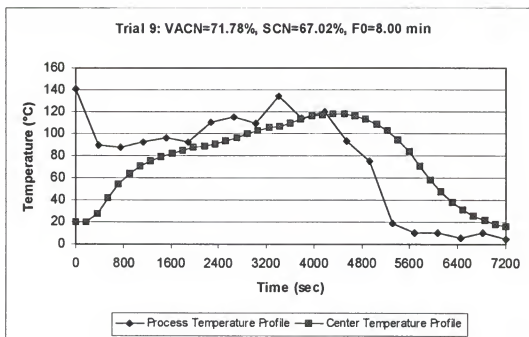


Trial 4: VACN=71.66%, SCN=64.22%, F0=8.02 min





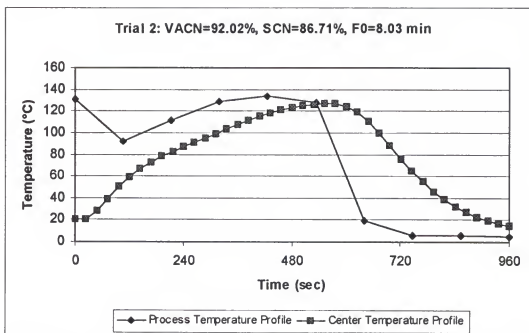
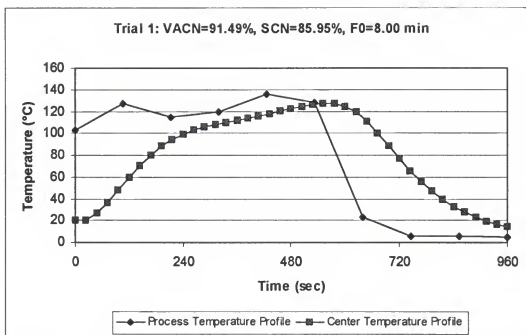


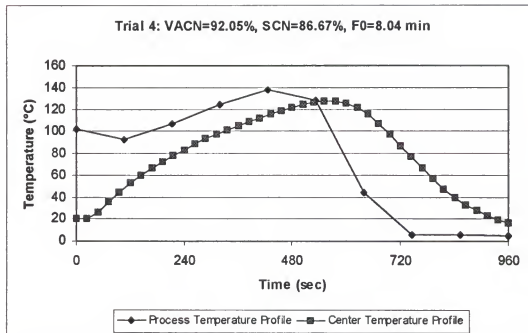
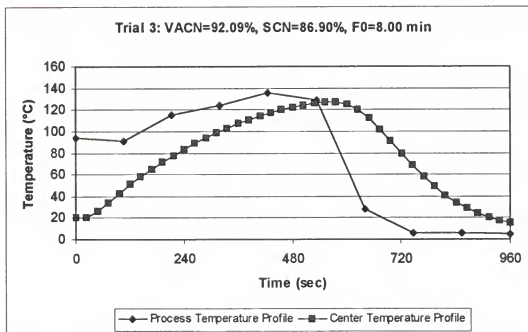


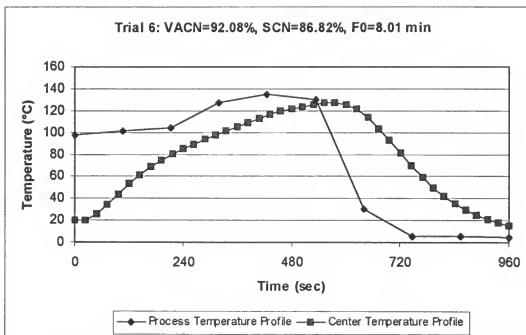
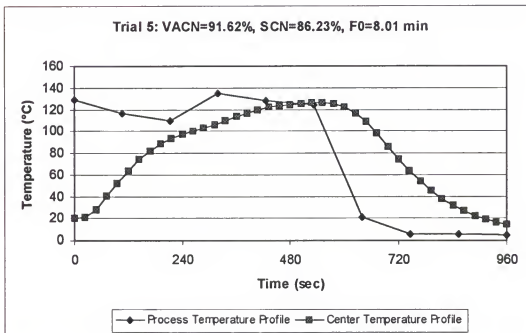
All the raw data can be obtained from Dr. M.Ö. Balaban at the Food Science and Human Nutrition Department of the University of Florida, Gainesville, FL.

APPENDIX C
PROCESS AND CENTER TEMPERATURE PROFILES FOR A FINITE CYLINDER
UNDER DIFFERENT PROCESSING CONDITIONS;
OBJECTIVE FUNCTION: VACN

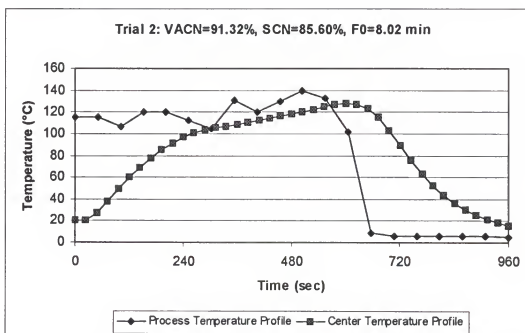
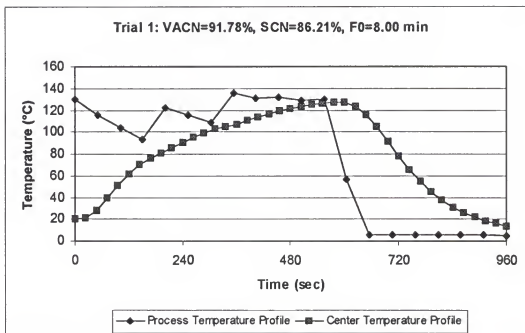
1. Finite Cylinder ($r=15\text{mm}$, $2l=15\text{ mm}$, $t=16\text{ min}$, $N=10$).

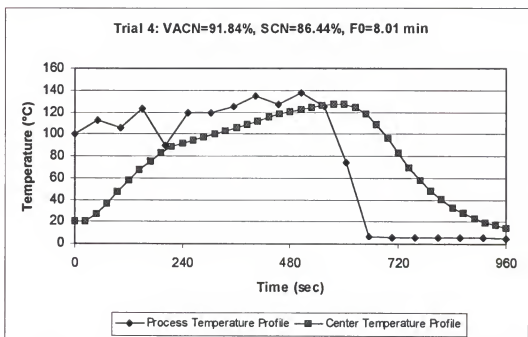
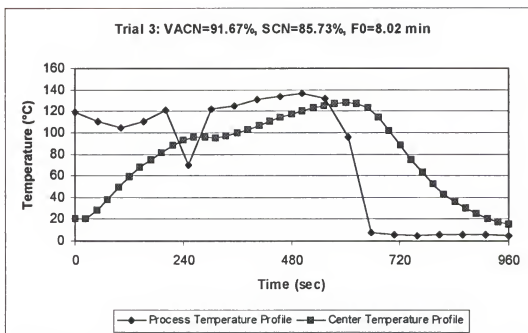


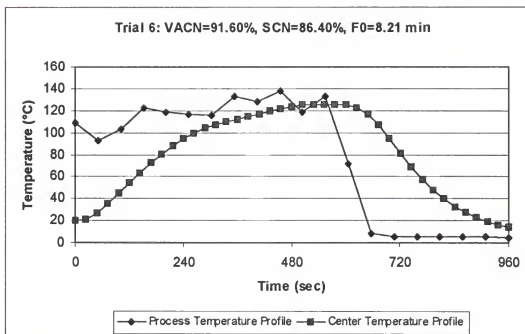
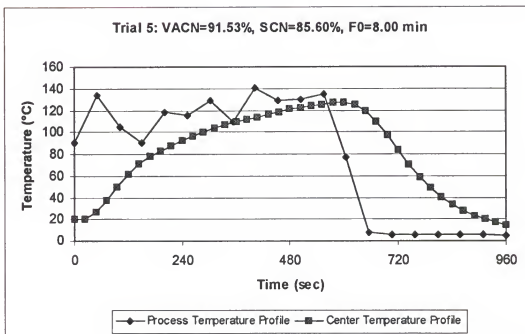




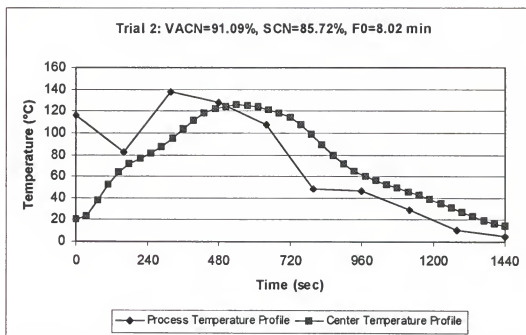
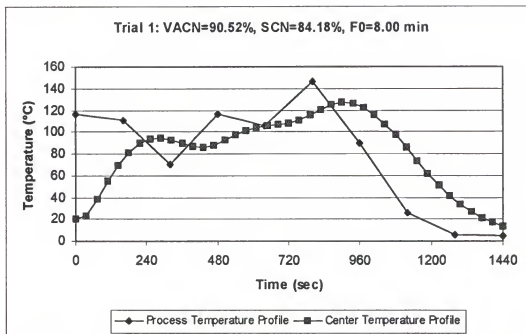
2. Finite Cylinder ($r=15\text{mm}$, $2l=15\text{ mm}$, $t=16\text{ min}$, $N=20$).

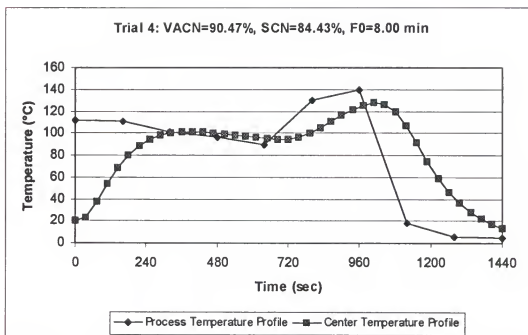
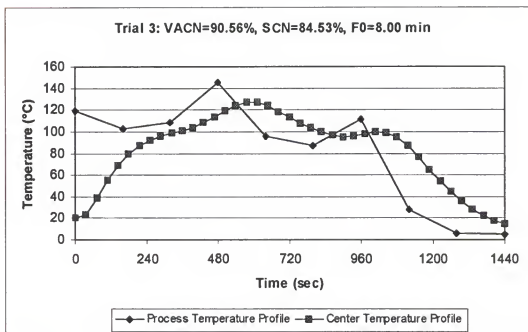


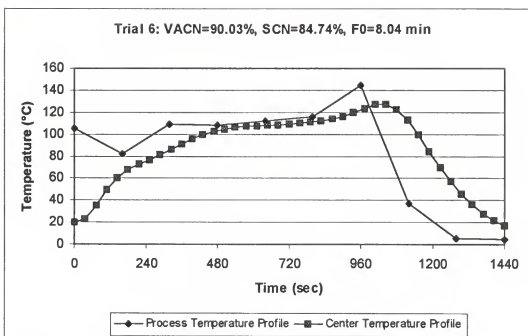
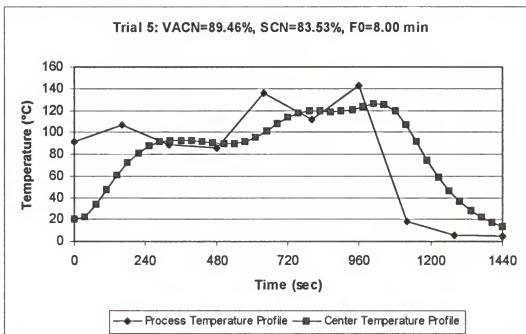




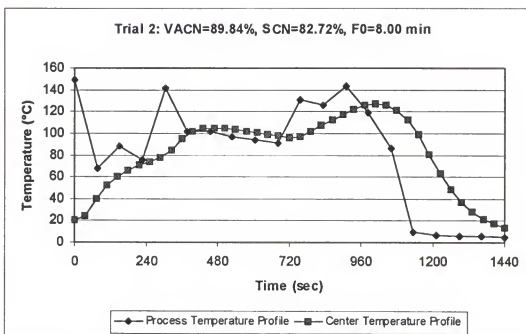
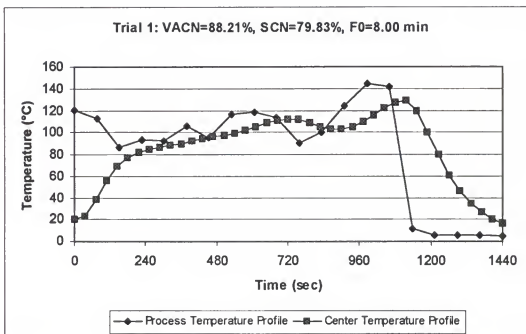
3. Finite Cylinder ($r=15\text{mm}$, $2l=15\text{ mm}$, $t=24\text{ min}$, $N=10$).

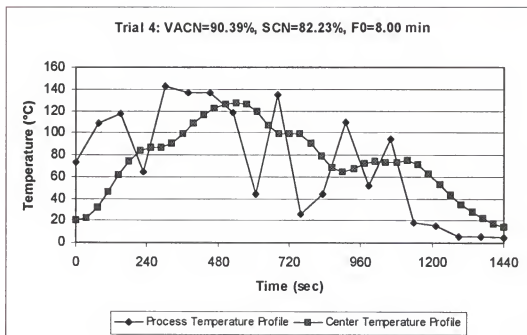
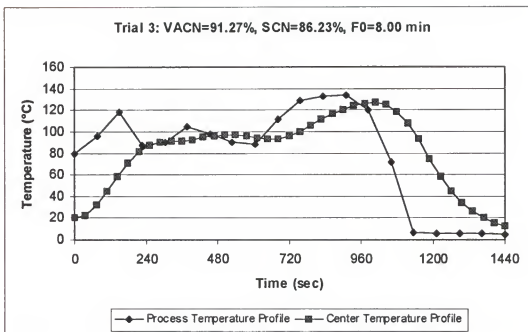


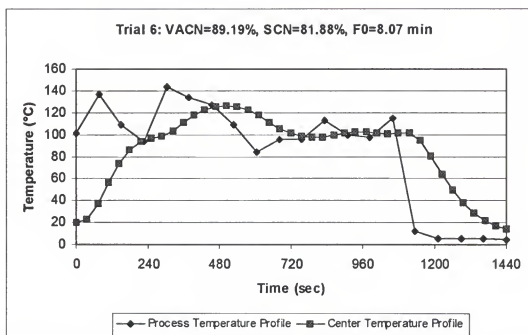
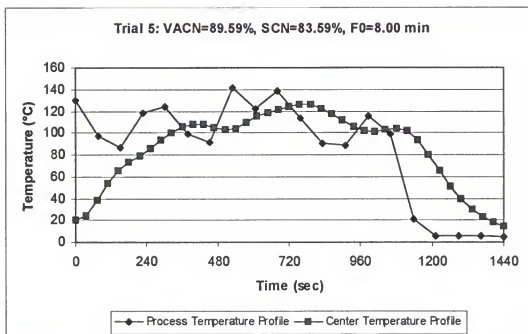




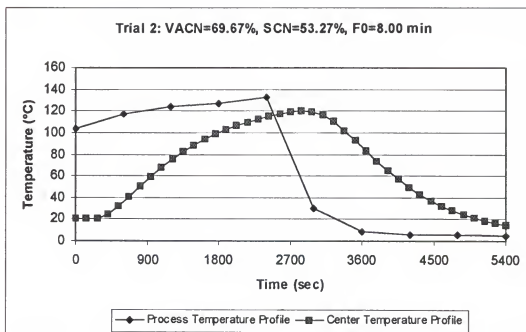
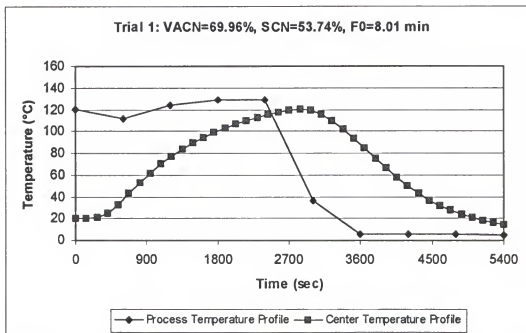
4. Finite Cylinder ($r=15\text{mm}$, $2l=15\text{ mm}$, $t=24\text{ min}$, $N=20$).

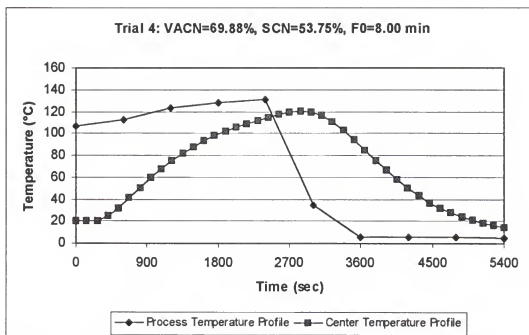
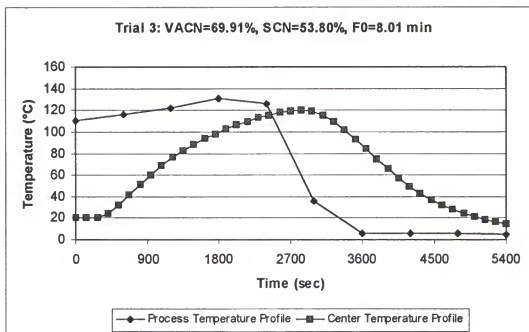


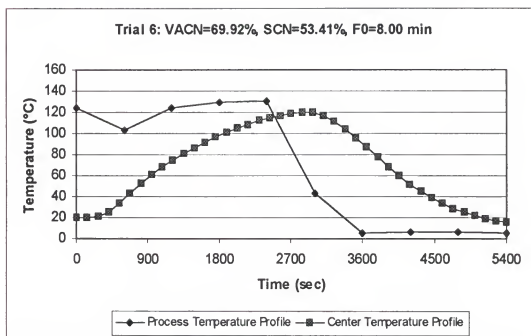
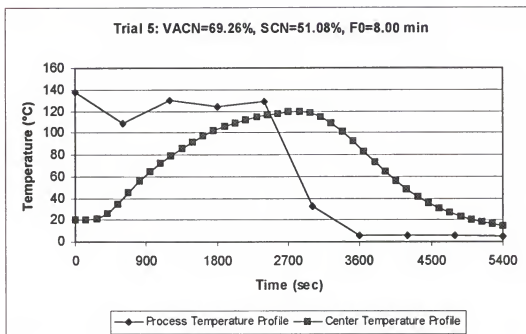




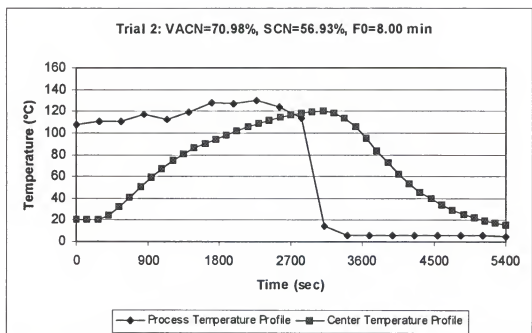
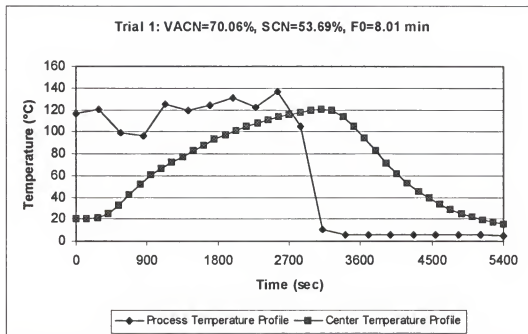
5. Finite Cylinder ($r=30\text{mm}$, $2l=60\text{ mm}$, $t=90\text{ min}$, $N=10$).

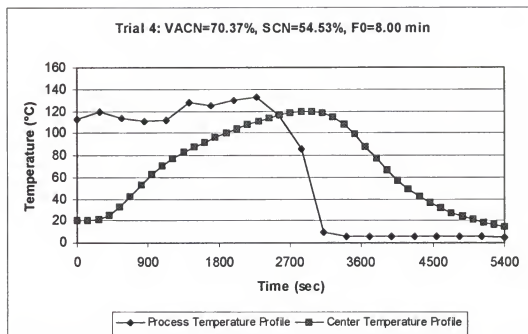
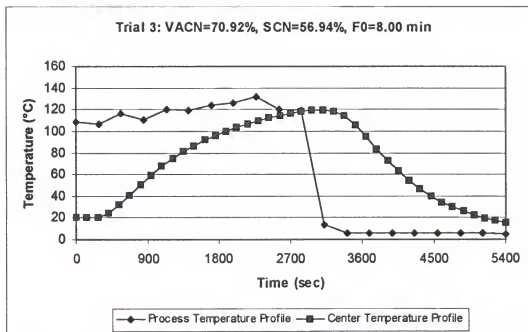


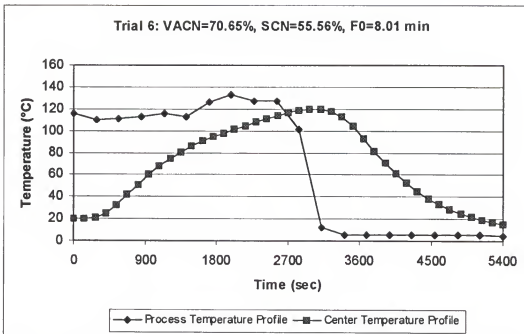
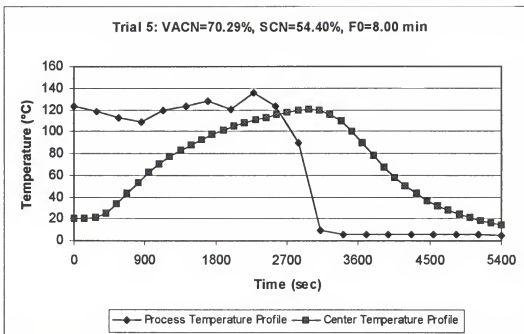




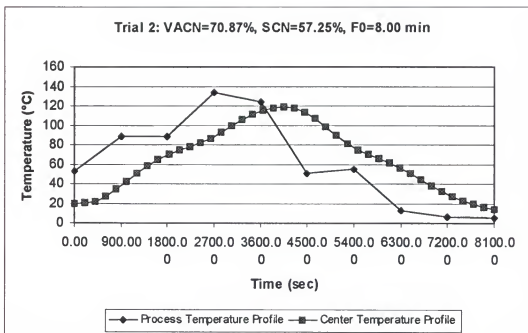
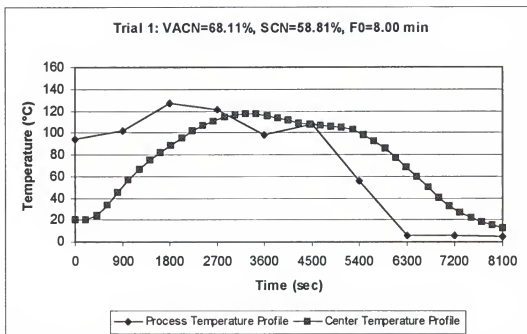
6. Finite Cylinder ($r=30\text{mm}$, $2l=60\text{ mm}$, $t=90\text{ min}$, $N=20$).

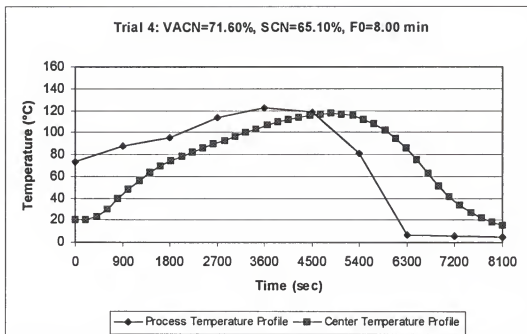
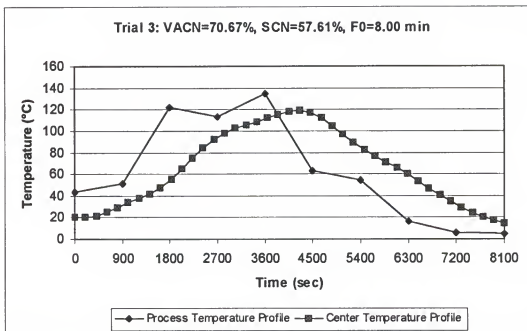


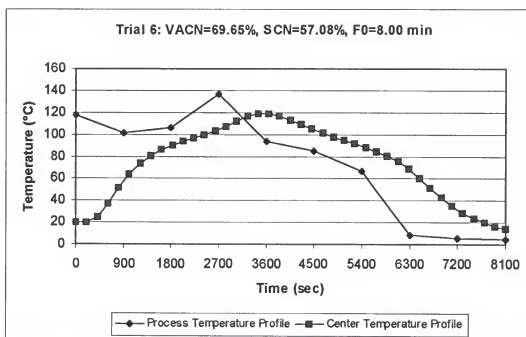
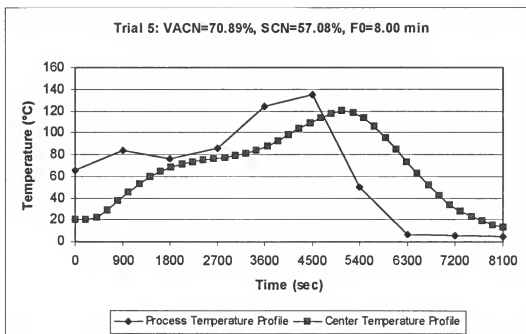




7. Finite Cylinder ($r=30\text{mm}$, $2l=60\text{ mm}$, $t=135\text{ min}$, $N=10$).



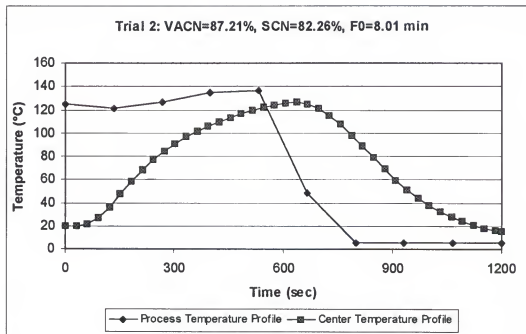
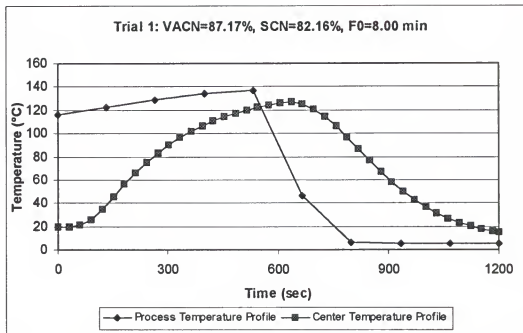


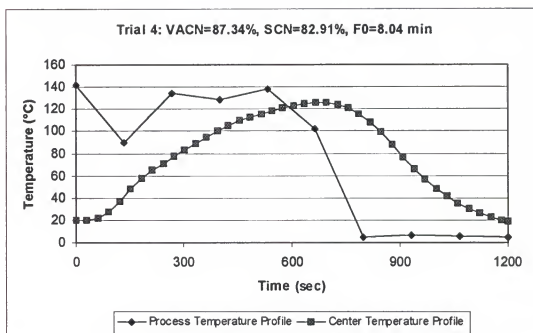
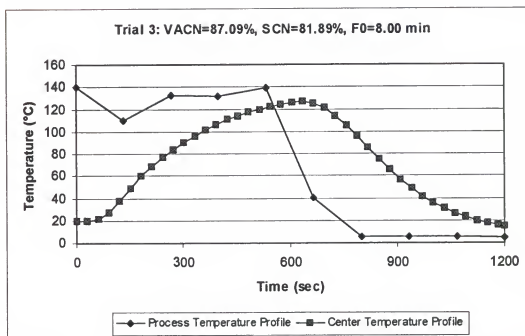


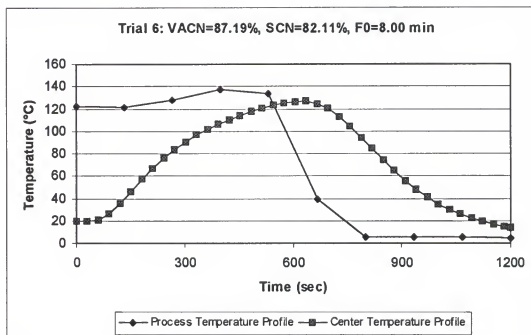
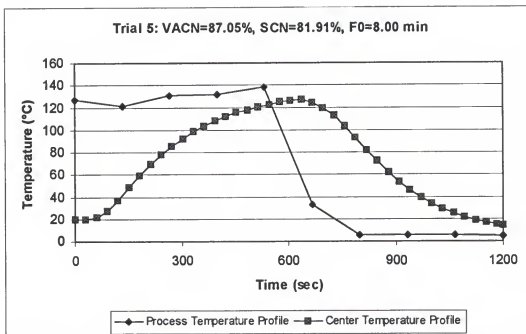
All the raw data can be obtained from Dr. M.Ö. Balaban at the Food Science and Human Nutrition Department of the University of Florida, Gainesville, FL.

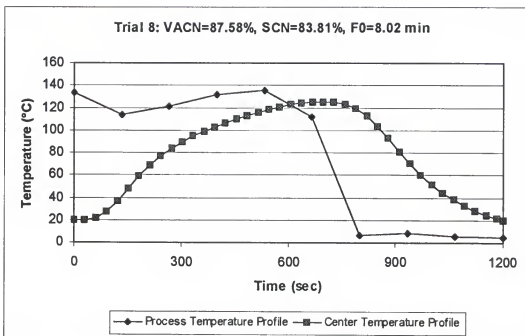
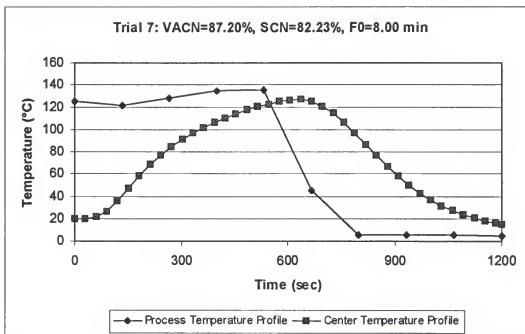
APPENDIX D
PROCESS AND CENTER TEMPERATURE PROFILES FOR A SPHERE
UNDER DIFFERENT PROCESSING CONDITIONS;
OBJECTIVE FUNCTION: SCN

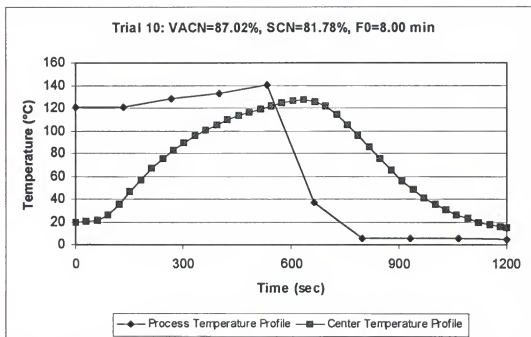
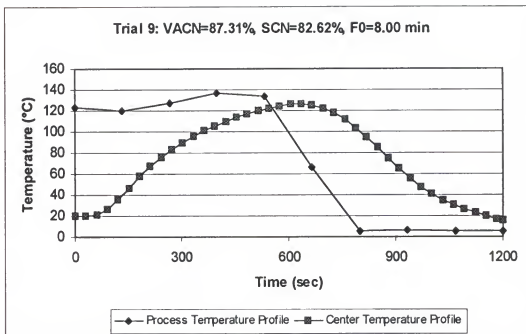
1. Sphere ($r=15\text{mm}$, $t=20\text{ min}$, $N=10$).



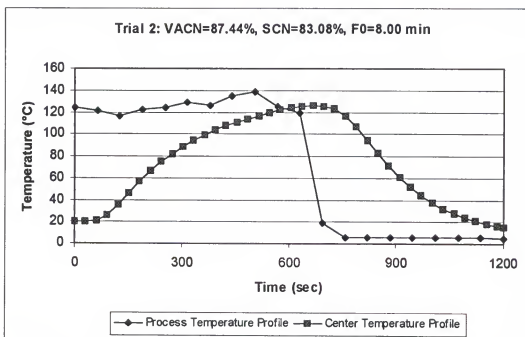
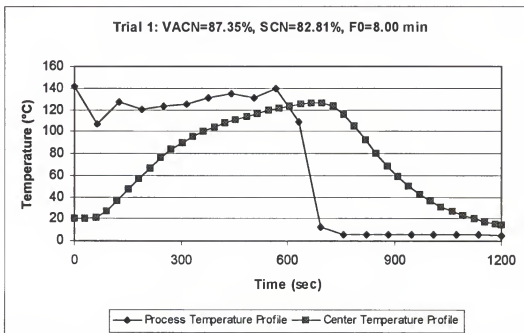


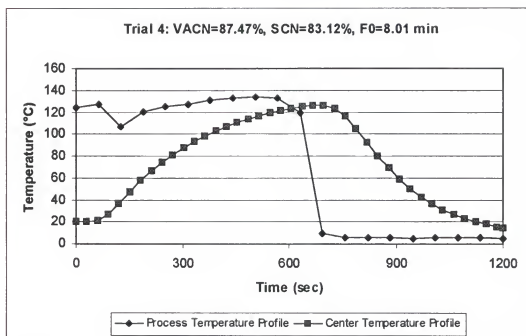
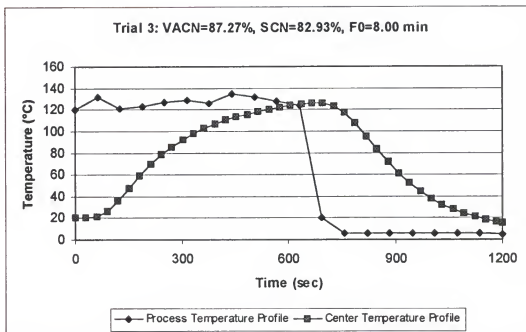


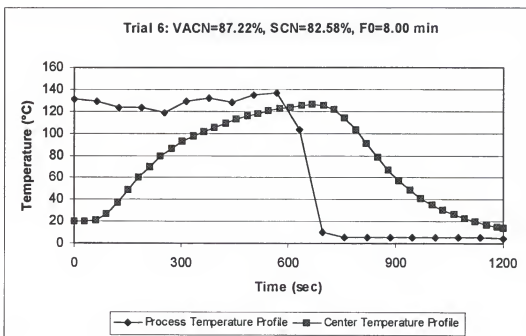
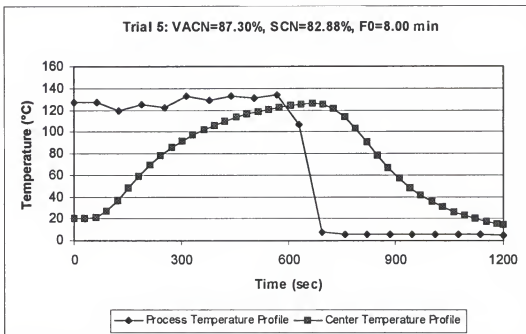


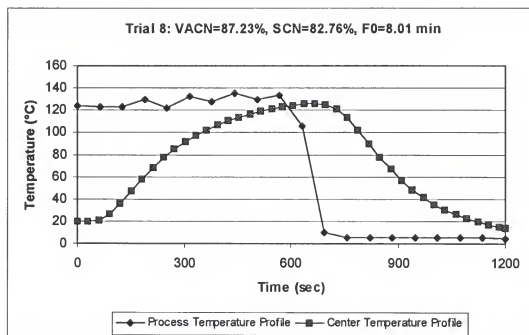
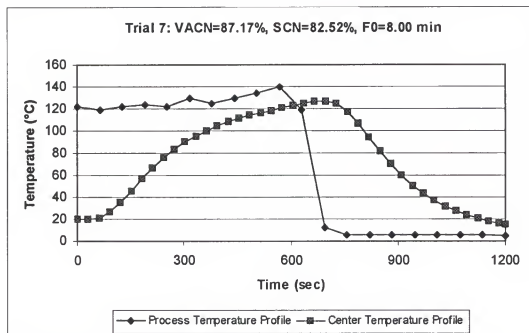


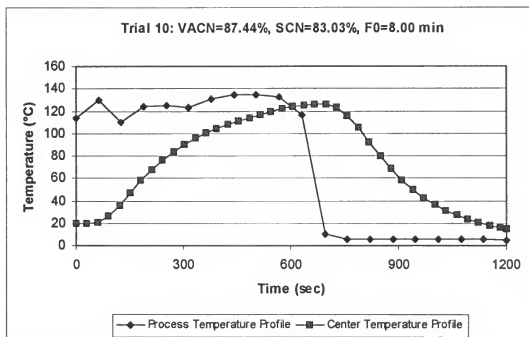
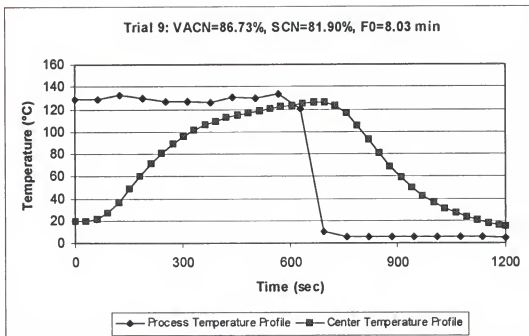
2. Sphere ($r=15\text{mm}$, $t=20\text{ min}$, $N=20$).



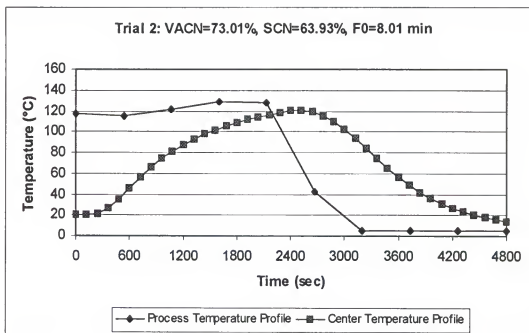
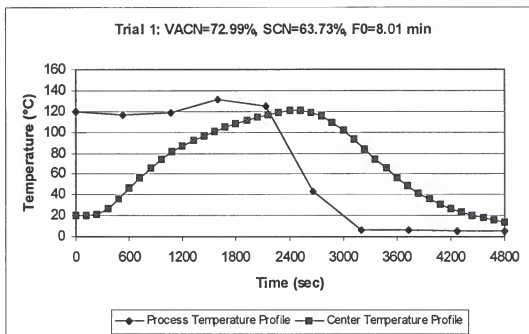


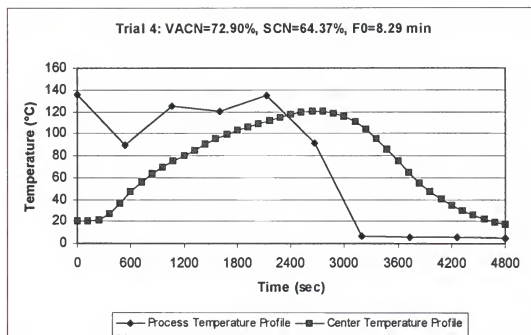
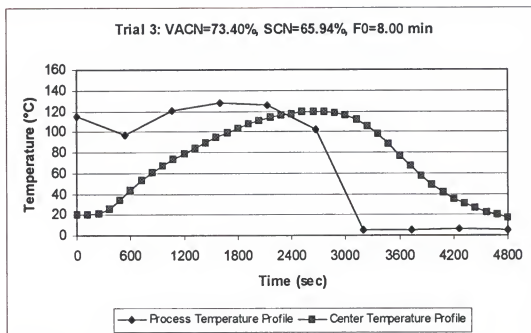


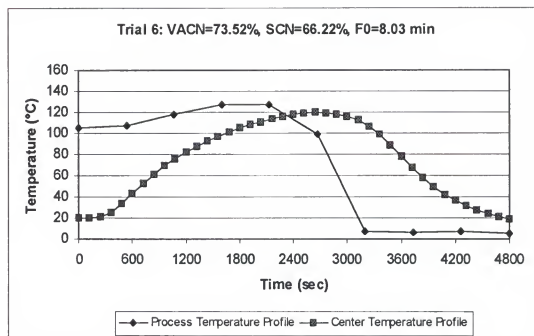
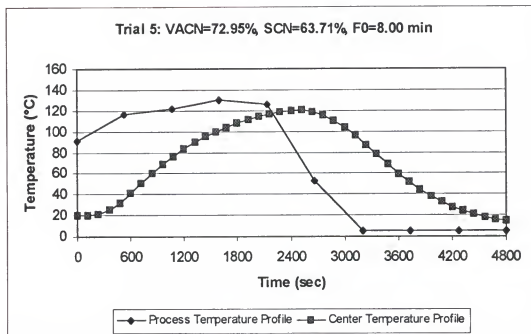


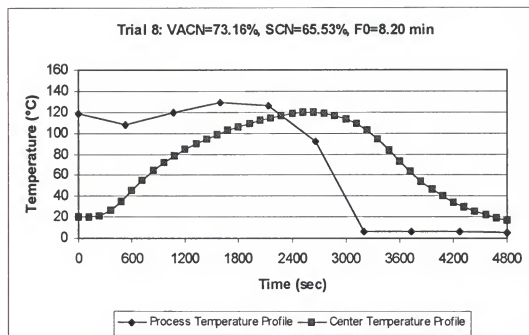
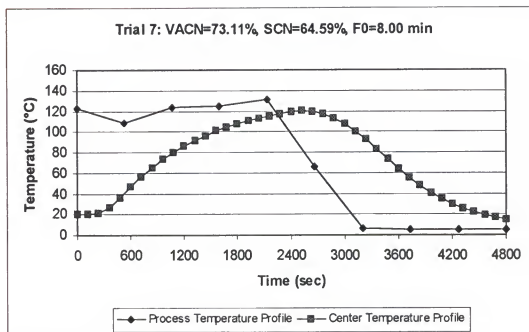


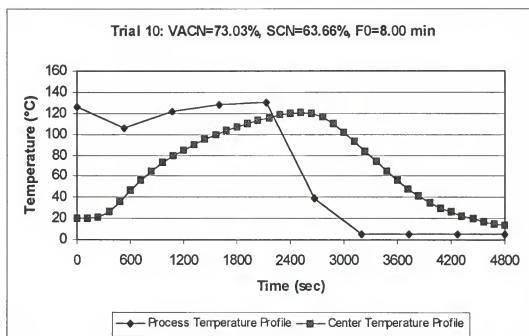
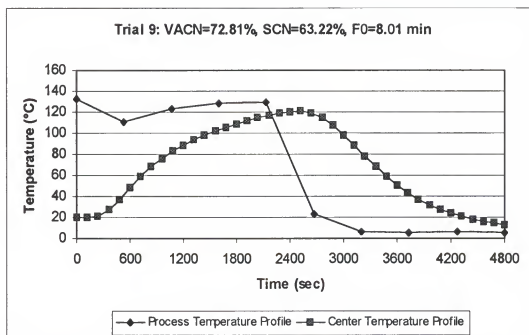
3. Sphere ($r=30\text{mm}$, $t=80\text{ min}$, $N=10$).



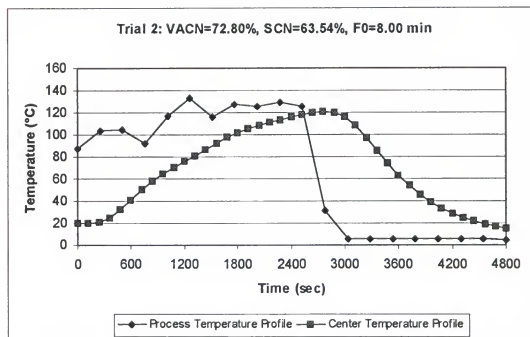
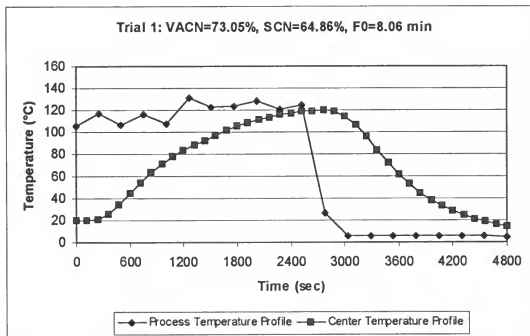


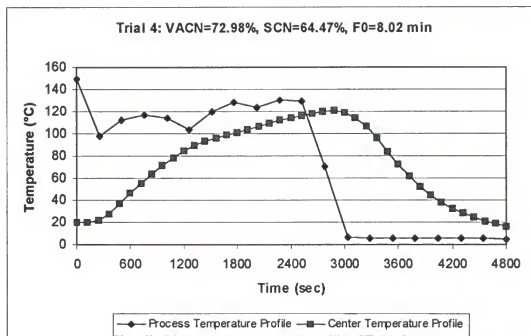
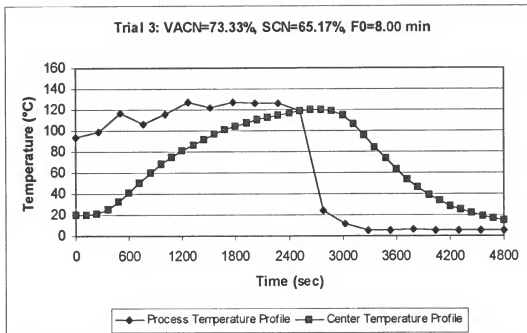


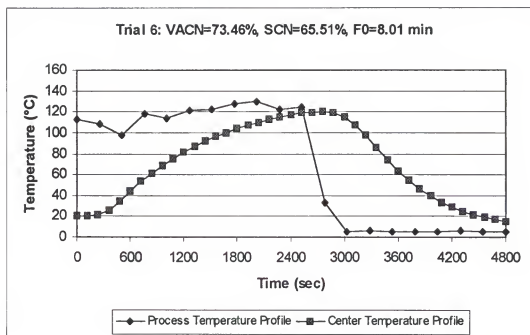
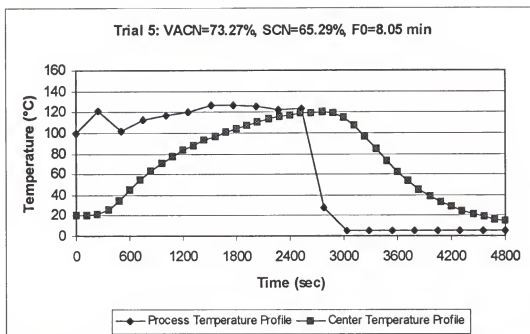


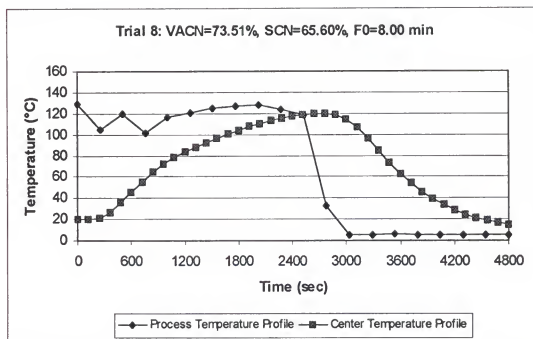
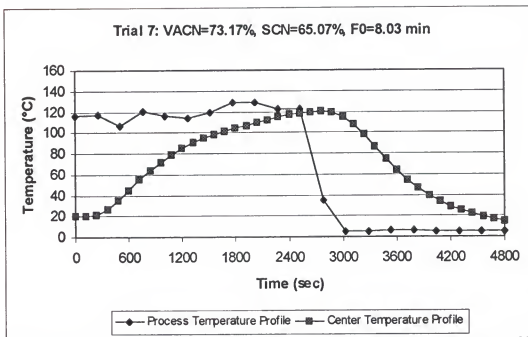


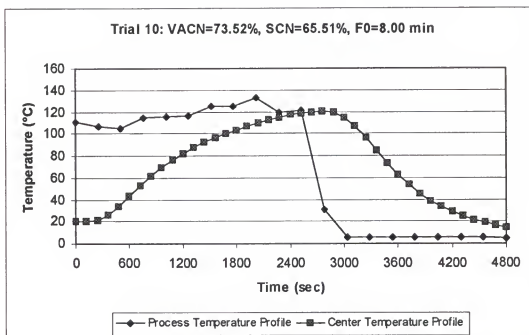
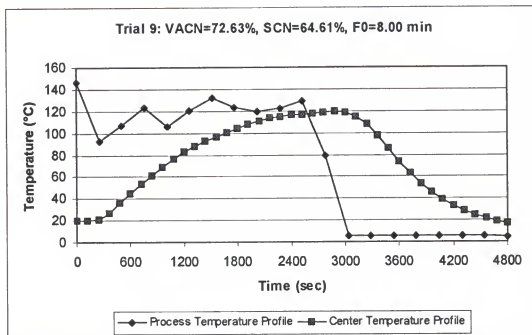
3. Sphere ($r=30\text{mm}$, $t=80\text{ min}$, $N=20$).







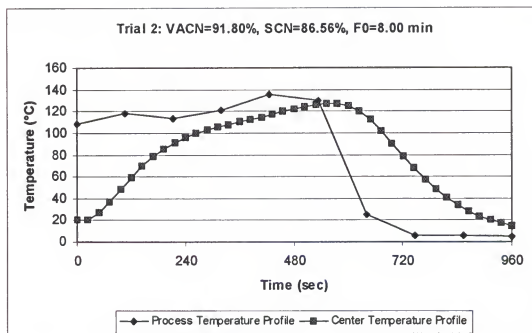
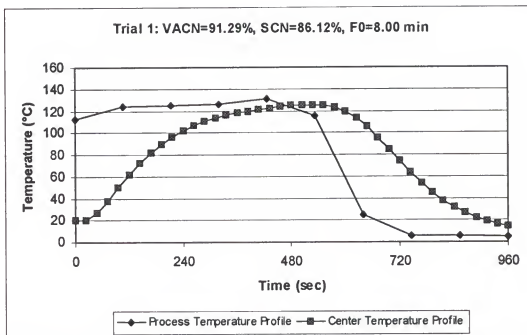


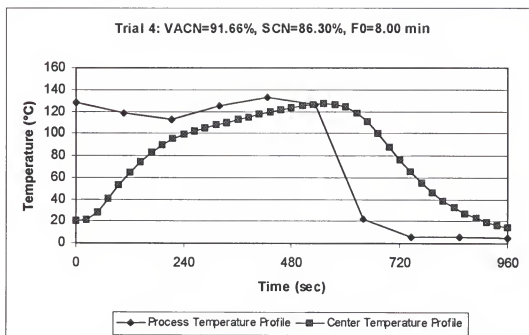
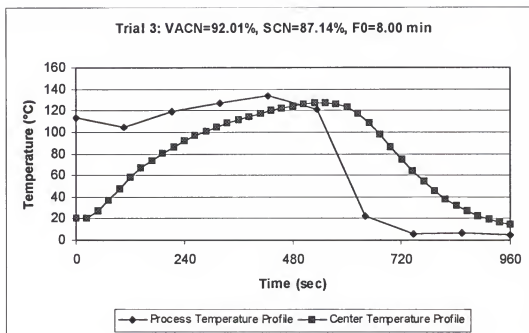


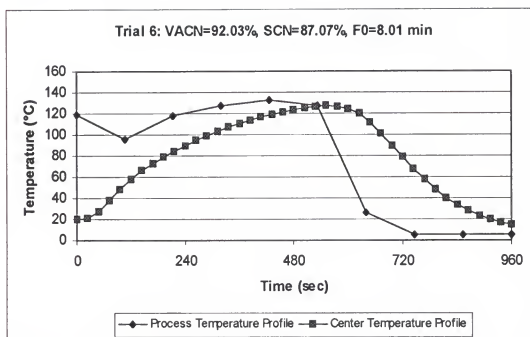
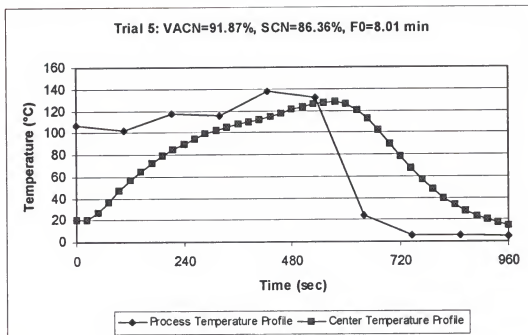
All the raw data can be obtained from Dr. M.Ö. Balaban at the Food Science and Human Nutrition Department of the University of Florida, Gainesville, FL.

APPENDIX E
PROCESS AND CENTER TEMPERATURE PROFILES FOR A FINITE CYLINDER
UNDER DIFFERENT PROCESSING CONDITIONS;
OBJECTIVE FUNCTION: SCN

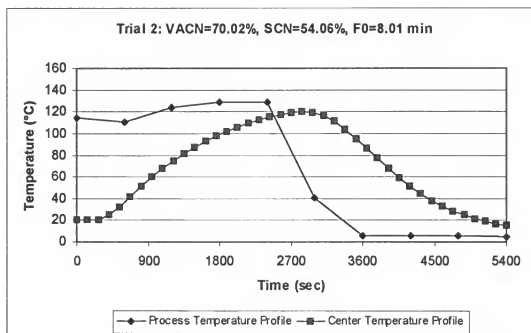
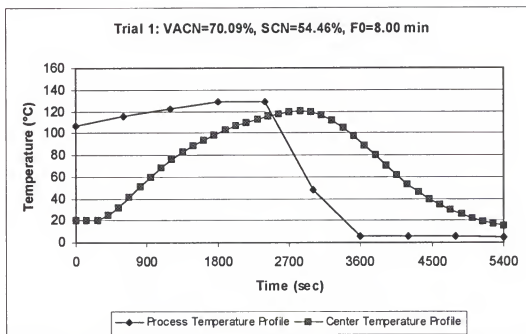
1. Finite Cylinder ($r=15\text{mm}$, $2l=15\text{ mm}$, $t=16\text{ min}$, $N=10$).

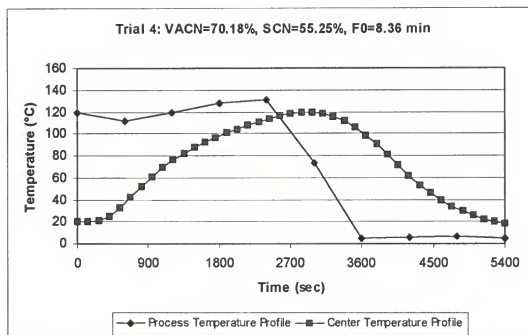
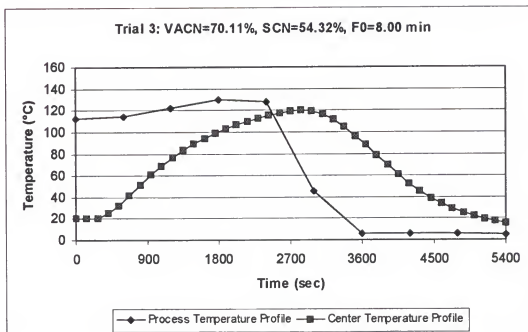


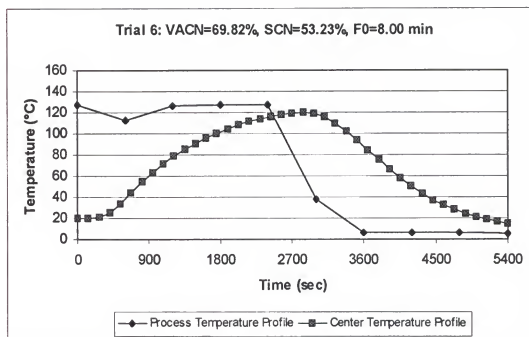
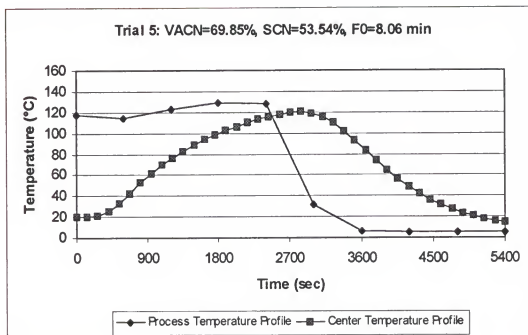




2. Finite Cylinder ($r=30\text{mm}$, $2l=60\text{ mm}$, $t=90\text{ min}$, $N=10$).



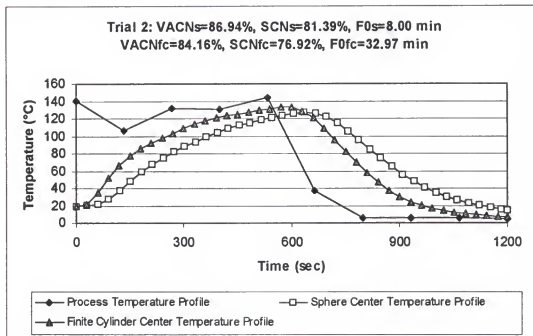
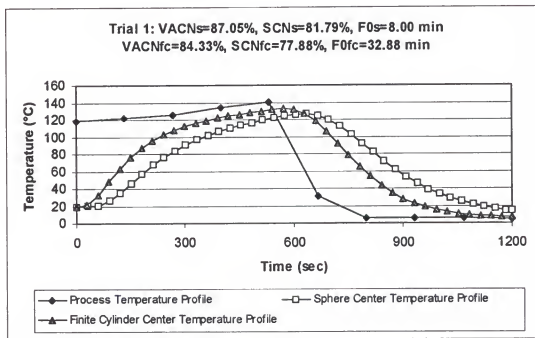




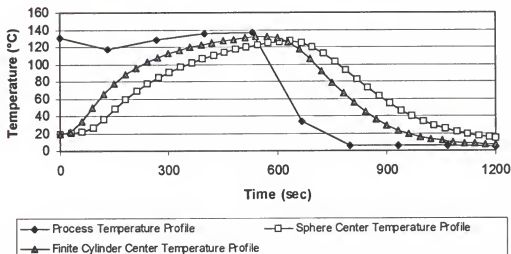
All the raw data can be obtained from Dr. M.Ö. Balaban at the Food Science and Human Nutrition Department of the University of Florida, Gainesville, FL.

APPENDIX F
PROCESS AND CENTER TEMPERATURE PROFILES
FOR DOUBLE GEOMETRY SYSTEM (A SPHERE AND A FINITE CYLINDER)
UNDER DIFFERENT PROCESSING CONDITIONS;
OBJECTIVE FUNCTION: VACN

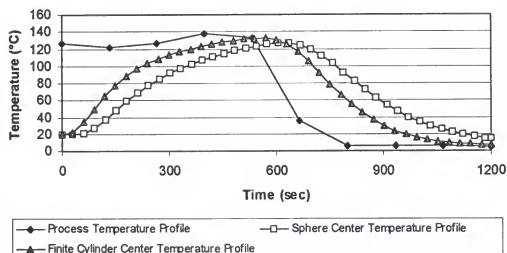
1. Sphere ($r=15$ mm) and Finite Cylinder ($r=15$ mm, $2l=15$ mm, $t=20$ min, $N=10$).



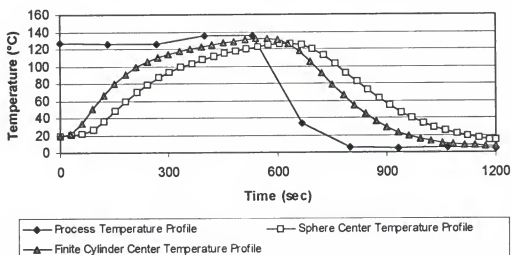
Trial 3: VACNs=87.15%, SCNs=82.00%, F0s=8.01 min
VACnfc=84.46%, SCNfc=78.03%, F0fc=32.68 min



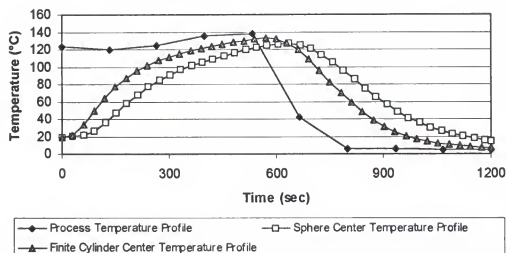
Trial 4: VACNs=87.16%, SCNs=82.04%, F0s=8.01 min
VACnfc=84.41%, SCNfc=78.09%, F0fc=32.88 min



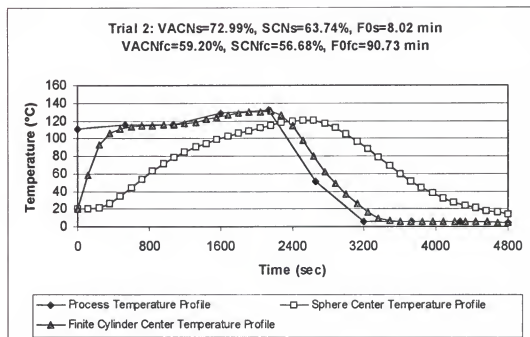
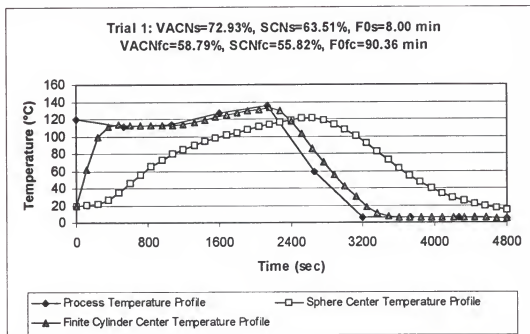
Trial 5: VACNs=87.10%, SCNs=81.92%, F0s=8.00 min
 VACNfc=84.37%, SCNfc=77.82%, F0fc=31.25 min



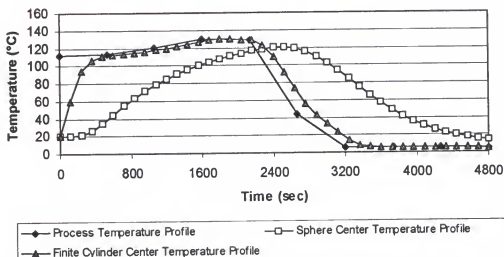
Trial 6: VACNs=87.15%, SCNs=81.99%, F0s=8.02 min
 VACNfc=84.53%, SCNfc=78.18%, F0fc=32.82 min



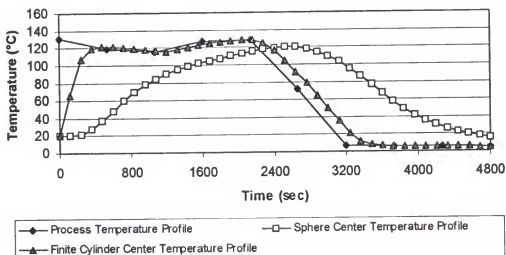
2. Sphere ($r=30$ mm) and Finite Cylinder ($r=15$ mm, $2l=15$ mm, $t=80$ min, $N=10$).



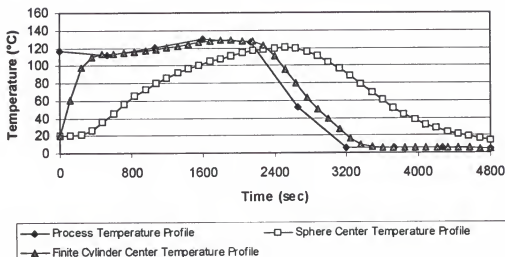
Trial 3: VACNs=73.04%, SCNs=63.86%, F0s=8.03 min
 VACNfc=66.16%, SCNfc=59.29%, F0fc=83.63 min



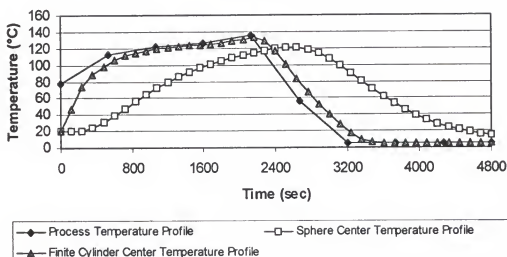
Trial 4: VACNs=72.75%, SCNs=63.91%, F0s=8.00 min
 VACNfc=57.95%, SCNfc=54.29%, F0fc=65.32 min



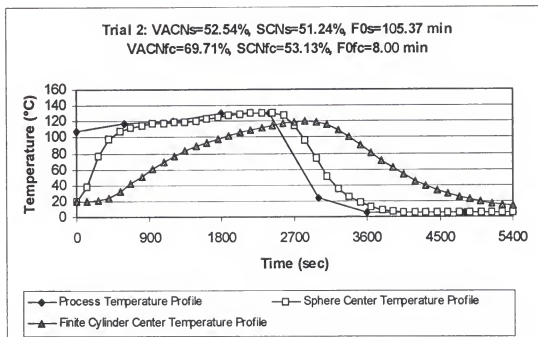
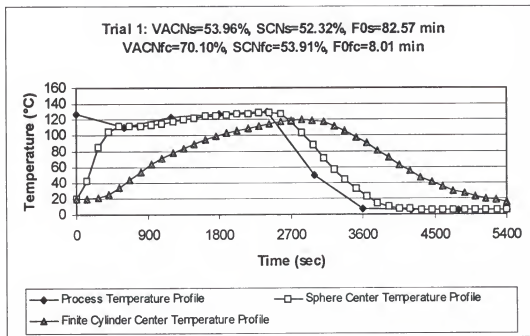
Trial 5: VACNs=73.12%, SCNs=64.19%, F0s=8.00 min
 VACNfc=59.59%, SCNfc=57.06%, F0fc=79.33 min



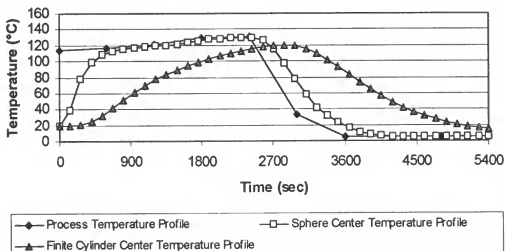
Trial 6: VACNs=72.76%, SCNs=63.04%, F0s=8.00 min
 VACNfc=58.47%, SCNfc=56.14%, F0fc=103.48 min



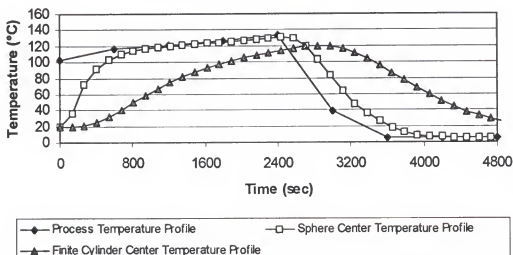
3. Sphere ($r=15$ mm) and Finite Cylinder ($r=30$ mm, $2l=60$ mm, $t=90$ min, $N=10$).



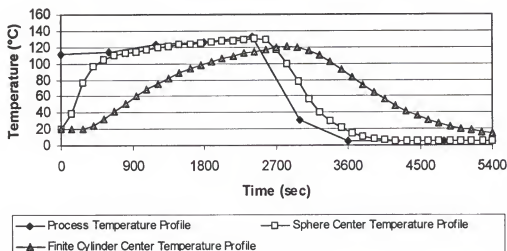
Trial 3: VACNs=53.07%, SCNs=51.75%, F0s=96.69 min
 VACNfc=69.89%, SCNfc=53.58%, F0fc=8.01 min



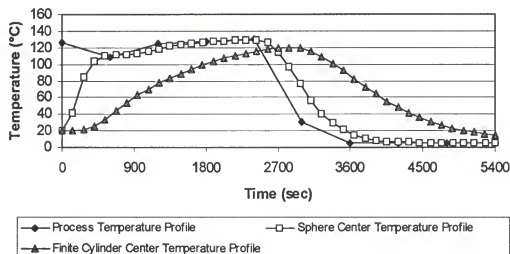
Trial 4: VACNs=53.00%, SCNs=51.71%, F0s=100.03 min
 VACNfc=69.80%, SCNfc=53.55%, F0fc=8.00 min



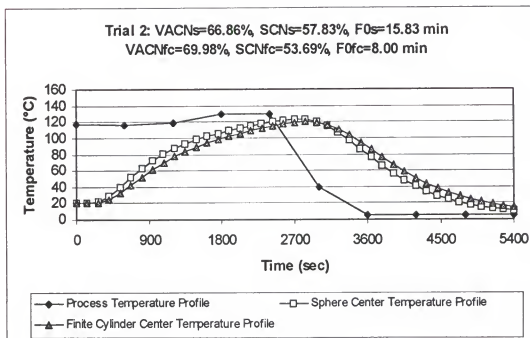
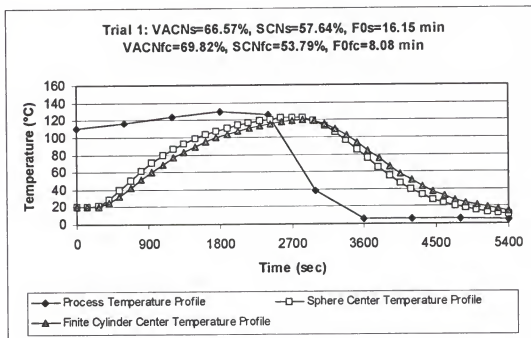
Trial 5: VACNs=52.91%, SCNs=51.55%, F0s=97.88 min
 VACNfc=69.75%, SCNfc=53.35%, F0fc=8.01 min



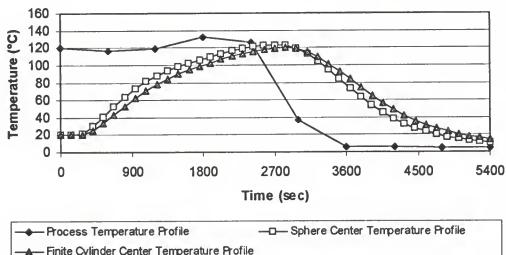
Trial 6: VACNs=53.09%, SCNs=51.46%, F0s=93.90 min
 VACNfc=69.84%, SCNfc=53.12%, F0fc=8.00 min



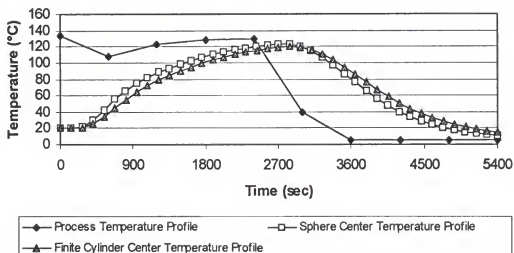
4. Sphere ($r=30$ mm) and Finite Cylinder ($r=30$ mm, $2l=60$ mm, $t=90$ min, $N=10$).

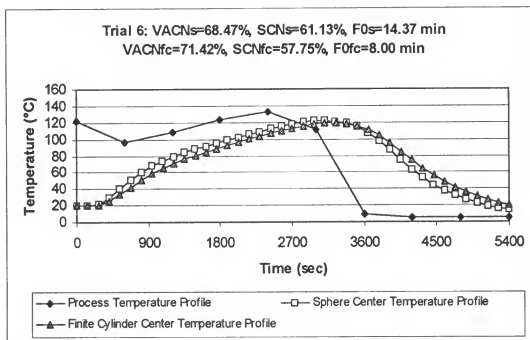
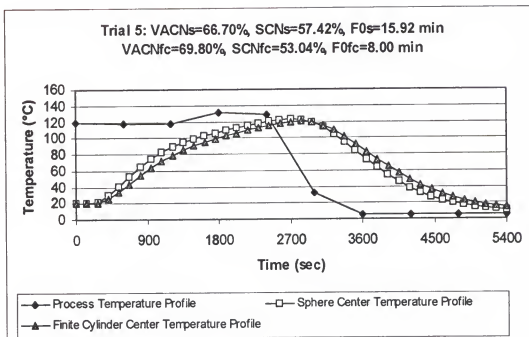


Trial 3: VACNs=66.73%, SCNs=57.57%, F0s=16.02 min
 VACNfc=69.86%, SCNfc=53.24%, F0fc=8.01 min



Trial 4: VACNs=66.87%, SCNs=57.73%, F0s=15.75 min
 VACNfc=69.85%, SCNfc=52.54%, F0fc=8.00 min

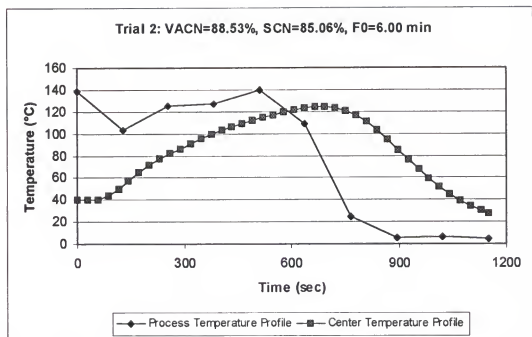
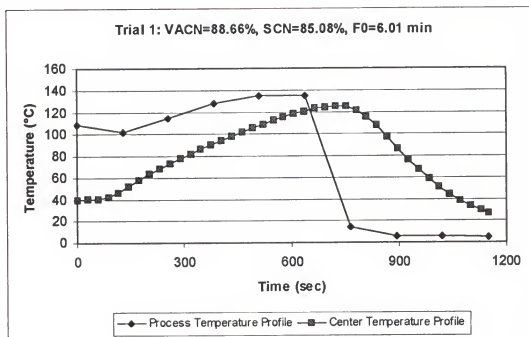


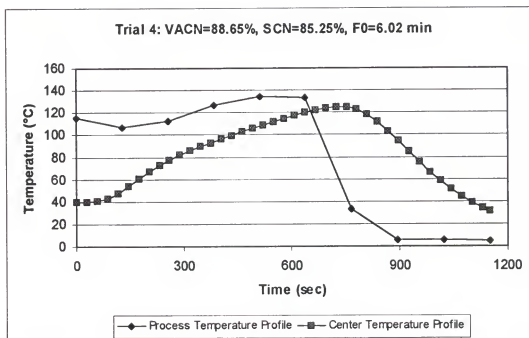
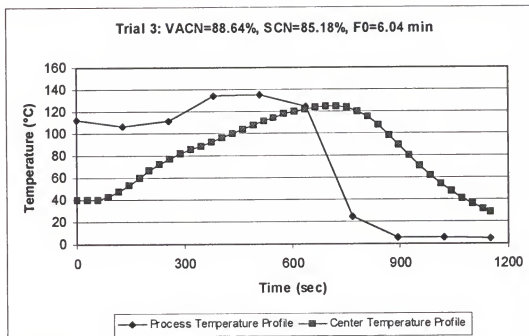


All the raw data can be obtained from Dr. M.Ö. Balaban at the Food Science and Human Nutrition Department of the University of Florida, Gainesville, FL.

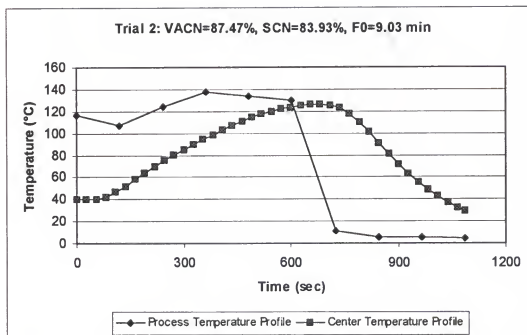
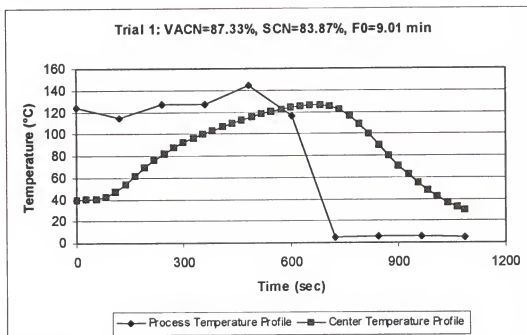
APPENDIX G
PROCESS AND CENTER TEMPERATURE PROFILES
FOR LITERATURE CASES

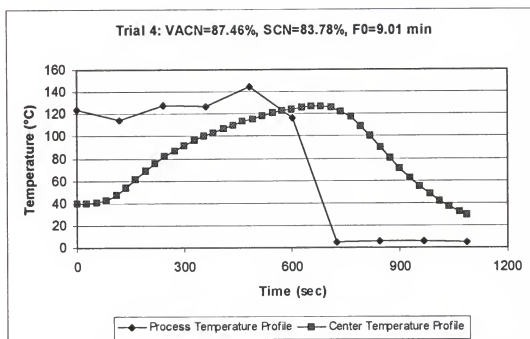
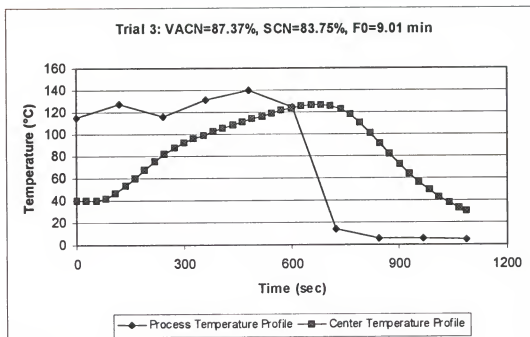
1. Case I:





2. Case II:





All the raw data can be obtained from Dr. M.Ö. Balaban at the Food Science and Human Nutrition Department of the University of Florida, Gainesville, FL.

REFERENCES

- Avriel, M. 1976. Nonlinear programming. Prentice-Hall, Englewood Cliffs, N.J.
- Banga, J.R., Martin, R.I.P., Gallardo, J.M., and Casares, J.J. 1991. Optimization of the thermal processing of conduction-heated canned foods: Study of several objective functions. *Journal of Food Engineering*. 14: 25-51.
- Box, M.J. 1965. A new method of constrained optimization and comparison with other methods. *Computer Journal*. 8: 42-52.
- Carslaw, H.S., and Jaeger, J.C. 1986. Conduction of heat in solids. Oxford University Press, New York, N.Y.
- Chau, K.V., and Gaffney, J.J. 1990. A finite-difference model for heat and mass transfer in products with internal heat generation and transpiration. *Journal of Food Science*. 55(2):484-487.
- Chau, K.V. and Snyder, G. 1988. Mathematical model for temperature distribution of thermally processed shrimp. *Transactions of the ASAE*, 31(2): 608-612.
- Clausing, A.M. 1989. Numerical methods in heat transfer. Lectures in mechanical engineering, University of Illinois, Urbana, IL.
- Erdoğdu, F. 1996. Modeling of temperature distribution in shrimp, and measurement of its effects on texture, shrinkage and yield loss. Master of Engineering Thesis. University of Florida, Gainesville.
- Erdoğdu, F., Balaban, M.O., and Chau, K.V. (1998a). Modeling of heat conduction in elliptical cross-section: I. Development and testing of the model. *Journal of Food Engineering*. 38(2):223-239.
- Erdoğdu, F., Balaban, M.O., and Chau, K.V. (1998b). Modeling of heat conduction in elliptical cross-section: II. Adaptation to thermal processing of shrimp. *Journal of Food Engineering*. 38(2):241-258.

- Evans, L.B. 1982. Optimization theory and its application in food processing. *Food Technology*. 36(7):88-93,96.
- Fastag, J., Koide, H., and Rizvi, S.S.H. 1996. Variable control of a batch retort and process simulation for optimization studies. *Journal of Food Process Engineering*. 19: 1-14.
- Hager, W.W. 1988. *Applied Numerical Linear Algebra*. Department of Mathematics, University of Florida, Gainesville, FL.
- Hayakawa, K.I. 1978. A critical review of mathematical procedures for determining proper heat sterilization processes. *Food Technology*. 78(3): 59-65.
- Hendrickx, M., Silva, C., Oliveira, F., and Tobback, P. 1993. Generalized (semi)-empirical formulae for optimal sterilization temperatures of conduction-heated foods with infinite surface heat transfer coefficients. *Journal of Food Engineering*. 19: 141-158.
- Holdsworth, S.D. 1985. Optimization of thermal processing: a review. *Journal of Food Engineering*. 4: 89-116.
- Kazmierczak, R.F., Jr. 1996. Optimizing complex bioeconomic simulations using an efficient search heuristic. Louisiana State University, Baton Rouge, Research Reports Number: 704.
- Lebowitz, S.F. and Bhowmik, S.R. 1989. Determination of retortable pouch heat transfer coefficients by optimization method. *Journal of Food Science*. 54(6):1407-1412.
- Loncin, M., and Merson, R.L. 1979. Optimization. In: *Food engineering: Principles and selected applications*. page: 330-358. Academic Press, New York.
- Lund, D.B. 1977. Design of thermal processes for maximizing nutrient retention. *Food Technology*. 31(2): 71-78.
- Lund, D.B. 1982. Applications of optimization in heat processing. *Food Technology*. 36(7): 97-100.
- Microsoft Corporation. (1994) *Visual Basic Professional*. Version 6.0. Redmond, WA.
- Miettinen, K.M. 1999. *Nonlinear multiobjective optimization*. Kluwer, Norwell, MA.
- Mishkin, M., Karel, M., and Saguy, I. 1982. Applications of optimization in food dehydration. *Food Technology*. 36(7): 101-109.

- Mishkin M., Saguy, I., and Karel, M. 1984. Optimization of nutrient retention during processing: Ascorbic acid in potato dehydration. *Journal of Food Science*. 49: 1262-1266.
- Nadkarni, M.M. and Hatton, T.A. 1985. Optimal nutrient retention during the thermal processing of conduction-heated canned foods: Application of the distributed minimum principle. *Journal of Food Science*. 50: 1312-1321.
- Norback, J.B. 1980. Techniques for optimization of food processes. *Food Technology*. 34(2):86-88.
- Noronha, J., Hendrickx, M., Suys, J., and Tobback, P. 1993. Optimization of surface quality retention during the thermal processing of conduction heated foods using variable temperature retort profiles. *Journal of Food Processing and Preservation*. 17: 75-91.
- Noronha, J., Hendrickx, M., Loey, A.V., and Tobback, P. 1995. New semi-empirical approach to handle time-variable boundary conditions during sterilization of non-conductive heating foods. *Journal of Food Engineering*. 24: 249-268.
- Noronha, J.F., Loey, A.V., Hendrickx, M., and Tobback, P. 1996a. An empirical equation for the description of optimum variable retort temperature profiles that maximize surface quality retention in thermally processed foods. *Journal of Food Processing and Preservation*. 20: 251-264.
- Noronha, J., Loey, A.V., Hendrickx, M., and Tobback, P. 1996b. Simultaneous optimization of surface quality during the sterilization of packed foods using constant and variable retort temperature profiles. *Journal of Food Engineering*. 30: 283-297.
- Ohlsson, T. 1980a. Optimal sterilization temperatures for flat containers. *Journal of Food Science*. 45: 848-852, 859.
- Ohlsson, T. 1980b. Optimal sterilization temperatures for sensory quality in cylindrical containers. *Journal of Food Science*. 45:1517-1521.
- Ozisik, M.N. 1993. Heat conduction. Wiley, New York.
- Ramesh, M.N. 1995. Optimum sterilization of foods by thermal processing-A review. *Food Science and Technology Today*. 9(4): 217-227.

- Saguy, I., and Karel, M. 1979. Optimal retort temperature profile in optimizing thiamin retention in conduction-type heating of canned foods. *Journal of Food Science*. 44: 1485-1490.
- Saguy, I. 1983. Optimization methods and applications. In: I. Saguy ed., *Computer aided techniques in food technology*, pages: 268-320. Marcel Dekker, New York.
- Silva, C., Hendrickx, M., Oliveira, F., and Tobback, P. 1992a. Critical evaluation of commonly used objective functions to optimize overall quality and nutrient retention of heat-preserved foods. *Journal of Food Engineering*. 17: 241-258.
- Silva, C., Hendrickx, F., Oliveira, F., and Tobback, P. 1992b. Optimal sterilization temperatures for conduction heating foods considering finite surface heat transfer coefficients. *Journal of Food Science*. 57(3):743-748.
- Silva, C.L.M., Oliveira, F.A.R., and Hendrickx, M. 1993. Modeling optimum processing conditions for the sterilization of prepackaged foods. *Food Control*. 4(2): 67-78.
- Silva, C.L.M., Oliveira, F.A.R., and Hendrickx, M. 1994a. Experimental validation of models for predicting optimal surface quality sterilization temperatures. *International Journal of Food Science and Technology*. 29: 227-241.
- Silva, C.L.M., Oliveira, F.A.R., and Pereira, P.A.M. 1994b. Optimum sterilization: A comparative study between average and surface quality. *Journal of Food Process Engineering*. 17: 155-176.
- Silva, C.L.M., Oliveira, F.A.R., and Hendrickx, M. 1994c. Quality optimization of conduction heating foods sterilized in different packages. *International Journal of Food Science and Technology*. 29: 515-530.
- Schulz, G.L. 1978. Trends in packaging for food service. *Journal of Food Protection*. 41(6): 464-467.
- Teixeira, A.A., Dixon, J.R., Zahradnik, J.W., and Zinsmeister, G.E. 1969a. Computer optimization of nutrient retention in the thermal processing of conduction-heated foods. *Food Technology*. 23:845-850.
- Teixeira, A.A., Dixon, J.R., Zahradnik, J.W., and Zinsmeister, G.E. 1969b. Computer determination of spore survival distributions in thermally-processed conduction-heated foods. *Food Technology*. 23: 352-354.

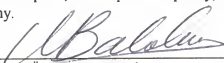
- Teixeira, A.A., Zinsmeister, G.E., and Zahradnik, J.W. 1975a. Experimental evaluation of mathematical and computer models for thermal process evaluation. *Journal of Food Science*. 40: 653-655.
- Teixeira, A.A., Stumbo, C.R., and Zahradnik, J.W. 1975b. Computer simulation of variable retort control and container geometry as a possible means of improving thiamine retention in thermally processed foods. *Journal of Food Science*. 40: 653-655.
- Terajima, Y., and Nonaka, Y. 1996. Retort temperature profile for optimum quality during conduction heating of foods in retortable pouches. *Journal of Food Science*. 61(4): 673-678, 682.
- Thijssen, H.A.C., Kerkhof, A.M., and Liefkens, A.A.A. 1978. Short-cut method for the calculation of sterilization conditions yielding optimum quality retention for conduction-type heating of packaged foods. *Journal of Food Science*. 43:1096-1101.
- Thijssen, H.A.C., and Kochen, L.H.P.J.M. 1980. Calculation of optimum sterilization conditions for packed conduction-type foods. *Journal of Food Science*. 45:1267-1272, 1292.
- Tucker, G.S., and Clark, P. 1990. Modeling the cooling phase of heat sterilization processes, using heat transfer coefficients. *International Journal of Food Science and Technology*. 25: 668-681.
- Umeda, T., Shindo, A., and Ichikawa, A. 1972. Complex method for solving variational problems with state-variable inequality constraints. *Industrial Engineering of Chemical Process Design and Development*. 11(1): 102-107.
- Welt, B.A., Teixeira, A.A., Chau, K.V., Balaban, M.O., and Hintenlang, D.E. 1997. Explicit finite difference methods for heat transfer simulation and thermal process design. *Journal of Food Science*. 62(2): 230-236.

BIOGRAPHICAL SKETCH


Ferruh Erdoğan was born on October 19, 1970, in Ereğli, Türkiye. He graduated from Ereğli-Cumhuriyet High School in 1987 and graduated from the Food Engineering Department at Hacettepe University in Ankara with the highest GPA in 1992, receiving the İhsan Doğramacı Success Award. While studying for his M.S. at the same university, he also worked in ERSU, a fruit juice factory for 8 months as a quality control engineer. In 1993, he started working in the Food Engineering Department at the Mersin University as a research assistant. Ferruh worked in Mersin for 8 months. In 1994, he won a nationwide exam to pursue M.S. and Ph. D. degrees in food engineering in the U.S.A.

Ferruh has worked with Dr. Balaban at the University of Florida receiving his master's degree in December of 1996. He received outstanding academic achievement awards from the College of Engineering (1997, 1998, 1999, and 2000) and the College of Agriculture (1999) and won a student paper competition in 1997 from the Institute of Food Technologists. Ferruh expects to receive his Ph.D. in agricultural and biological engineering in August of 2000. Ferruh is currently a member of the Institute of Food Technologists (IFT), American Society of Agricultural Engineers (ASAE), Institute for Thermal Processing Specialists (IFTPS), Society of Industrial and Applied Mathematics (SIAM), and Florida Gamma Beta Chapter of Alpha Epsilon. Later in his career, he would like to be a member of the academy teaching of applied mathematics in food engineering.

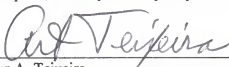
I certify that I have read this study and that in my opinion it conforms to acceptable standards of scholarly presentation and is fully adequate, in scope and quality, as a dissertation for the degree of Doctor of Philosophy.


Murat Ö. Balaban, Chair
Professor of Agricultural and Biological
Engineering

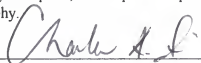
I certify that I have read this study and that in my opinion it conforms to acceptable standards of scholarly presentation and is fully adequate, in scope and quality, as a dissertation for the degree of Doctor of Philosophy.


Khe V. Chau
Professor of Agricultural and Biological
Engineering

I certify that I have read this study and that in my opinion it conforms to acceptable standards of scholarly presentation and is fully adequate, in scope and quality, as a dissertation for the degree of Doctor of Philosophy.


Arthur A. Teixeira
Professor of Agricultural and Biological
Engineering

I certify that I have read this study and that in my opinion it conforms to acceptable standards of scholarly presentation and is fully adequate, in scope and quality, as a dissertation for the degree of Doctor of Philosophy.


Charles A. Sims
Professor of Food Science and Human
Nutrition

I certify that I have read this study and that in my opinion it conforms to acceptable standards of scholarly presentation and is fully adequate, in scope and quality, as a dissertation for the degree of Doctor of Philosophy.


Chung K. Hsieh
Professor of Mechanical Engineering

This dissertation was submitted to the Graduate Faculty of the College of Engineering and to the Graduate School and was accepted as partial fulfillment of the requirements for the degree of Doctor of Philosophy.

August 2000

A handwritten signature in black ink, appearing to read 'M. Jack Ohanian', written over a horizontal line.

M. Jack Ohanian
Dean, College of Engineering

Winfred M. Phillips
Dean, Graduate School

LD
1780
20 00

Eldo